5-2014

Generation Scheduling for Power Systems with Demand Response and a High Penetration of Wind Energy

Guodong Liu
University of Tennessee - Knoxville, gliu5@utk.edu

To the Graduate Council:

I am submitting herewith a dissertation written by Guodong Liu entitled "Generation Scheduling for Power Systems with Demand Response and a High Penetration of Wind Energy." I have examined the final electronic copy of this dissertation for form and content and recommend that it be accepted in partial fulfillment of the requirements for the degree of Doctor of Philosophy, with a major in Electrical Engineering.

Kevin L. Tomsovic, Major Professor

We have read this dissertation and recommend its acceptance:

Fangxing Li, Yilu Liu, Tsewei Wang

Accepted for the Council:

Carolyn R. Hodges

Vice Provost and Dean of the Graduate School

(Original signatures are on file with official student records.)

Generation Scheduling for Power Systems with Demand Response and a High Penetration of Wind Energy

A Dissertation Presented for the

Doctor of Philosophy

Degree

The University of Tennessee, Knoxville

Guodong Liu

May 2014

Dedicated to My Parents

Acknowledgements

I would like to express my deepest gratitude to my advisor, Professor Kevin Tomsovic, for his time and dedication, patience and supervision, professionalism and inspirational teaching, and above all, for providing me with a high-quality education and introducing me to the world of research.

My gratitude also goes to Dr. Yilu Liu, Dr. Fangxing Li and Dr. Tsewei Wang for their time and effort in serving as my committee member. Their invaluable suggestions and comments enhanced the quality of this work.

Also, I am thankful to all the professors, stuff and students in the CURENT Engineering Research Center, including those already left. Their friendship, encouragement, and help were indeed beneficial to my studies and research work.

Additionally, I would like to thank to Dr. Yan Xu at Oak Ridge National Laboratory (ORNL) for supporting me during the last year of my Ph.D. study. Besides, I benefit a lot from all the inspiring discussions in friendly atmosphere.

Finally, I would like to express my appreciation and love to my family, especially my wife, Junjue Hu, for their unconditional love and support, which made it possible for me to finish this work.

These violent delights have violent ends, and in their triumph die, like fire and powder, which, as they kiss, consume.

–William Shakespeare: Romeo and Juliet, Act II, Scene VI

Abstract

With renewable energy sources and demand response programs expanding in many power systems, traditional unit commitment and economic dispatch approaches are inadequate. The power system is changing to one where there is control with uncertainty for both generation and load. Alternative power system scheduling methods capable of aggregating the uncertainty of wind power and demand response, while maintaining reliable and economic performance are investigated in this work. The research addresses four aspects of these changes.

First , a probabilistic method is proposed to maintain uniform system reliability level in the hour-ahead economic dispatch by quantifying different levels of required spinning reserve. The method considers the probability distributions of wind speed and load forecast errors, as well as outage replacement rates of generators by using the expectation of demand not served (EDNS) as an evaluation index.

Second, a probabilistic model of security-constrained unit commitment (SCUC) is proposed to determine the optimal amount of spinning reserve when integrating wind generation. An algorithm, which includes the stochastic wind forecast results into a day-ahead unit commitment and extracts its value for system operation of system, is developed. The proposed model determines the optimal amount of spinning reserve in terms of an optimal trade-off between economic efficiency and system reliability.

Third, a new duplex demand response model is proposed to allow demand to bid into both the energy and spinning reserve markets. A co-optimized day-ahead energy and spinning reserve market is proposed to minimize the expected net cost under

any credible system state, i.e., expected total cost of operation minus total benefit of demand. The problem is solved by MILP. Compared with conventional demand shifting bids, the proposed model can reduce system operating cost.

Fourth, a robust UC model to minimize the generalized social cost is proposed. Compared to the traditional UC to maximize the social welfare, the proposed model more effectively manages uncertainty in demand response to price changes. The solution is robust against all possible modeled realizations of the uncertain demand response.

Table of Contents

List of Tables

List of Figures

Nomenclature

i	Index of generators, running from 1 to NG.
j	Index of demand, running from 1 to ND.
t	Index of time periods, running from 1 to NT.
k	Index of transmission lines, running from 1 to NK.
m	Index of energy blocks offered by generators (demand), running from 1 to $Noit$ ($Nojt$).
ω, s	Index of scenarios of generators, running from 1 to NW.
r, q	Index of wind farms,running from 1 to NM.
n	Index of buses, running from 1 to NB.
l	Index of probability intervals, running from 1 to NL.
u_{Git}	1 if unit i is scheduled on during period t and 0 otherwise.
u_{Djt}	1 if demand j is scheduled on during period t and 0 otherwise.
$b_{s,t,l}$	1 if uncertainty within interval l plus outage of units in scenario s during period t causes loss of load and 0 otherwise.
$p_{Git}(m)$	Power output scheduled from the m-th block of energy offer by unit i during period t (MW). Limited to $p_{Git}^{max}(m)$.

$p_{Djt}(m)$	Power consumption scheduled from the m-th block of energy bid by demand j during period t (MW). Limited to $p_{Djt}^{max}(m)$.
P_{it}	Power output scheduled from unit i during period t (MW).
D_{jt}	Power consumption scheduled for demand j during period t (MW).
R_{it}^{U}	Scheduled up-spinning reserve for unit i during time period t (MW).
R_{it}^{D}	Scheduled down-spinning reserve for unit i during time period t (MW).
R_{jt}^{U}	Scheduled up-spinning reserve for demand j during time period t (MW).
R_{jt}^{D}	Scheduled down-spinning reserve for demand j during time period t (MW).
$P_{it\omega}$	Power output of unit i during period t in scenario ω (MW).
$D_{jt\omega}$	Power consumption of demand j during period t in scenario ω (MW).
$r_{it\omega}^{U}$	Deployed up-spinning reserve from unit i during time period t in scenario ω (MW).
$r_{it\omega}^{D}$	Deployed down-spinning reserve from unit i during time period t in scenario ω (MW).
$r_{jt\omega}^{U}$	Deployed up-spinning reserve from demand j during time period t in scenario ω (MW).
$r_{jt\omega}^{D}$	Deployed down-spinning reserve from demand j during time period t in scenario ω (MW).

$r_{Git\omega}(m)$	Deployed spinning reserve from m-th block of energy offer by unit i during period t in scenario ω (MW).
$r_{Djt\omega}(m)$	Deployed spinning reserve from m-th block of energy bid by demand j during period t in scenario ω (MW).
$L_{jt\omega}$	Involuntary load shedding from demand j during period t in scenario ω (MW). Limited to L_{jt}^{max}.
$P_{i,r,t}^{w}$	Power output of wind turbine i in wind farm r during period t (MW).
$e_{i,r,t}^{w}$	Wind power forecast error of turbine i in wind farm r during period t (MW).
P_{t}^{w}	Total wind power output during period t (MW).
e_{t}^{w}	Total wind power forecast error during period t (MW).
$\sigma_{i,r,t}^{w}$	Standard deviation of $e_{i,r,t}^{w}$ (MW).
σ_{t}^{w}	Standard deviation of e_{t}^{w} (MW).
σ_{t}^{l}	Standard deviation of load forecast error during period t (MW).
e_{t}^{d}	Total net demand forecast error during period t (MW).
σ_{t}^{d}	Standard deviation of e_{t}^{d} (MW).
$p_{s,t}$	Probability of scenario s during period t.
$\mu_{s,t}$	Redundant or deficient power of generators in scenario s during period t (MW).
$x_{s,t}$	Total system forecast error in scenario s during period t (MW).
$P_{i,t}^{w}$	Power output of wind turbine i during period t (MW).

$EENS_{s,t}$	Expected energy not served in scenario s during period t (MWh).
$EENS_t$	Expected energy not served during period t (MWh).
$EENS^{\max}$	Maximum amount of expected energy not served (MWh).
$LOLP_t$	Loss of load probability during period t.
$LOLP^{\max}$	Maximum value of Loss of load probability.
$EDNS_{\omega t}$	Expected demand not served in scenario ω during period t (MW).
$EDNS_t$	Expected demand not served during period t (MW).
$EDNS^{\max}$	Maximum amount of expected demand not served (MW).
$\lambda_{Git}(m)$	Marginal cost of the m-th block of energy offer by unit i during period t (\$/MWh).
$\lambda_{Djt}(m)$	Marginal benefit of the m-th block of energy bid by unit i during period t (\$/MWh).
A_i	Operating Cost of unit i at the point of P_i^{min} (\$/h).
B_j	Consumption benefit of demand j at the point of D_j^{min} (\$/h).
C_{it}^U	Capacity cost offer of unit i during period t for providing up-spinning reserve (\$/MW/h).
C_{it}^D	Capacity cost offer of unit i during period t for providing down-spinning reserve (\$/MW/h).
C_{jt}^U	Capacity cost offer of demand j during period t for providing up-spinning reserve (\$/MW/h).
C_{jt}^D	Capacity cost offer of demand j during period t for providing down-spinning reserve (\$/MW/h).

π_ω	Probability of scenario ω.
$VOLL_{jt}$	Value of load shed from demand j during period t (\$/MWh).
P_i^{max}	Maximum output of unit i (MW).
P_i^{min}	Minimum output of unit i (MW).
D_{jt}^{max}	Maximum consumption of demand j during period t (MW).
D_{jt}^{min}	Minimum consumption of demand j during period t (MW).
λ_{jt}^{max}	Maximum bidding price of demand j during period t (\$/MWh).
λ_{jt}^{min}	Minimum bidding price of demand j during period t (\$/MWh).
$-\alpha_{jt}$	Price elasticity of demand j during period t ($\$/MW^2h$).
$\triangle t$	Duration of time period t (h).
τ	Spinning reserve market lead time (h).
E_j	Maximum energy consumption of demand j during the scheduling horizon (MWh).
D_{jt}^F	Fixed demand of demand j during period t (MW).
GSF_{ki}	Generation shift factor to line k from unit i.
GSF_{kj}	Generation shift factor to line k from demand j.
F_k^{max}	Transmission limit of line k (MW).
RU_i	Up-ramping rate of unit i (MW/h).
RD_i	Down-ramping rate of unit i (MW/h).
RU_j	Up-ramping rate of demand j (MW/h).

RD_j	Down-ramping rate of demand j (MW/h).
$R_t^{\min}$	Minimum amount of spinning reserve during period t (MW).
$\xi_{it\omega}$	Health indicator of unit i during period t in scenario ω.
$H_{t\omega}$	Health indicator of system during period t in scenario ω.
T	System lead time (h).
TR	Minimum spinning reserve requirement (MW).
n_r	Number of wind turbines in wind farm r.
ρ_{rr}	Correlation coefficient between two wind power forecast error in the same wind farm r.
ρ_{qr}	Correlation coefficient between two wind power forecast error in wind farm q and farm r.
$q_{i,t}$	Capacity cost of spinning reserve of generator i during period t (\$/MWh).
ORR_i	Outage replacement rate of generator i.
$A_{s,t}$	Set of available generators in scenario s during period t.
$U_{s,t}$	Set of unavailable generators in scenario s during period t.
I_w	Set of all wind turbines.
Γ_0	Control parameter of robustness level.
C_i	Energy cost function of generator i.
S_i	Start-up cost function of generator i.
ED	Economic dispatch.

UC	Unit commmitment.
SCUC	Security-constraint unit commitment.
DR	Demand response.
DRP	Demand response provider.

Chapter 1

Introduction

The work in this dissertation is inspired by two facts in today's power system. Firstly, the large-scale integration of renewable energy sources especially wind is advancing rapidly in numerous power systems. How to accommodate the uncertainties of wind power without compromising the operating efficiency? Secondly, demand response plays an increasingly important role in reliable and economic operation of power systems and the electricity markets. How to make use of the flexibilities of demand side so as to improve the operating efficiency. This first chapter describes the background and motivation for this work. In addition, the main contributions and outline of this dissertation is provided.

1.1 Background

1.1.1 Renewable Energy

Due to increasing prices of fossil fuels, environmental impact and energy security concerns coupled with improvements in wind turbines, there has been a great increase in the penetration level of wind power around the world. Wind energy is expected to contribute 20 % of the total energy in the U.S. by the year 2030 (Lindenberg, 2008). Twenty four states and the District of Columbia have set renewable portfolio

standards, which require utilities to procure at least a certain percentage of their energy consumption from renewable energy sources, such as wind, solar and biomass. For example, California Energy Commission has set a Renewable Portfolio Standard that require 20 % of the energy mix to be produced from renewable sources by 2012 and 33 % by 2020 (Louton and Hawkins, 2007). Among all of the renewable resources, wind power production occupies most of the renewable energy market worldwide due to its technological maturity, widespread availability, speed of development and the very fact that the generating cost of wind farm is much lower than that of other renewable resources.

As numerous power systems in the U.S. and Europe have come to rely on wind power for supplying bulk quantities of power, system operators have to deal with the fact that the output of wind units depends on the weather condition. Consequently, wind units cannot be scheduled or dispatched like traditional units at the will of system operators. In fact, wind power can only be predicted with limited accuracy. Typically, the standard deviation of wind power forecast error is about 10 % for hour-ahead forecasting, 15 % for 12 hour-ahead forecasting and 20 % and more for day-ahead forecasting compared to its output (Watson et al., 1994; Fabbri et al., 2005; Ahlstrom et al., 2005). Therefore, the integration of wind power introduces additional uncertainty and great challenge to system operators.

1.1.2 Power system Scheduling

The scheduling of power system requires maintaining a continuous balance between supply and demand due to the fact that no practical technology is available for large-scale storage of electricity. Usually, this balance is achieved in multiple stages: day-ahead, hour-ahead and real-time scheduling. In day-ahead scheduling, a day-ahead unit commitment program is executed to decide the most economic unit combination with considerations of various restrictions of units. Hour-ahead scheduling responds to the deviation between supply and demand that arise as actual operating hour

approaches by rescheduling the flexible units committed in day-ahead scheduling or committing additional rapid-start units, which is usually expensive. Real-time scheduling further corrects the supply and demand deviations in real time. In deregulated power systems, these balancing stages are cleared in corresponding markets that are operated by Independent System Operators (ISOs) or Regional Transmission Operators (RTOs). Take California for example, the scheduling process of California ISO (CAISO) is described in Louton and Hawkins (2007) and briefly summarized here.

Day-ahead market (DAM). Scheduling Coordinators submit hourly bids (for supply and demand) for each resource to be used in the DAM. Ancillary Service (AS) bids are also submitted in the DAM, which is optimized in conjunction with energy bids to minimize the total bid cost of clearing congestion, balancing energy supply and demand, and reserving AS. In the DAM, a Residual Unit Commitment Program (RUC) is executed to ensure that sufficient capacity is committed, on-line and available for dispatch in real time to meet the CAISO forecast of CAISO demand for each trading hour of the operating day. Bidding into the DAM is closed at 1000 hours and results are published by 1300 hours on the day preceding the operating day.

Hour-ahead market. In the actual operating day, generators and loads adjust their positions to forecast errors or unexpected events by bidding in the hour-ahead market. CAISO will run the Hour-ahead Scheduling Process (HASP) to lock in changes to schedules 75-minutes before each actual operating hour starts. The imbalance between hourly supply and load will be eliminated by rescheduling the committed units through economic dispatch (ED) or committing short start or fast start units if possible. Similar to day-ahead schedules, hour-ahead schedules are also hourly blocks with 20-minute ramps between the hours.

Real-time market. Generally, the objective of a Real-time market (RTM) is system balancing and load following on a forward-looking basis above and beyond

the normal function of the Automatic Generation Control (AGC). The real time economic dispatch software normally runs every five-minute starting at approximately 7.5 minutes prior to the mid point of the next five-minute dispatch interval and produces a dispatch instruction for that dispatch interval.

Regulation. The real-time economic dispatch gives the dispatch results of each five-minute interval, during this five-minute timeframe, deviation from generation schedules is compensated with regulation, which is dispatched through AGC. The CAISO automatically dispatches regulation through AGC every four-seconds to meet moment-to-moment fluctuations in customer load demand and to correct for the unintended fluctuations in generation. This generating capacity under AGC is also referred to as regulating reserve, which is cleared in ancillary service market. The actual dispatch of regulating reserve is empirical rather than economic.

While the benefit of wind power integration is well understood in society as it has very low operating cost, reduces the emission of pollutants, and relieves dependence on foreign petroleum and gas (Thresher et al., 2007; Blatchfort, 2009), the increasing penetration of wind power is challenging for power system operations, including frequency control and transient stability (Lalor et al., 2005; Ericsen et al., 2005). In particular, the requirement of maintaining a continuous balance between the supply and demand of electricity and the fact that large scale of electricity storage is not practical greatly complicate the scheduling of power system in the presence of wind power. In fact, wind power fluctuations affect balancing operations in all time scales ranging from real-time control to day-ahead commitment.

In real-time operation, the minute-by-minute variability of wind power causes system imbalance and necessitates generators which could rapidly adjust their power output in responde to imbalances. The intermittency and limited accuracy of forecast wind power exacerbate this problem. As to hour-ahead dispatch, the unpredictability of wind power may cause more severe imbalance since the wind power forecast error is

greater with longer forecast horizon. In order to accommodate to a sudden shortage or increase in wind power, operators may need to start up additional units or shut down committed units, which leads to higher operating cost and wild fluctuations in electricity prices. In day-ahead scheduling, the traditional unit commitment (UC) program with deterministic spinning reserve requirements is inadequate due to the variability and limited predictability of wind power. As wind power cannot be predicted with great accuracy, additional spinning reserve needs to be carried to guarantee the operational reliability (Söder., 1993; Ummels et al., 2007). Therefore, new UC and ED methods capable of taking account of probabilistic characteristics of wind power need to be developed.

1.1.3 Reserve Requirements

Reserve is the most important resources for power system operators to respond to disturbances, such as sudden generation and transmission line outages and stochastic fluctuations in electricity demand. Generally, reserve can be classified into two categories: spinning and supplemental. Spinning reserve is provided by online generators, which can be deployed within a few seconds or minutes. It can not only follow the normal load variations through automatic generation control, but also respond to system contingencies so as to keep the system-wide power balance. Supplemental reserves sometimes are also called "replacement reserves", which can also be provided by generators that are not synchronized yet. The deployment of supplemental reserves permits the repositioning of generation levels such that the faster spinning reserve becomes available to respond to further disturbances.

Spinning reserve Requirements is the primary focus of this work because it directly and immediately responds to system imbalance and prevent load disconnections. While its availability has a significant value because it mitigates the considerable social and economic cost of occasional outages, the continuous provision of spinning reserve is costly since additional generating units must be committed and some units

have to be operated at less than optimal output. Thus, research on spinning reserve requirements has actual economic benefits.

Traditionally, power systems keep a fixed (deterministic) amount of spinning reserve available to compensate for the worst credible contingency, such as loss of the largest generator or the largest importing transmission facility (Wood and Woolenberg, 1996; Wood, 1982). These fixed amounts of spinning reserve requirements are developed for each power system and are tailored to achieve a desired level of risk in each power system. However, these deterministic spinning reserve requirements will be inadequate due to the variability and limited predictability of wind power.

1.1.4 Demand Response

Since the birth of power system, the prevailing paradigm of power system operations has been load-following: flexibility from generation side has been required to track demand, regardless of its patterns, locations, unpredictability and the stress that is imposed on the system. People have been so accustomed to the paradigm of having power at the flick of a switch that the extreme reliability of power system and the costly flexibility that are required to maintain it are usually overlooked. When renewable energy resources, such as wind and solar, are integrated, this paradigm becomes technically more difficult and potentially compromises the efficiency (Tan and Kirschen, 2006; Rahimi and Ipakchi, 2010; Baboli et al., 2011). Under such circumstances, a paradigm of mutual-following is called for in our energy consumption philosophy. In other words, we could also exploit the flexibility of demand side or demand response (DR) to accommodate the imbalance.

While large-scale wind power is integrated into power systems, operators cannot exclusively rely on adjustment and regulation from generation side since the flexibility of conventional generators is restricted by technical constraints, such as ramming rates and capacity limits. Under these circumstances, the flexibility in electricity

consumption becomes immediately important. In fact, a large proportion of the energy that people consume across the residential, commercial and industrial sector is dedicated to duties that can be postponed for certain amount of time with minimal impact on comfort. These kinds of consumption includes heating and cooling, washer and dryer, refrigeration, agricultural pumping, industrial production and, more interestingly, electric vehicle charging. Generally, these flexible energy consumption tasks can be described as requests for certain amount of energy over a given time horizon.

An ideal approach for exploiting the flexibility of demand would be the use of real-time pricing for consumers. However, this is not practical and is unlikely to occur in the immediate future due to both economical and political reasons. An alternative possible approach would be collecting the flexibility of demand through an aggregator or DRP which will participate in the energy and reserve market on behalf of small consumers (FERC, 2008). The DRP enrolls customers to participate in different DR programs and bids the aggregated responses in the energy and reserve markets. By this way, the flexibility of all customers, even small ones, can be made full use of. It should also be noted that customers can also participate solely in the DR programs if certain requirements, such as minimum curtailment level, can be satisfied.

In fact, the importance of DR has been recognized and in some cases, it is actually implemented for obtaining reliable and efficient electricity markets in several countries (Singh and Østergaard, 2010). DR can reduce the load at peak periods, which could reduce the under utilization of generators with marginal costs (Wight, 2006). In addition, DR can benefit individual customers by reducing their electricity charges through shifting consumption to lower price hours. Beside participation in energy markets, advances in control and communication technologies offer the possibility for DR to participate in reserve markets and provide contingency reserve during emergency conditions of the system by changing the normal consumption pattern (Wang et al., 2003). The additional scheduling flexibility introduced by DR facilitates more reliable and efficient power system operation, reduces transmission

line congestion and mitigates price manipulations and leads to significant gains in social welfare (Strbac and Kirschen, 1999; Earle, 2000; Kirschen et al., 2000).

1.1.5 Power System Reliability

Reliability of a power system refers to the probability of its satisfactory operation over the long run. It denotes the ability to supply adequate electric service on a nearly continuous basis, with few interruptions over an extended time period.

NERC (North American Electric Reliability Council) defines power system reliability as follows (Kundur et al., 2004):

> *Reliability, in a bulk power electric system, is the degree to which the performance of the elements of that system results in power being delivered to consumers within accepted standards and in the amount desired. The degree of reliability may be measured by the frequency, duration, and magnitude of adverse effects on consumer service.*

Reliability for a bulk power system are typically separated into two distinct, but related, functional areas:

Adequacy the ability of the power system to supply the aggregate electric power and energy requirements of the customer at all times, taking into account scheduled and unscheduled outages. of system components.

Security the ability of the power system to withstand sudden disturbances such as electric short circuits or non-anticipated loss of system components.

Adequacy and security are considered the basic inputs to the generation side of system reliability. In spite of distinct concepts, they are closely correlated. A system with adequate capacity can maintain enough security to reduce periods of involuntary load shedding.

In order to keep a power system reliable, the reliability of a power system should be evaluated by certain method. This is where reliability indices come in. The commonly

accepted quantitative indices of reliability assessment are Loss of Load Probability (LOLP) and Expect Energy Not Served (EENS). LOLP is defined as the likelihood (probability) that a system demand will exceed the generating capacity during a given period. It is often expressed as the fraction of the expected number of days out of a year in which peak load exceeds generation capacity. It should be noted that LOLP does not indicate the severity of load shedding incidents. Compared to LOLP, EENS is computationally intensive but indicates the extent that supply fails to meet the demand. Thus, this dissertation takes EENS as the reliability index.

1.2 Motivation

While the benefit of wind power integration is well understood in society, the essential characteristic of the wind energy exploitation is its intrinsic dependence on weather conditions. Consequently, the large scale integration of wind power into bulk power system introduces a new source of uncertainty in the power system operation and planning. As wind power cannot be predicted with great accuracy, additional spinning reserve needs to be carried to absorb unpredictable wind power fluctuations (Söder., 1993; Ummels et al., 2007). Therefore, developing new UC and ED methods capable of taking into account the probabilistic characteristics of wind power, load and generators to quantify the optimal amount of spinning reserve is of fundamental importance. In this dissertation, a tool for system operators to estimate optimal amount of spinning reserve within an electricity market framework is proposed.

As large-scale wind power is integrated in power system, the flexibility in electricity consumption becomes immediately important and necessary since adjustment and regulation from conventional generators is restricted by technical constraints, such as ramming rates and capacity limits. Under this circumstances, the system operator must provide mechanisms to encourage the market participation of flexible demand. Nevertheless, how to define the market products that flexible demand can offer so as to make the utmost of demand flexibility? In addition, how to incorporate DR into

the market clearing process to achieve the most efficient operation? These questions are challenging and will be investigated in this dissertation.

Although price responsive demand response has been widely accepted as important in the reliable and economic operation of the future grid, the response from demand can be highly uncertain due to a limited understanding of consumers' response to pricing signals. To model the behavior of consumers, the price elasticity of demand has been explored and utilized in both research and real practice (Rahimi and Ipakchi, 2010). Still, the price elasticity of demand is not precisely known and may vary greatly with operating conditions and types of customers. In addition, consumers may modify their demand as prices change without being centrally dispatched. To accommodate the uncertainty of demand response, alternative UC methods robust to the uncertainty of the demand response require investigation.

1.3 Dissertation Outline

The chapters of the dissertation are as follows:

Chapter 2 reviews the literature related to integration of wind power and demand response for ED and UC.

Chapter 3 develops an uncertainty model for forecast wind power. Based on this model, the reliability index expectation of demand not served (EDNS) is formulated. This index takes into account the uncertainties of wind speed, load forecast and generator availability. A probabilistic model is proposed in the hour-ahead economic dispatch by using EDNS as a reliability constraint. Based on the monotonic relationship between EDNS and total spinning reserve, an iterative optimization scheme is used to find the solution through adjusting total spinning reserve to satisfy a predefined EDNS value. The proposed probabilistic method can maintain a uniform system reliability level, i.e., the reliability index EDNS is uniform, for all dispatch intervals.

Chapter 4 proposes a probabilistic model for security-constrained unit commitment (SCUC) to determine the optimal spinning reserve required in the day-ahead market considering the integration of wind power generation. In particular, a new formulation of EENS which considers the probability distribution of forecast errors of wind and load, as well as outage replacement rate (ORR) of generators is formulated and integrated into the SCUC model.

Chapter 5 develops a full demand response model in which the DRP can bid into the energy and spinning reserve markets. The proposed full demand response model is incorporated into a co-optimized day-ahead energy and spinning reserve market. The market clearing problem is formulated as a two-stage stochastic SCUC and solved by MILP. The most economic solution with a probabilistic spinning reserve scheme is obtained by balancing the energy plus spinning reserve cost and the cost of EENS.

Chapter 6 introduces a robust UC model to minimize the generalized social cost taking into account the uncertainty in the price elasticity of demand. By optimizing the worst case scenario, the UC solution is robust against all possible realizations of the modeled uncertain demand response. Compared to a conventional UC with deterministic price elasticity of demand, the proposed robust model reduces the average Locational Marginal Prices (LMPs) as well as price volatility.

Chapter 7 summarizes the work in this dissertation and provides suggestions for future work.

1.4 Contributions

The main contributions of this dissertation are:

1. The formulation of probabilistic model of wind power forecast error, based on the wind speed forecast results is proposed. The dependence between two forecast errors within the same wind farm and that across wind farms are taken into account.

2. The reliability index EDNS is formulated by including the uncertainties of wind speed, load forecast and generator availability. A probabilistic ED model is proposed to address the amount of spinning reserve required for wind turbine integration in order to ensure a minimum reliability level. The monotonic relationship between EDNS and total spinning reserve is proved and an iterative optimization scheme is used to find the solution.

3. A new mixed integer linear formulation of EENS is proposed. The formulation incorporates the probability distribution of forecast errors of wind and demand. The proposed formulation can be applied to any form of probability distribution of wind power forecast error as long as it is continuous.

4. A new SCUC model, which integrates the stochastic wind forecast results into the day-ahead UC and extracts its value for system operation, is proposed. The model determines the amount of spinning reserve needed to minimize the total cost of operation, i.e., balancing energy cost, start-up cost, reserve cost and expected cost of load shedding.

5. A full demand response model in which DRP can bid both in the energy and spinning reserve markets is proposed. The proposed full demand response model can exploit more flexibility from demand than other models in the literature.

6. The proposed full demand response model is incorporated into a co-optimized day-ahead energy and spinning reserve market in which the expected net cost under any credible system state, i.e., expected total cost of operation minus total benefit of demand, is minimized. The market clearing problem is formulated as a two-stage stochastic SCUC and solved by MILP.

7. A new robust UC model is developed to take into account uncertain price elasticity of demand and minimize the generalized social cost, which consists of generation cost, and opportunity cost of reduced demand or the alternative cost of electricity consumption.

Chapter 2

Literature Review

Literatures related to quantifying spinning reserve, ED and UC and incorporating demand response into market will be reviewed and summarized in this chapter.

2.1 Quantifying Spinning Reserve

This section reviews the various formulations that have been developed to produce optimal and secure generation schedules. The aim of all these methods is to determine the commitment and dispatch of a set of generating units to supply the forecast load over a short-term horizon (usually one day to one week). These methods differ in their objective function and the formulation of the constraint responsible for guaranteeing the provision of spinning reserve.

2.1.1 Direct Enforcement of Spinning Reserve Constraint

Currently in practice, there are two basic methods of quantifying required spinning reserve: deterministic and probabilistic. The deterministic method typically sets the quantity of spinning reserve as the capacity of the largest generator or some fraction of the peak load of the system (Wood and Woolenberg, 1996; Wood, 1982). By this

method, the system is able to continue operation without load shedding when any single unit is lost.

The conventional UC formulation falls in this category. The objective function considers only the sum of the running and startup costs of all units over all periods of the scheduling horizon.

$$\min_{P_{it},u_{it}} \{\sum_{t=1}^{NT} \sum_{i=1}^{NG} [C_i(P_{it}, u_{it}) + S_i(u_{it})]\} \tag{2.1}$$

This objective function must be minimized subject to a number of constraints, the most concerned one of which is clearly that at least the specified amount of spinning reserve during each period is provided.

$$\sum_{i=1}^{NG} R_{it} \geq R_t^{min} \qquad \forall t \tag{2.2}$$

Besides the spinning reserve enforcement, each generating unit is subject to its own operating constraints, which include minimum and maximum production levels, minimum up- and down-time constraints, and maximum ramp-up and ramp-down constraints. Last but not least, the total generation must match the system demand for each interval.

The deterministic spinning reserve requirements are developed specifically for each system, and thus the acceptable level of reliability varies from system to system, as well as the spinning reserve requirements. Those requirements of different systems are shown as in Table 2.1, where Union for the Co-ordination of Transmission of Electricity (UCTE) is the association of transmission system operators in continental Europe and p_d^{max} is the system peak demand.

The deterministic approach has served the industry reasonably well in the past. It has resulted in high security levels and the study effort is minimized. However, no distinction of system size is taken into consideration. This is because each requirement is developed specifically for each system, and while a given requirement would procure

Table 2.1: Spinning reserve requirements in different power systems

System	Requirement (R_t^{min})
Australia and New Zealand	$max(u_{it}P_{it})$
BC Hydro	$max(u_{it}P_i^{max})$
Belgium	UCTE rules, currently at least 460 MW
California	$50\% \times max\left(5\% \times P_{hydro} + 7\% \times P_{other},\ P_{largest\,contigency}\right)$ $+P_{non-firm\,import}$
France	UCTE rules, currently at least 500 MW
Manitoba Hydro	$80\% max\left(u_{it}P_i^{max}\right) + 20\% \left(\sum_{i=1}^{NG} P_i^{max}\right)$
PJM (Southern)	$max(u_{it}P_i^{max})$
PJM (Western)	$1.5\% p_d^{max}$
PJM (Other)	$1.5\% p_d^{max}$+probabilistic calculation on typical days and hours
Spain	The recommended maximum is: $\left(10p_{d,zone}^{max} + 150^2\right)^{1/2} - 150$
The Netherlalnds	UCTE rules, currently at least 300 MW
UCTE	The recommended maximum is: $\left(10p_{d,zone}^{max} + 150^2\right)^{1/2} - 150$
Yukon Electrical	$max(u_{it}P_i^{max}) + 10\% p_d^{max}$

a reasonable amount of spinning reserve in one system, it might result in excessive or insufficient spinning reserve if applied to different systems. In addition, this deterministic method neither guarantees uniform reliability nor does it consider load forecast error or forced outage rates (FOR) of the different generators. For example, this method may be conservative when the largest generator has a very low FOR, while exposing the system to high risk at the other extreme.

2.1.2 Enforcement of the Spinning Reserve Constraint Using Reliability Indices

Compared to deterministic method, the probabilistic method takes load forecast error and FOR of generators into consideration by satisfying some reliability indices, such as loss of load probability (LOLP) and/or expected energy not served (EENS).

Numerous approaches have been developed to incorporate probabilistic reserve criteria in the formulation of UC and ED. In Anstine et al. (1963), the commitment risks of generators are used to determine the spinning reserve in unit commitment for the first time. In Söder. (1993), the conventional hydro-thermal model is extended to take into account load and wind speed forecast errors. The reserve levels are determined by setting the possibility of unacceptable frequency deviations due to load and wind speed fluctuations. Bouffard and Galiana (2004) address the problem of reliability-constrained market-clearing in pool-based electricity markets with unit commitment. In general, probabilistic reliability criteria that implicitly set the reserve requirement are defined by LOLP and EENS. Specifically, they impose an upper bound on LOLP and EENS and incorporate them into the UC program to ensure the reliability of system. However, the optimal reliability index or upper bound is another decision hard to make.

$$LOLP_t \leq LOLP^{\max} \qquad \forall t \tag{2.3}$$

$$EENS_t \leq EENS^{\max} \qquad \forall t \tag{2.4}$$

2.1.3 Spinning Reserve Optimization

To the dilemma mentioned above, the question of how much spinning reserve should be provided arises. Intuitively, it can be said that as the amount of spinning reserve provided increases, the system risk reduces; then by maximizing the spinning reserve procurement, the system risk is minimized. However, the spinning reserve comes at a cost, which ideally should be kept at its minimum and the operating cost is reduced. On the other hand, if a small amount of spinning reserve is provided, the operating cost of system decreases but the expected cost of outages increases. Between these two extremes an optimum exists (i.e. a point at which the operating cost plus the expected cost of outages is minimized) as shown in Figure 2.1.

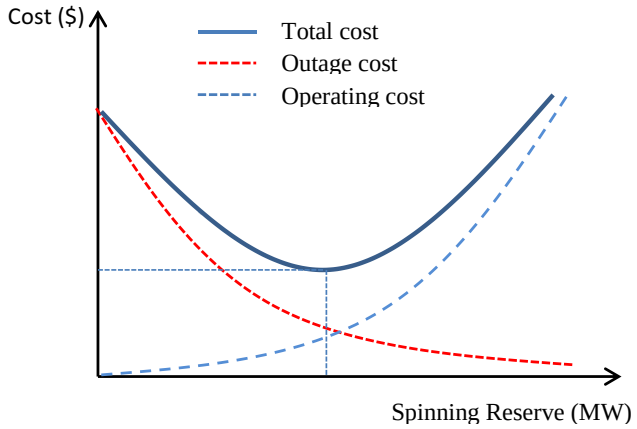

Figure 2.1: Cost as a function of spinning reserve procurement

Gooi et al. (1999) integrate a probabilistic reliability assessment with the traditional reserve constrained unit commitment function. Reliability of individual units and load forecast error are considered for scheduling. The generation can then be scheduled to meet a given risk index, which should be selected on the basis of a tradeoff between the total schedule cost obtained from the UC solution and the expected cost of EENS which ran be derived from the probabilistic reserve requirement. In Wu and Gooi (1999), the ramp constraints of generators are taken into account. Nevertheless, this approach is computationally intensive because iterative unit commitment is performed to determine the optimal risk.

In Ortega-Vazquez and Kirschen (2007), the scheduling of reserves is performed in two steps. First, the amount of spinning reserve that minimizes the sum of total schedule cost and the expected cost of EENS is calculated for every period of the scheduling horizon taken separately as in (2.5). This calculation takes into account the load as well as the cost and reliability characteristics of the available units. Second, these hourly spinning reserve requirements are used as input to a traditional reserve-constrained UC program that produces a generation schedule that takes into account

all the standard constraints and the inter-temporal constraints and couplings.

$$\min_{P_{it},u_{it},R_{it}} \{\sum_{t=1}^{NT}\sum_{i=1}^{NG}[C_i(P_{it},u_{it}) + S_i(u_{it}) + VOLL_t \cdot EENS_t]\} \tag{2.5}$$

Compared to Gooi et al. (1999), This approach has the advantage of being self-contained in the sense that it does not require a LOLP or EENS target because the spinning reserve provision is based on an internal cost/benefit analysis. Nevertheless, this method cannot guarantee the optimal schedule since the UC result in step two may be different from that in step one due to the forced decomposition in this step.

2.1.4 Quantifying Spinning Reserve with Integration of Wind Power

In recent years, quantifying spinning reserve faces new challenges due to the rapid growth of wind power penetration. Wind generation has been used to replace conventional power technologies in many countries recently due to increasing prices of fossil fuels, environmental impacts and energy security concerns. However, the output of a wind turbine generator varies with wind speed that can be predicted with only limited accuracy. Spinning reserve is the additional generating capacity available by increasing power output of generators already connected to the power system. This reserve is needed to protect the system against unexpected events such as generator outages, unforeseen load changes and so on. The uncertainty of wind power output must be taken into account when quantifying the spinning reserve.

A common and straightforward solution for variability and limited predictability of wind power is to commit more reserve from conventional generation units. Doherty and O'Malley (2005) use the number of load sheds per year as the reliability criterion to quantify the spinning reserve in a system with large wind power penetration. The net load forecast error is modeled as a normal distribution, but this criterion does not consider the extent that supply fails to meet the demand. Bouffard and

Galiana (2008) formulate a short-term forward electricity market-clearing problem with stochastic security capable of accounting for non-dispatchable and variable wind power generation sources. The normal distribution of net load forecast error is discretized. In addition, a scenario tree is introduced to simulate the intra-period transitions. Ortega-Vazquez and Kirschen (2009) proposed to estimate the spinning reserve requirements considering wind power generation and load forecast errors as well as the possible contingencies that might arise for a given commitment prior to the day-ahead scheduling. A UC program then performs the scheduling enforcing the traditional spinning reserve constraint based on the previously computed optimal spinning reserve requirements. The Gaussian distribution of net demand forecast error is approximated by seven intervals and a capacity outage probability table (COPT) is used to calculate the EENS of system (Billinton and Allan, 1996).

In Wang et al. (2008), adequacy of flexibility is used to guarantee the security of system in case of wind power volatility. Benders cuts are created and added to the master UC to revise the commitment solution for iterations with violations. Another stochastic optimization scheduling model considering wind power production as stochastic input is presented in Meibom et al. (2011), which makes use of a scenario tree tool to commit the scenario reduction and reschedules based on the most up-to-date forecast information. Wang and Gooi (2011) proposed a method for estimating spinning reserve requirement in microgrids considering uncertainties caused by load and non-dispatchable units, such as wind turbines (WTs) and photovoltaics (PVs). Various uncertainties are discretized then combined into an aggregated uncertainty distribution. In addition, an iterative method is proposed to take into account multiple generator failures.

In general, these methods fall in the category of stochastic optimization which is suitable for solving UC in systems with high wind power penetration in form. However, a large number of scenarios trigger the curse of dimensionality. Even with the scenario reduction technique, the computation efficiency of stochastic

optimization is still low. In fact, the computational complexity is the main obstacle to its application in real systems scheduling.

2.2 Unit Commitment and Economic Dispatch

Quantifying spinning reserve cannot be done without unit commitment (UC) and economic dispatch (ED) results. Spinning reserve level and its allocation is closely related to the combination of units and their outputs. In many systems, energy market and reserve market are actually co-optimized and cleared simultaneously. Ignoring the coupling that exists between the energy and the reserve scheduling can lead to suboptimal or infeasible results. Due to this reason, quantifying spinning reserve can be seen as solving UC or ED problem with spinning reserve in consideration.

The UC problem is the problem of scheduling generation for the following day in order to meet forecast demand in the system while considering numerous operating constraints on generators and the transmission network. It is a mixed integer linear program which is solved by system operators daily in order to both operate the system but also for the purpose of clearing the market. Once the schedules of slow-responding resources are fixed according to their day-ahead schedule, and as the actual operating interval approaches, the ED problem is solved. It is a continuous convex problem and can be solved efficiently by various nonlinear programming techniques. The purpose of economic dispatch is to adjust fast-responding resources to the prevailing system conditions which are inevitably different from what was forecast in the day-ahead time frame.

2.2.1 Unit Commitment

The formulation of unit commitment problem follows Baldick (1995).

$$\min_{P_{it},u_{it},R_{it}} \{\sum_{t=1}^{NT}\sum_{i=1}^{NG}[C_i(P_{it},u_{it}) + S_i(u_{it}) + q_{it}R_{it}]\} \tag{2.6}$$

$$\sum_{i=1}^{NG} P_{it} = \sum_{j=1}^{ND} D_{jt} \qquad \forall t \tag{2.7}$$

$$P_i^{min} u_{it} \leq P_{it} \leq P_i^{max} u_{it} \qquad \forall i, \forall t \tag{2.8}$$

$$P_{it} + R_{it} \leq P_i^{max} \qquad \forall i, \forall t \tag{2.9}$$

$$0 \leq R_{it} \leq u_{it}(RU_i \tau) \qquad \forall i, \forall t \tag{2.10}$$

$$\sum_{i=1}^{NG} R_{it} \geq R_t^{min} \qquad \forall t \tag{2.11}$$

$$P_{it} - P_{i,t-1} \leq RU_i u_{i,t-1} + R_i^{start}(u_{it} - u_{i,t-1}) \qquad \forall i, \forall t \tag{2.12}$$

$$P_{it} - P_{i,t-1} \geq -RD_i u_{it} - R_i^{shut}(u_{i,t-1} - u_{it}) \qquad \forall i, \forall t \tag{2.13}$$

$$R_i^{start} = \max RU_i, P_i^{min} \qquad \forall i \tag{2.14}$$

$$R_i^{shut} = \max RD_i, P_i^{min} \qquad \forall i \tag{2.15}$$

$$\sum_{i=1}^{NG} GSF_{ki} P_{it} - \sum_{j=1}^{ND} GSF_{kj} D_{jt} \leq F_k^{max} \qquad \forall k, \forall t \tag{2.16}$$

The objective of unit commitment problem is to minimize the system operating cost, which consists of fuel cost, start-up cost and reserve cost. The constraint (2.7) ensures the balance between supply and demand. The generation capacity constraints (2.8) and (2.9) limit the amount of power and reserves that can be supplied by a generator. The constraint (2.10) limits the maximum spinning reserve from a generator. The constraint (2.11) requires at least certain amount of spinning reserve is provided. (2.12) and (2.13) are the constraints of ramping rates of generators. It should be noted that the trajectories of generators' start-up and shut-down process are neglected in this model. Constraint (2.12) ensures that the increment in the output power ($\triangle P_{it} = P_{it} - P_{i,t-1}$) cannot be greater than the ramp limits of the generator, or if it is starting-up to its minimum stable generation. The ramp down constraint (2.13) is formulated in an equivalent way. The transmission flow limits are

simulated using DC power flow in (2.16). The minimum up/down time constraints are imposed through binary variable u_{it} (see Appendix B).

Solution techniques for the unit commitment problem have evolved over time. Simple priority rules were used originally, as discussed by Wood and Woolenberg (1996). Due to the fact that there is a loose coupling of generator operations via (2.7), one of the earliest approaches for improving the solution of the unit commitment problem was Lagrangian relaxation, which is described by Muckstadt and Koenig (1977). Lagrangian relaxation was thereafter widely adopted by system operators in actual operations. Recently, advances in mixed integer programming have led to the gradual replacement of Lagrangian decomposition algorithms by branch and bound techniques for solving the unit commitment problem, as discussed by Carrión and Arroyo (2006).

Recently, various studies have utilized two stage stochastic unit commitment models for assessing the impacts of renewable energy integration (Bouffard and Galiana, 2008; Wang et al., 2008; Meibom et al., 2011; Morales et al., 2009). Firstly, a large scenario set is generated by Monte Carlo method or Autoregressive Moving Average (ARMA) model. Then, scenario reduction method may be used to reduce the scenario set (Dupačŏvá et al., 2003). A stochastic optimization model with recourse is used to model the problem. Finally, the model is solved by MILP or Benders' decomposition. However, it still cannot be used in real systems scheduling due to computational complexity.

A two-stage adaptive robust unit commitment model for the security constrained unit commitment problem in the presence of nodal net injection uncertainty is proposed recently (Bertsimas et al., 2013). Compared to the stochastic programming approach, the proposed model is more practical in that it only requires a deterministic uncertainty set, rather than a probability distribution on the uncertain data. The unit commitment solutions of the this model are robust against all possible realizations of the modeled uncertainty.

2.2.2 Economic Dispatch

The formulation of economic dispatch problem follows Han et al. (2001).

$$\min_{P_{it},R_{it}} \{\sum_{t=1}^{NT}\sum_{i=1}^{NG}[C_i(P_{it}) + q_{it}R_{it}]\} \tag{2.17}$$

$$\sum_{i=1}^{NG} P_{it} = \sum_{j=1}^{ND} D_{jt} \qquad \forall t \tag{2.18}$$

$$P_i^{min} \leq P_{it} \leq P_i^{max} \qquad \forall i, \forall t \tag{2.19}$$

$$P_{it} + R_{it} \leq P_i^{max} \qquad \forall i, \forall t \tag{2.20}$$

$$0 \leq R_{it} \leq RU_i\tau \qquad \forall i, \forall t \tag{2.21}$$

$$\sum_{i=1}^{NG} R_{it} \geq R_t^{min} \qquad \forall t \tag{2.22}$$

$$-RD_i \triangle t \leq P_{it} - P_{i,t-1} \leq RU_i \triangle t \qquad \forall i, \forall t \tag{2.23}$$

$$\sum_{i=1}^{NG} GSF_{ki}P_{it} - \sum_{j=1}^{ND} GSF_{kj}D_{jt} \leq F_k^{max} \qquad \forall k, \forall t \tag{2.24}$$

Compared to UC, Economic dispatch (ED) is to determine optimal dispatch of a set of committed generating units to supply the forecast load over a shorter time horizon (usually 10 minutes to several hours). The objective function is to minimize the operating cost of generators. The constraint (2.18) ensures the balance between supply and demand. The generation capacity constraints (2.19) and (2.20) limit the amount of power and reserves that can be supplied by a generator. The constraint (2.21) limits the maximum spinning reserve from a generator. The constraint (2.22) requires at least certain amount of spinning reserve is provided. Constraint (2.23) is the constraints of ramping rates of generators. The transmission flow limits are simulated using DC power flow in (2.24).

ED is a continuous convex problem and can be solved efficiently by various nonlinear programming techniques. Traditionally and practically, quadratic programming are widely used by system operators.

2.3 Incorporating Demand Response into Market

Considerable efforts have been devoted to incorporate demand response into the market clearing process to achieve the most efficient dynamics in the past decades. In Wang et al. (2003), a market model in which generators and consumers can submit offers and bids on both energy and reserve are proposed, but the network and multi-period constraints are neglected. In addition, the reserve constraint is deterministic in this model. A probabilistic reserve model with demand-side participation is proposed in Bai et al. (2008). In this model, demand is able to submit bids of load reduction in energy market and load shedding upon request through the reserve market. In Singh et al. (2011) the price responsive demand shifting bidding of consumers is introduced in a day-ahead market with network constraints. The ACOPF model is used in the formulation without considering the unit commitment. The demand response modeled with inter-temporal characteristics is incorporated into SCUC for economic and security purposes in Khodaei et al. (2011). However, demand response is modeled as shiftable load and only participates in energy market in Singh et al. (2011); Khodaei et al. (2011). In Parvania and Fotuhi-Firuzabad (2010), a short-term stochastic SCUC model that simultaneously schedules generators energy and spinning reserve and also reserve from DRPs is proposed. A mixed integer representation of reserve provided by DRPs and its associated cost function are used in the proposed two-stage stochastic mixed integer programming formulation. In Karangelos and Bouffard (2012), the demand recovery effect after deployment of spinning reserve from DR is further considered. It should be noted that DRPs only participate in spinning reserve market in Parvania and Fotuhi-Firuzabad (2010); Karangelos and Bouffard (2012).

In the above literature, demand response is modeled as a deterministic price-elastic demand curve. However, the actual price-elastic demand curve is uncertain and variable in time. In addition, consumers may modify their demand as prices change without being centrally dispatched. Therefore, power system scheduling, particularly UC, needs to be robust against the uncertainty in demand price elasticity. In Wang et al. (2013), a scenario set of demand price elasticities is proposed to represent the stochastic DR, i.e., customers have different responses to the electricity prices in different scenarios, but the probability distribution of these demand elasticities is difficult to identify. In Zhao et al. (2013) and Zhao and Zeng (2012), the price elasticity of demand is assumed to be varying within a given range. A robust UC approach is proposed to maximize the social welfare under the worst case joint wind power output and price-elastic demand curve scenario. This method allowing for increased demand elasticity results in a paradoxical apparent reduction of the total social welfare, i.e., the worst case is the scenario with the highest price elasticity of demand (Wolfgang and Doorman, 2011). In fact, the worst case should be when the price elasticity of demand is over-estimated and the real price elasticity of demand is much lower. In this case, the generation capacity is insufficient and electricity price spikes may appear.

Chapter 3

Hour-ahead Economic Dispatch Considering Wind Power

In this chapter, we propose a probabilistic economic dispatch (ED) model to maintain a uniform system reliability level based on expectation of demand not served (EDNS) in each dispatch interval. The model of wind power, net demand and generators are presented in Section 3.1. Then, the reliability index EDNS is formulated in Section 3.2. It takes account of the uncertainties of wind speed, load forecast and availability of generators. In Section 3.3, a probabilistic hour-ahead economic dispatch model is proposed using EDNS as a reliability constraint. Based on the monotonic relationship between EDNS and total spinning reserve, an iterative optimization scheme is used to find the solution through adjusting total spinning reserve to satisfy a predefined EDNS value. In Section 3.4, the proposed model is applied to the IEEE Reliability Test System. The results show the validity of the model and the relationships of various uncertainties with the system spinning reserve levels. Finally, Section 3.5 summarizes the work and presents conclusions.

The main content in this chapter can also be found in Liu and Tomsovic (2012a).

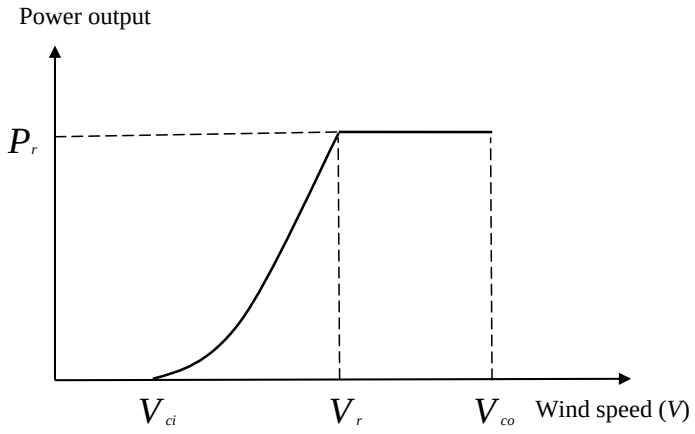

Figure 3.1: A typical input-output curve of a wind turbine

3.1 Model of Wind Power, Net Demand and Generators

3.1.1 Wind Power Forecast Error

The power output of a wind turbine generator depends on both the wind speed and its input-output characteristic. The wind turbine generator begins to produce electrical energy at a wind speed called cut-in speed and reaches the rated output at rated speed. The electrical output is maintained constant at the rated value for further increase in wind speed up to the cut-out speed, beyond which the unit is shut down for security reasons. Between the cut-in and rated speed, the relationship between the electrical output and wind speed is nonlinear, due to the combined effects of aero-turbine and generator characteristics. A typical input-output curve of a wind turbine is shown in Fig. 3.1, where P_r is the rated power output, V_{ci} is the cut-in wind speed, V_r is the rated wind speed and V_{co} is the cut-out wind speed (Billinton and Chowdhury, 1992).

A wind speed forecast can provide expected wind speed and estimated standard deviation of forecast error, which can be modeled as a Gaussian distribution with

mean zero (Söder., 1993). With the input-output characteristic of a wind turbine, the probability distribution of wind power from each turbine can be obtained. Consequently, we can obtain the expectation and standard deviation of total wind power forecast error. Due to the nonlinear input-output relationship of a wind turbine, the probability distribution of wind power forecast error from individual wind turbine is not Gaussian. Researchers have shown that the wind power forecast error of individual turbine follows β distribution (Fabbri et al., 2005). Still, the large number and geographical dispersion of wind turbines permit the invocation of Central Limit theorem (Papoulis and Pillai, 2002) to justify the assumption of Gaussian distribution of the total wind power forecast error.

Consider a power system with NM wind farms and n_r wind turbines in wind farm r. $P^w_{i,r,t}$ is a random variable of power output of wind turbine i in wind farm r at time t with expectation $E\left(P^w_{i,r,t}\right)$ and standard deviation $\sigma^w_{i,r,t}$. The wind power forecast error of this turbine is

$$e^w_{i,r,t} = P^w_{i,r,t} - E\left(P^w_{i,r,t}\right) \tag{3.1}$$

The total wind power forecast error is the sum of errors from each individual wind turbine: $e^w_t = \sum_{r=1}^{NM}\sum_{i=1}^{n_r} e^w_{i,r,t}$. Given the assumption above, e^w_t has Gaussian distribution with expectation $E\left(e^w_t\right)$ and standard deviation $\sigma^w_t = \sigma\left(e^w_t\right)$, which we will calculate as

$$\begin{aligned} E\left(e^w_t\right) &= E\left(\sum_{r=1}^{NM}\sum_{i=1}^{n_r} e^w_{i,r,t}\right) \\ &= \sum_{r=1}^{NM}\sum_{i=1}^{n_r}\left(E\left(P^w_{i,r,t}\right) - E\left(P^w_{i,r,t}\right)\right) \\ &= 0 \end{aligned} \tag{3.2}$$

and

$$\begin{aligned}
\left(\sigma_t^w\right)^2 &= E\left(\left(e_t^w\right)^2\right) - E^2\left(e_t^w\right) \\
&= E\left(\left(\sum_{r=1}^{NM}\sum_{i=1}^{n_r} P_{i,r,t}^w - \sum_{r=1}^{NM}\sum_{i=1}^{n_r} E\left(P_{i,r,t}^w\right)\right)^2\right) \\
&= E\left(\left(P_t^w\right)^2\right) - \left(\sum_{r=1}^{NM}\sum_{i=1}^{n_r} E\left(P_{i,r,t}^w\right)\right)^2 \qquad (3.3)
\end{aligned}$$

where $E\left(\left(P_t^w\right)^2\right) = E\left(\left(\sum_{r=1}^{NM}\sum_{i=1}^{n_r} P_{i,r,t}^w\right)^2\right)$ is the second moment of total wind power output.

Given the probability distribution of forecast wind power for each wind turbine with corresponding expectation and standard deviation, the dependence between two forecast errors within the same wind farm r can be modeled with correlation coefficient ρ_{rr}. Across wind farms q and r dependence can be modeled with correlation coefficient ρ_{qr}. In some cases $\rho_{qr} = 0$ or is small, because the wind farms are far away geographically. In the case two wind farms are not greatly separated, then $\rho_{qr} \neq 0$. We can obtain the second moment of total forecast wind power as

$$\begin{aligned}
E\left(\left(P_t^w\right)^2\right) &= \sum_{i\in I_w} E\left(\left(P_{i,t}^w\right)^2\right) + \sum_{i\in I_w}\sum_{j\in I_w, j\neq i} E\left(P_{i,t}^w P_{j,t}^w\right) \\
&= \sum_{r=1}^{NM}\sum_{i=1}^{n_r} E\left(\left(P_{i,r,t}^w\right)^2\right) + 2\sum_{r=1}^{NM}\sum_{i=1}^{n_r}\sum_{j=i+1}^{n_r}\left(\rho_{rr}\sigma_{i,r,t}^w\sigma_{j,r,t}^w + E\left(P_{i,r,t}^w\right)E\left(P_{j,r,t}^w\right)\right) \\
&\quad +2\sum_{r=1}^{NM}\sum_{q=r+1}^{NM} 2\sum_{i=1}^{n_r}\sum_{j=i+1}^{n_q}\left(\rho_{rq}\sigma_{i,r,t}^w\sigma_{j,q,t}^w + E\left(P_{i,r,t}^w\right)E\left(P_{j,r,t}^w\right)\right) \qquad (3.4)
\end{aligned}$$

where I_w is the set of all wind turbines and $E\left(\left(P_{i,r,t}^w\right)^2\right)$ is the second moment of the forecast wind power of turbine i in wind farm r during period t. Thus, we have the mean and standard deviation of total wind power forecast error based on wind speed forecast.

3.1.2 Net Demand Forecast Error

The load could be modeled as forecast load plus a Gaussian distributed error, which has expectation zero and standard deviation σ_t^l (Söder., 1993; Bouffard and Galiana, 2008; Ortega-Vazquez and Kirschen, 2009). The net demand D_t is defined as the system load minus the total wind power and needs to be balanced by other generators in the system. In this case, we assume the load forecast and wind forecast errors are uncorrelated, so the forecast error of net demand e_t^d is the sum of the load forecast error and wind power forecast error. This follows Gaussian distribution with expectation zero and standard deviation as:

$$\sigma_t^d = \sqrt{\left(\sigma_t^l\right)^2 + \left(\sigma_t^w\right)^2} \tag{3.5}$$

3.1.3 Generator Reliability Model

A two-state Markov model used in this dissertation is shown in Fig. 3.2 such that both failure and repair times are exponentially distributed with parameters λ_i and μ_i, respectively (Billinton and Allan, 1996). The time dependent unavailability and availability of unit i can be calculated respectively as

$$U_i\left(T\right) = \frac{\lambda_i}{\lambda_i + \mu_i}\left(1 - e^{-(\lambda_i + \mu_i)T}\right) \tag{3.6}$$

$$A_i\left(T\right) = 1 - U_i(T) \tag{3.7}$$

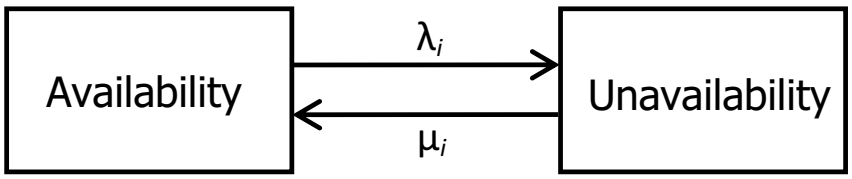

Figure 3.2: A two-state model of generator

For generators, the system lead time T is relatively short such that a failed unit cannot be repaired or replaced within this short period, i.e., μ_i can be neglected. Under this assumption, the unavailability and availability of unit i can be further simplified to:

$$U_i(T) = 1 - e^{-\lambda_i T} \approx \lambda_i T = ORR_i \tag{3.8}$$

$$A_i(T) = 1 - U_i(T) = 1 - ORR_i \tag{3.9}$$

3.2 Formulation of EDNS

The EDNS is the expected load shedding when the net demand forecast error plus the outputs of unavailable generators is larger than the available spinning reserve. For every scenario of generator outages, the EDNS is calculated by a partial expectation. Then, the summation of them weighted by the corresponding probability is the EDNS of the system.

$$EDNS_t = \sum_{\omega=0}^{NW} EDNS_{\omega t}\pi_\omega \tag{3.10}$$

where $EDNS_{\omega t}$ is the EDNS of scenario ω during time interval t, and π_ω is the probability of scenario ω and can be calculated using the outage replacement rates (ORR) of generators.

Since the net demand forecast error e_t^d is modeled as Gaussian distribution with mean zero and standard deviation σ_t^d, $EDNS_{\omega t}$ can be expressed as in (3.11).

$$\begin{aligned} EDNS_{\omega t} &= E\left(e_t^d - \sum_{i\in A_\omega} R_{it} + \sum_{m\in U_\omega} P_{mt} \mid e_t^d > \sum_{i\in A_\omega} R_{it} - \sum_{m\in U_\omega} P_{mt}\right) \\ &\quad \times P\left(e_t^d > \sum_{i\in A_\omega} R_{it} - \sum_{m\in U_\omega} P_{mt}\right) \\ &= \frac{\sigma_t^d}{\sqrt{2\pi}} e^{-\frac{\left(\sum_{i\in A_\omega} R_{it} - \sum_{m\in U_\omega} P_{mt}\right)^2}{2\left(\sigma_t^d\right)^2}} \\ &\quad - \left(\sum_{i\in A_\omega} R_{it} - \sum_{m\in U_\omega} P_{mt}\right)\left(1 - \Phi\left(\frac{\sum_{i\in A_\omega} R_{it} - \sum_{m\in U_\omega} P_{mt}}{\sigma_t^d}\right)\right) \end{aligned} \tag{3.11}$$

where A_ω is the set of available units, U_ω is the set of unavailable units, R_{it} is the spinning reserve of generator i during time interval t, P_{mt} is the power output of generator m during time interval t, and $\Phi(\cdot)$ is the cumulative distribution function of standard Gaussian distribution. The EDNS of the system is the sum of EDNS in all scenarios multiplied by the corresponding probabilities as in (3.10).

3.3 Probabilistic Economic Dispatch Model

The model pursues an optimal solution for conventional power generators with predefined reliability standard $EDNS^{\max}$. The objective function is formulated as:

$$\min_{P_{it},R_{it}} \sum_{t=1}^{NT} \sum_{i=1}^{NG} \left[C_i\left(P_{it}\right) + q_{it} R_{it}\right] \tag{3.12}$$

where NT is the number of time intervals, NG is the number of committed generators, C_i is the cost function of energy for generator i, and q_{it} is the cost of spinning reserve for generator i. The objective function is subject to the following constraints:

1. Balance of energy

$$\sum_{i=1}^{NG} P_{it} = D_t \qquad \forall t \tag{3.13}$$

2. Output limits of generators

$$P_i^{\min} \leq P_{it} \leq P_i^{\max} \qquad \forall i, \forall t \tag{3.14}$$

$$P_{it} + R_{it} \leq P_i^{\max} \qquad \forall i, \forall t \tag{3.15}$$

3. Spinning reserve limits of generators

$$0 \leq R_{it} \leq R_i^{\max} \qquad \forall i, \forall t \tag{3.16}$$

4. Ramping rates of generators

$$-RD_i \Delta t \leq P_{it} - P_{i,t-1} \leq RU_i \Delta t \qquad \forall i, \forall t \tag{3.17}$$

   where RU_i is the maximum ramping up rate of generator i, RD_i is the maximum ramping down rate of generator i and Δt is the time duration of each interval.

5. Reliability constraint

$$\sum_{\omega=0}^{NW} EDNS_{\omega t} \pi_\omega \leq EDNS^{\max} \qquad \forall t \tag{3.18}$$

In the optimization above, EDNS is explicitly expressed by the spinning reserves and power outputs of generators. Unfortunately with this constraint, computations will be complex, especially when multiple generator outages are considered. Nevertheless, given the same committed units and net demand forecast error, the relationship between EDNS and total system spinning reserve SR is monotonic (see Appendix A). That means, for each EDNS value, there is a unique value of corresponding SR. Thus, the results of optimization with EDNS as a constraint is equivalent to that

with corresponding SR as a constraint. That is:

$$\sum_{i=1}^{NG} R_{it} = SR_t \qquad \forall t \tag{3.19}$$

An iterative optimization scheme (Xia et al., 2005) is used to solve this modified model as shown in Fig. 3.3. The preset reliability index $EDNS^{\max}$ is achieved by iterative quadratic programming. To begin, we need to set lower and upper bounds for the spinning reserve. Then, binary search is used here to reduce the gap between the lower and upper bounds by updating the value of lower or upper bounds after each iteration. This is repeated till convergence.

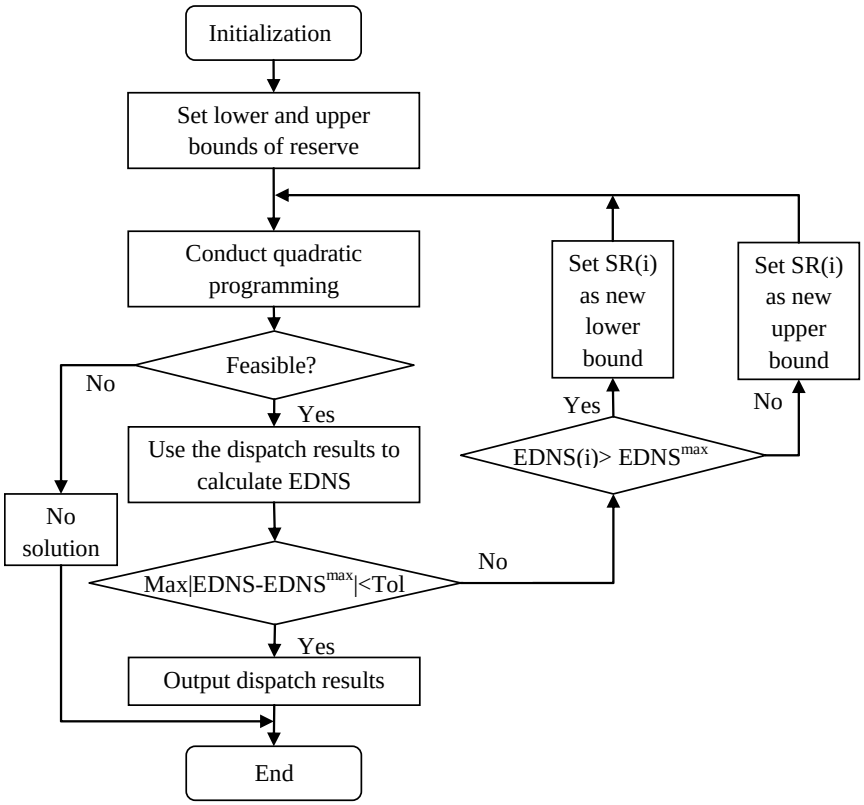

Figure 3.3: Iterative optimization scheme

Table 3.1: Forecast net demand

Interval	1	2	3	4	5	6
Load (MW)	2830.7	2858.6	2893.0	2942.8	2999.5	2927.4

Compared to the economic dispatch model with EDNS as a constraint, the proposed iterative optimization has two advantages. First of all, the formulation of EDNS is very complicated as shown in equation 3.11. With this complicated constraint, the economic dispatch model with EDNS as constraint is cumbersome, while the proposed iterative optimization perfectly preserves the traditional economic dispatch model with direct enforcement of spinning reserve as shown in 2.1.1, which has been successfully used in power industry for many years. In addition, the computational time of economic dispatch with EDNS as a constraint is much longer than the proposed iterative optimization, because, with EDNS as a constraint, the partial derivative of EDNS to the each optimization variable (P_{it} or R_{it}) needs to be calculated for every iteration inside the "quadprog" function, while for the proposed iterative optimization this trouble is avoided.

3.4 Case Study

In this section, the proposed probabilistic model is tested on the IEEE Reliability Test System (Grigg et al., 1999). For simplicity, we assume that all units offer reserve at rate q_i equal to 10% of their highest incremental cost of producing energy (Bouffard and Galiana, 2004). Since the economic dispatch of system under peak load is more challenging, we use the peak load 2999.5 MW as the load of the 5th time interval. The load forecast error is Gaussian distribution with mean 0 and standard deviation 1% (Söder., 1993). The forecast net demand, which is the system forecast load without the expected output of wind generators, is shown in Table 3.1.

In order to show the effect of wind penetration on the system reliability, we add three wind farms with 75 wind generators in each farm. The capacity of wind

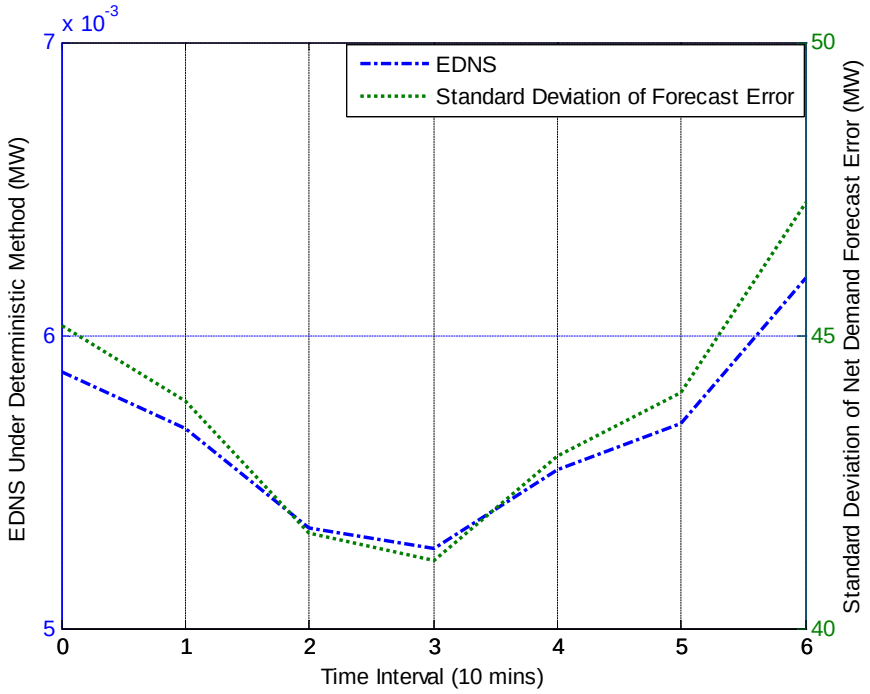

Figure 3.4: EDNS of deterministic method follows standard deviation of net demand forecast error

generators are all 1.5 MW. So, the total wind power capacity is 337.5 MW, or about 10.4% of the total generation capacity. The dependence between two wind power forecast errors within the same wind farm is set to be 0.3. Across wind farms 1 and 2 dependence is set to be 0.3 (Doherty and O'Malley, 2005). In addition, the wind speed forecasting error is set to be a Gaussian distribution with mean 0 and standard deviation within the range of 5%˜20%.

The model is coded in a MATLAB environment and solved using the "quadprog" function of it. With a pre-specified error tolerance of 0.0001 MW, the running time is less than 2 minutes on a 2.66 GHz Windows-based PC with 4 G bytes of RAM. Each iteration of quadratic programming needs less than 10 seconds.

3.4.1 Comparison of the Deterministic and Probabilistic Methods

Firstly, we solve the deterministic model maintaining the quantity of spinning reserve as the capacity of the largest generator in the system, which is 400 MW. Then, we calculate the EDNS of the dispatching result of the deterministic method. By setting the maximum EDNS of this result as the constraint for the probabilistic method, we calculate the dispatching result of that method.

The EDNS of deterministic method and standard deviation of net demand forecast error are shown in Fig. 3.4. We can see that the reliability of system under deterministic reserve requirement changes with the fluctuation of net demand forecast error. That means the deterministic requirement of spinning reserve does not provide a uniform system reliability level.

The EDNS and spinning reserve under the two methods are shown in Fig. 3.5. From these figures, we can see that although the amount of spinning reserve by the deterministic method is constant, the reliability index EDNS is fluctuating. In contrast, the reliability of the system by probabilistic method is constant, while the spinning reserve is changing. Thus, the probabilistic method can give system operators a more tangible measure of system reliability.

3.4.2 Relationship Between EDNS Requirement and Spinning Reserve

The quantities of spinning reserve under different EDNS requirements are shown in Fig. 3.6. We can see that as the EDNS value increases from 0.0062 MW to 0.0077 MW (Xia et al., 2005), indicating a worsening reliability, the quantity of spinning reserve decreases about 8 MW. This indicates the trade-off between reliability and economics, i.e., if higher reliability is required, then economy will be sacrificed.

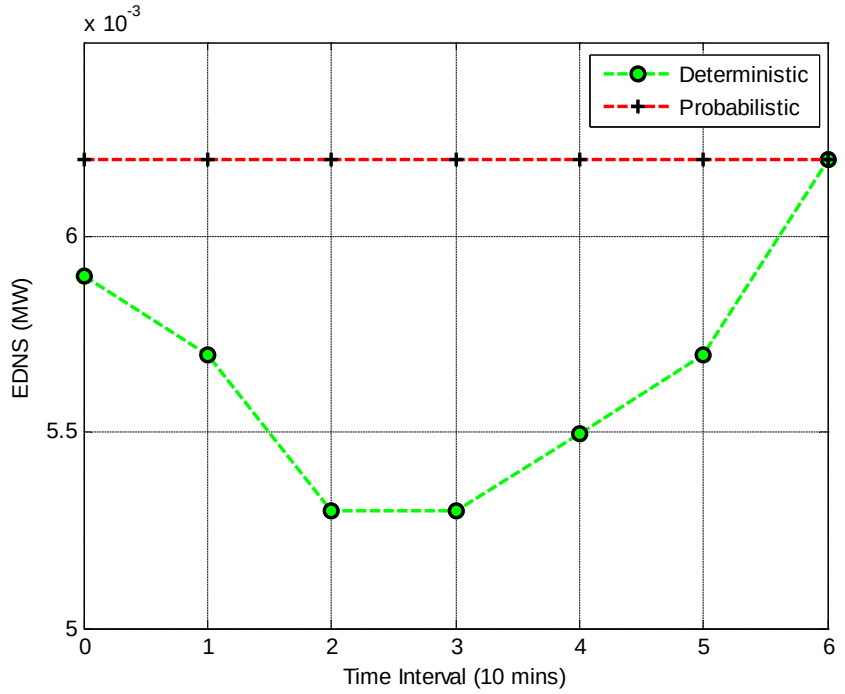

(a) EDNS value

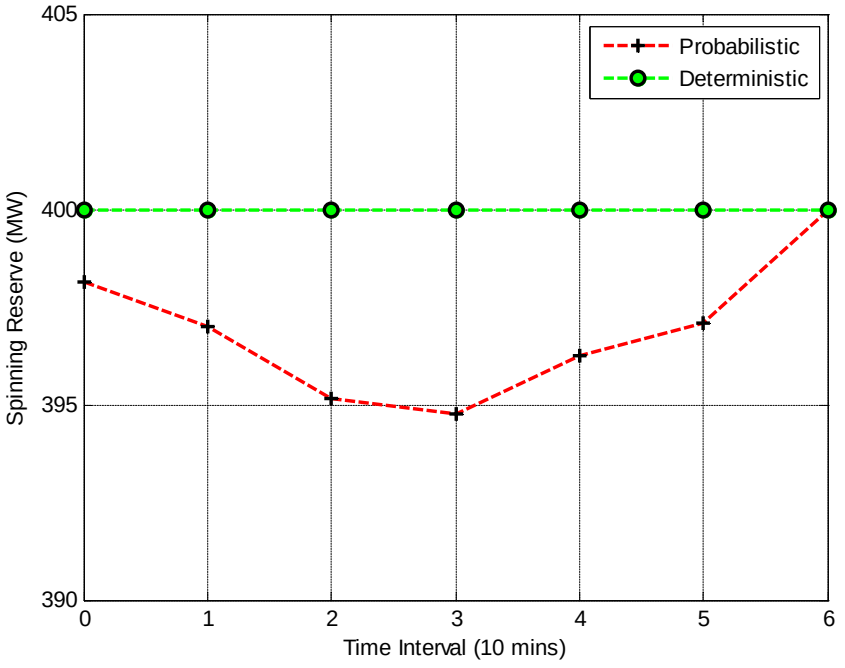

(b) Spinning reserve

Figure 3.5: Comparison of EDNS and spinning reserve of two methods: fluctuating EDNS with deterministic reserve, while constant EDNS with probabilistic reserve

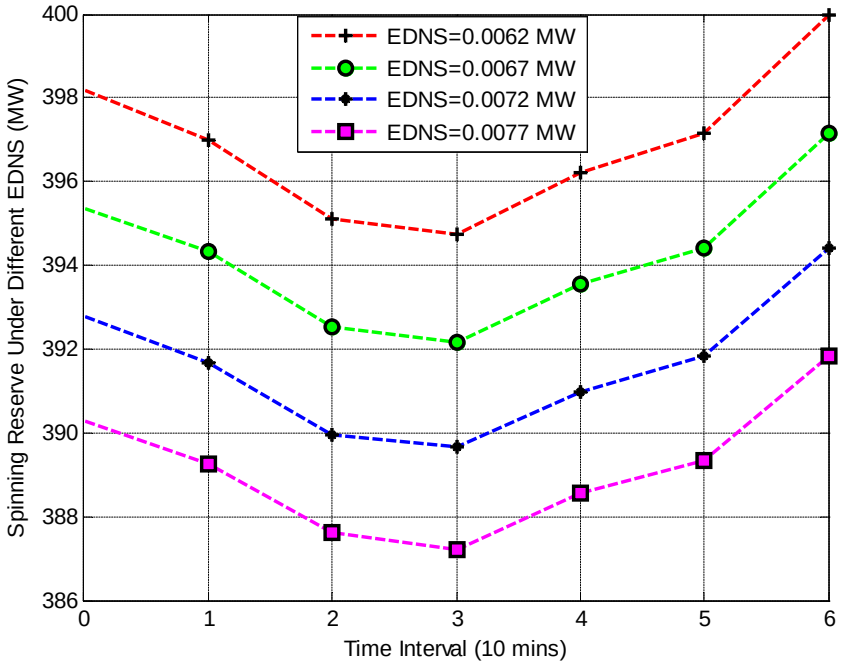

Figure 3.6: Spinning reserve under different ENDS requirements: lower ENDS, higher reserve level

Since there is a trade-off between reliability and economics, the question of optimal trade-off, i.e. optimal value of EDNS comes in. This question will be analyzed and solved in Chapter 4.

3.4.3 Relationship Between Load Forecast Error and Spinning Reserve

The quantities of spinning reserve under different load forecast errors and uniform reliability (EDNS=0.0062 MW) are shown in Fig. 3.7. We can see that as the standard deviation of load forecast error increases from 0.8% to 1.1% (Söder., 1993), the total spinning reserve rises about 5 MW. In this case, under uniform reliability requirements, more spinning reserve is required to make up for the poor load forecast. In other words, improving the accuracy of load forecast will reduce the amount of spinning reserve needed.

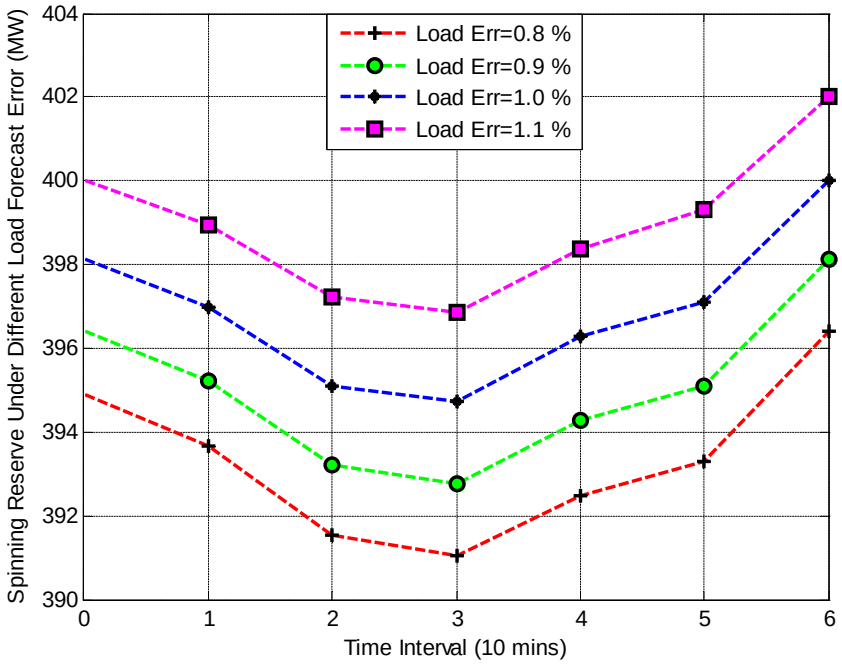

Figure 3.7: Spinning reserve under different load forecast error: higher forecast error, higher reserve level

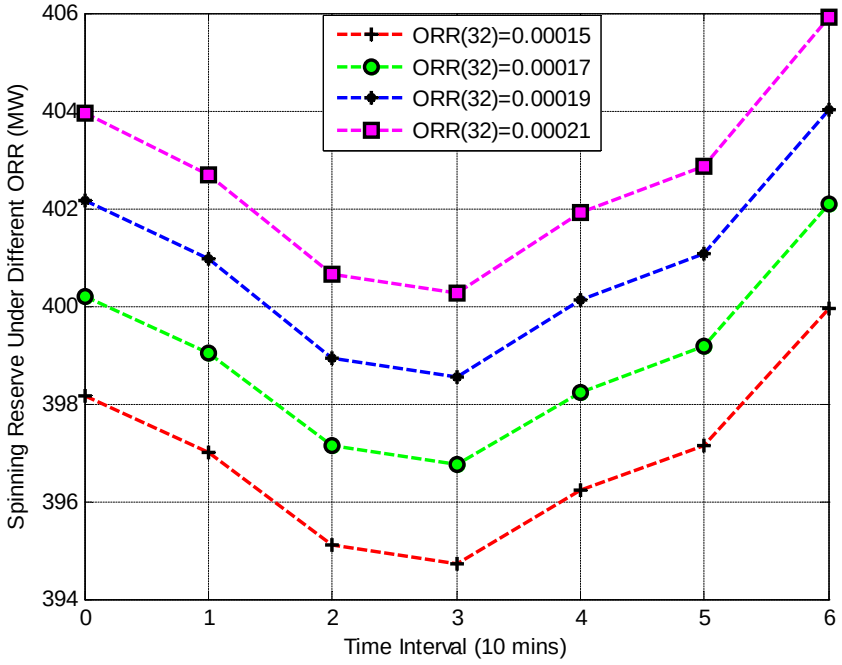

Figure 3.8: Spinning reserve under different ORR: higher ORR, higher reserve level

3.4.4 Relationship Between ORR and Spinning Reserve

The quantities of spinning reserve under different ORR of generators are shown in Fig. 3.8. Here we can see that as the ORR of generator 32 (nuclear generator with capacity 400 MW) increases from 0.00015 to 0.00021 (Grigg et al., 1999), the total system reserve rises about 6 MW to maintain uniform reliability (EDNS=0.0062 MW). This shows the reliability of the system has a close relationship with that of generators, especially those with large capacities. Compared to the deterministic method, the probabilistic method accounts for the reliability of generators and provides a uniform system reliability level. In addition, improvement in the reliability of generators will reduce the amount of spinning reserve needed.

3.4.5 Relationship Between Wind Speed Forecast Error and Spinning Reserve

The quantities of spinning reserve under different standard deviations of wind speed forecast error are shown in Fig. 3.9. As can be seen, about 4 to 6 MW spinning reserve is added to maintain the same reliability level (EDNS=0.0062 MW) as the stand deviation of forecast wind speed is scaled from 0.8σ to 1.1σ (Doherty and O'Malley, 2005).

In this case, under uniform reliability requirements, more spinning reserve is required to make up for the poor wind speed forecast. In other words, improving the accuracy of wind speed forecast will reduce the amount of spinning reserve needed.

3.4.6 Relationship Between Correlation Coefficients of Wind Turbines and Spinning Reserve

The quantities of spinning reserve under different correlation coefficients between wind turbines in the same wind farm are shown in Fig. 3.10a. It can be seen that, as ρ_{rr} increase from 0.3 to 0.6 (Doherty and O'Malley, 2005), the total spinning reserve

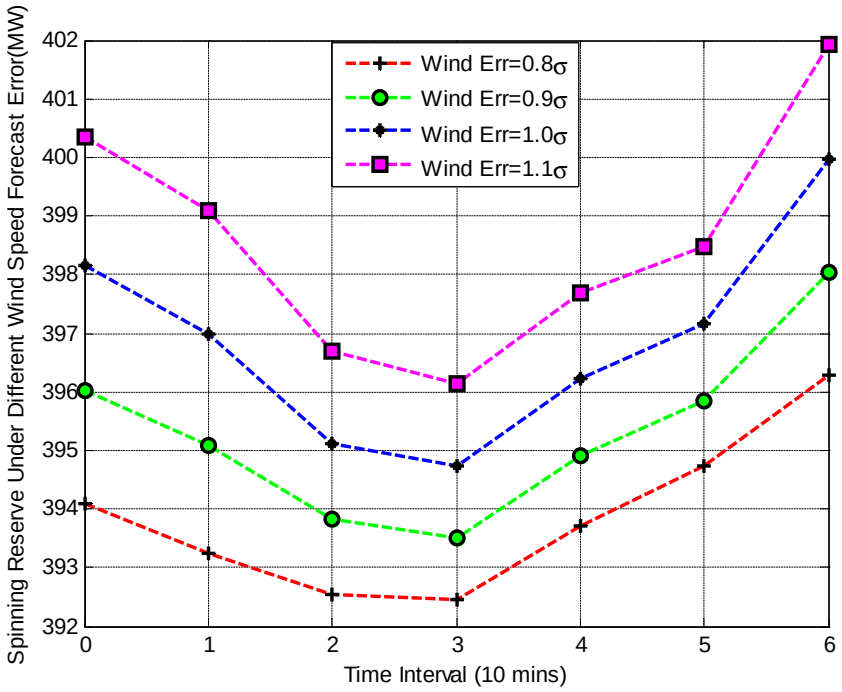

Figure 3.9: Spinning reserve under different standard deviations of wind speed forecast error: higher forecast error, higher reserve level

increases about 4 MW consequently in order to maintain the uniform system reliability level (EDNS=0.0062 MW). The relationship between correlation coefficients of wind turbines across wind farm 1 and 2 and spinning reserve are shown in Fig. 3.10b. Similar pattern can be found since both of them are related to spinning reserve through changing the total wind power forecast error.

Fig. 3.10 indicates that the spinning reserve is closely related to the correlation coefficients of wind turbines. As the correlation coefficients of wind turbines decrease as the distance between wind turbines increase, graphically widespread wind turbines reduce the amount of spinning reserve needed.

3.4.7 Factory Testing of the Algorithm

In order to make sure the algorithm can still work under various conditions, factory testing are done and results are reported in this subsection. Of all the uncertainties,

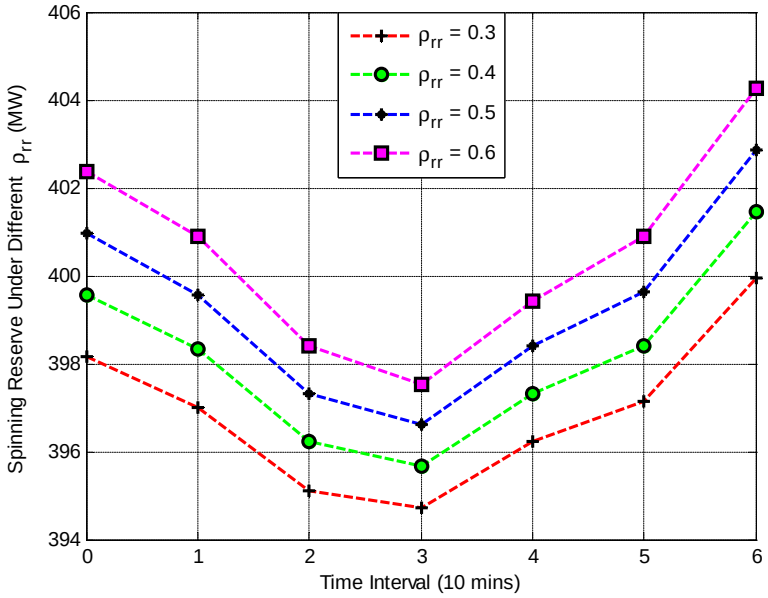

(a) Spinning reserve under different correlation coefficients between wind turbines in the same wind farm

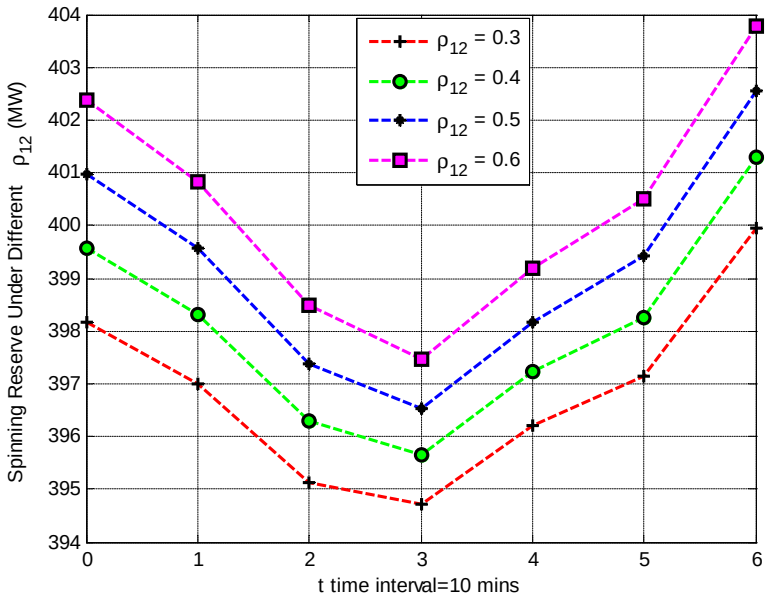

(b) Spinning reserve under different correlation coefficients between wind turbines across wind farm 1 and 2

Figure 3.10: Spinning reserve under different correlation coefficients between wind turbines: higher correlated wind turbines, higher reserve level

i.e. load forecast error, wind speed forecast error and ORR of generators, we change any two and calculated the spinning reserve by the proposed algorithm. The simulation results are shown in Fig. 3.11, Fig. 3.12 and Fig. 3.13.

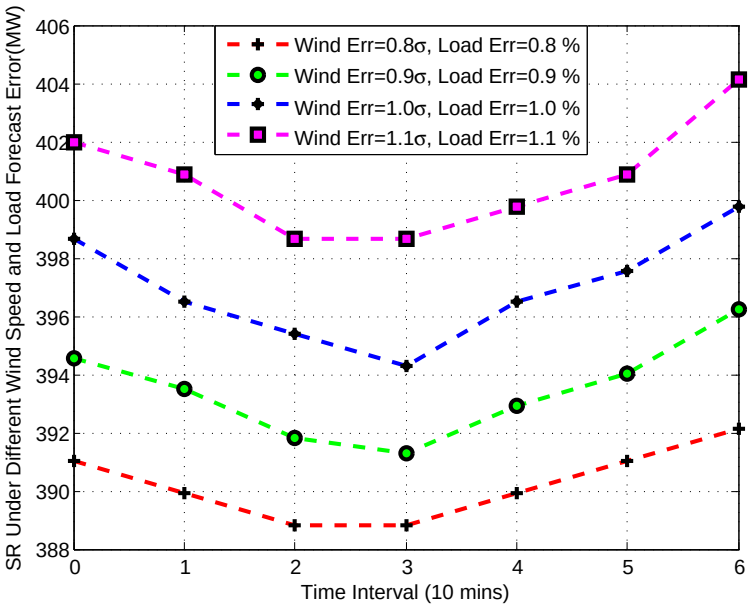

Figure 3.11: Spinning reserve under different load and wind speed forecast error

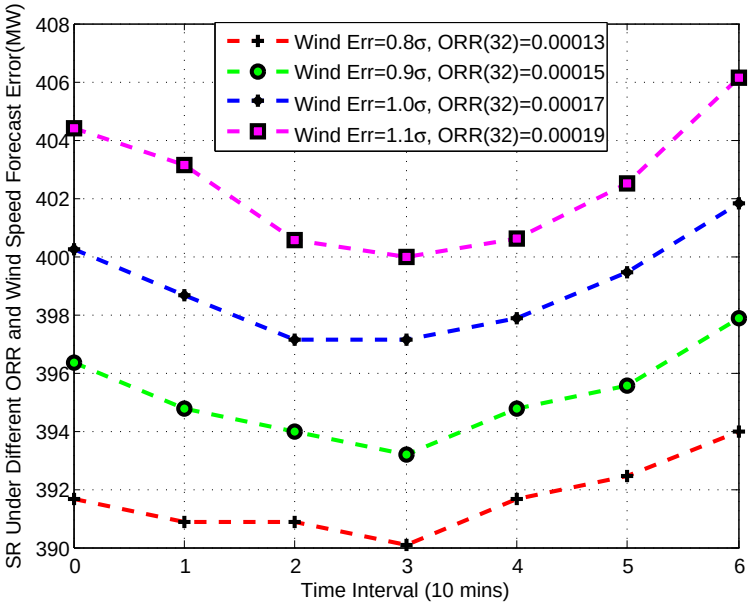

Figure 3.12: Spinning reserve under different ORR and wind speed forecast error

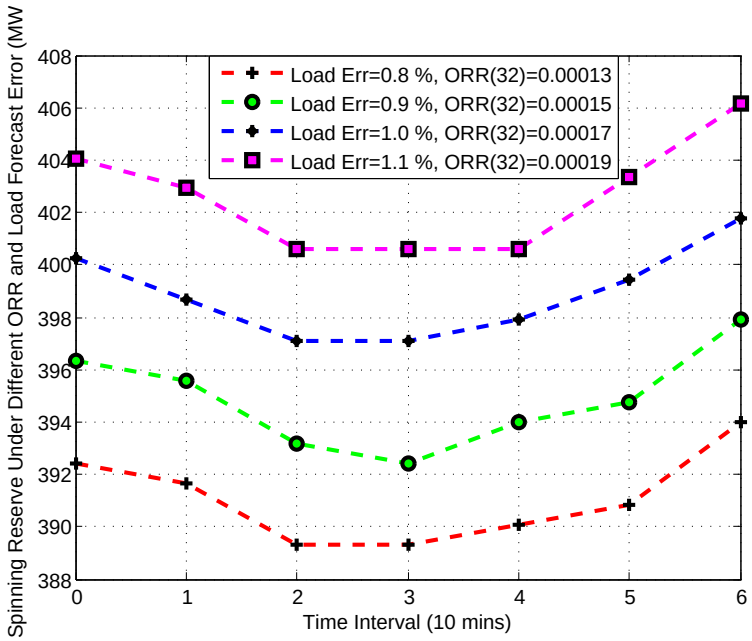

Figure 3.13: Spinning reserve under different ORR and load forecast error

First of all, we can see that the algorithm works well under various conditions. In addition, as two uncertainties change simultaneously, their effects on the amount of spinning reserve is not equal to the summation of each uncertainty's effect separately. This can be explained by the formulation of EDNS as equation (3.11), which is definitely not linear.

3.5 Conclusion

In this section, a new probabilistic method is used to quantify the spinning reserve of system and allocate the spinning reserve to relative generators. It uses EDNS as a constraint, which relates the reliability of system with the spinning reserve by calculating the extent of required load shedding. The method also considers the probability distribution of forecast errors of wind and load, as well as generator forced outage rate. The simulation results on the IEEE Reliability Test System show the strong relationship between EDNS and the quantity of spinning reserve. Under this probabilistic method, we can see the effect of uncertainties, such as ORR, load forecast

error and wind speed forecast error, on the reliability of system. In addition, the results show the effect of correlation coefficients of wind power forecast errors on the spinning reserve. The results suggest that the reliability of system is related to many uncertainties, from generators to load. The proposed probabilistic method can maintain the reliability of system at a uniform level considering all these uncertainties.

Chapter 4

Day-ahead Unit Commitment Considering Wind Power

The main contribution of this chapter is to propose an approach to determine the spinning reserve required over the next few hours or days considering integration of wind power generation. An algorithm, which integrates the stochastic wind forecast results into a day-ahead unit commitment (UC) and extracts its value for the operation of system, is developed. A new model of security constrained unit commitment (SCUC), which minimizes the cost of energy, spinning reserve and expected energy not served (EENS) is proposed and solved using mixed integer linear programming (MILP) technique. The formulation of EENS takes into account the probability distribution of forecast errors of wind and load, as well as outage replacement rates (ORR) of various generators. The rest of this chapter is organized as follows. In Section4.1, the model of forecast wind power, forecast net demand and generators are described. Then, the new formulation of EENS is given in Section 4.2. In Section 4.3, the model of SCUC is proposed. After that, results of case studies are presented in Section 4.4. Finally, the conclusions are given in Section 4.5.

The main content in this chapter can also be found in Liu and Tomsovic (2012b).

4.1 Model of Forecast Wind Power, Forecast Net Demand and Generators

As mentioned in Section 3.1 wind speed forecast error can be modeled as a Gaussian distribution with mean zero. Due to the nonlinear input-output relationship of the wind turbine, the probability distribution of wind power forecast error from individual wind turbine is not Gaussian. In this chaper, we will propose a new method which can be applied to any form of probability distribution of wind power forecast error as long as it is smooth. Without loss of generality, we still use the model of wind power forecast error in Section 3.1.

The load could be modeled as forecast load plus a Gaussian distributed error, which has expectation zero and standard deviation σ_t^l. The net demand D_t is defined as the system load minus the total wind power and needs to be balanced by other generators in the system. In this chapter, we assume the load forecast and wind forecast errors are uncorrelated, so the forecast error of net demand e_t^d is the sum of the load forecast error and wind power forecast error. This follows Gaussian distribution with expectation zero and standard deviation as in Section 3.5. In more general case, we can get the probability distribution function of net demand by convolving the wind power forecast error with load forecast error.

For generators, the two-stage Markov model are used as in Section 3.1.

4.2 Formulation of EENS

The EENS is the expected energy not served while the net demand forecast error plus the output of unavailable generators is larger than the available spinning reserve. The unit of EENS used in this chapter is MWh. As stated before, the net demand forecast error is a continuous random variable, while the uncertainties of generators are a set of binary random variables. In order to combine these binary random variables with the continuous random variable, the formulation of EENS is divided into two steps. In

the first step, a set of scenarios is constructed based on "$n-1$" or "$n-2$" contingency rules. In the next step, the probability distribution of net demand forecast error is combined with the realization of uncertainties of generators in each scenario, then discretized into NL intervals. The EENS in a scenario is calculated by summing the expectation of all intervals giving rise to load shedding. The summation of all EENS weighted by probabilities of corresponding scenarios is the total EENS of the system.

In the first step, only single order contingency events are taken into account since multiple order contingency events have relatively small probabilities while consuming far more computational resources. Note the difference between a planning calculation where in general one needs to consider the possibility of multiple outages and units under maintenance. The probability of all scheduled generators available except generator i is

$$p_{it} = u_{it}U_i \prod_{j=1,j\neq i}^{NG} (1 - u_{jt}U_j) \tag{4.1}$$

In addition, these probabilities can be further simplified by replacing the higher order terms in the product expansions by upper bounds. Therefore, they can be restated as

$$p_{it} \approx u_{it}U_i \tag{4.2}$$

In the second step, the uncertainties of generators and net demand forecast error are combined to obtain the total system forecast error for each scenario. Taking scenario s during period t for example, we calculate the redundant or deficient power of generators according to the realization of them in this scenario as

$$\mu_{s,t} = \sum_{i\in A_{s,t}} R_{it} - \sum_{j\in U_{s,t}} P_{jt} \tag{4.3}$$

It should be pointed out that $U_{s,t}$ is empty, when $s = 0$. This is the base scenario. Then, we subtract $\mu_{s,t}$ from e_t^d to find the total system forecast error $x_{s,t}$ for scenario s as

$$x_{s,t} = e_t^d - \mu_{s,t} \tag{4.4}$$

Note that the probability distribution of $x_{s,t}$ is obtained through shifting e_t^d to the left or right over a distance of $|\mu_{s,t}|$. If $\mu_{s,t} > 0$, that means there is redundant power from generators, then e_t^d shifts to the right and the expectation of load shedding is reduced as in Fig. 4.1. Otherwise, e_t^d shifts to the right and the expectation of load shedding is increased. Next, the probability distribution of $x_{s,t}$ is divided into NL odd number intervals with $a_{s,t,l}$ as the probability of interval l. The width of each interval is σ_t^d. For interval l, the mid-value of this interval $\left(\frac{NL+1}{2} - l\right)\sigma_t^d - \mu_{s,t}$ is taken as the value of the whole interval. A seven-interval approximation is shown as in Fig. 4.1.

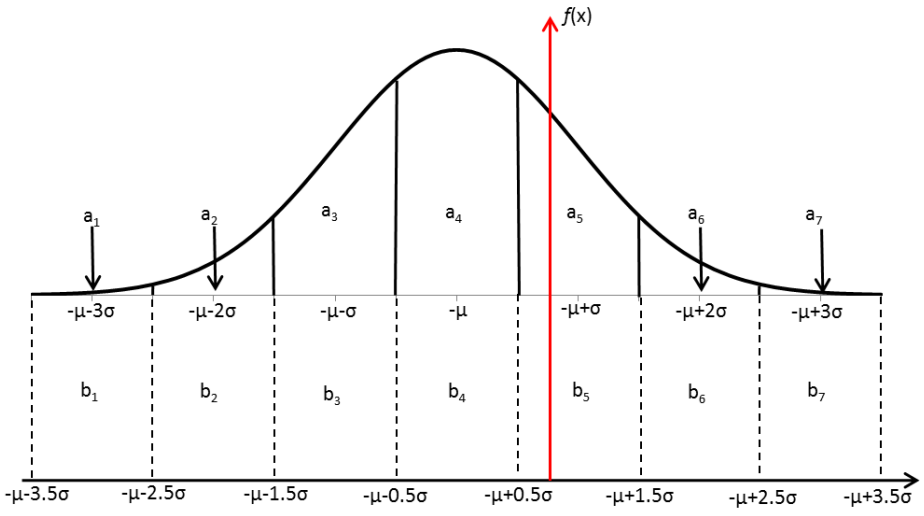

Figure 4.1: Seven-interval approximation of probability distribution of total system forecast error

Since we only need the intervals satisfying

$$\left(\frac{NL+1}{2}-l\right)\sigma_t^d-\mu_{s,t}>0 \tag{4.5}$$

another binary variable $b_{s,t,l}$ is introduced to distinguish intervals satisfying (4.5) from others. Hence, the *EENS* in scenario s during period t can be formulated as

$$EENS_{s,t}=\sum_{l=1}^{NL}\left(\left(\frac{NL+1}{2}-l\right)\sigma_t^d-\mu_{s,t}\right)a_{s,t,l}b_{s,t,l} \tag{4.6}$$

Each of these binary variables $b_{s,t,l}$ is associated with one realization of the total system forecast error, such that

$$b_{s,t,l}=\begin{cases}1 & \text{if } \left(\frac{NL+1}{2}-l\right)\sigma_t^d-\mu_{s,t}>0\\ 0, & \text{otherwise}\end{cases} \tag{4.7}$$

Expression (4.7) implies that the new binary variable is equal to 1 if and only if the associated realization of total system forecast error falls on the positive side of the $f(x)$ axis as in Fig. 4.1. The nonlinear conditional expression in (4.7) can be recast into an equivalent MILP form by constraints:

$$b_{s,t,l}\le b_{s,t,l+1}\quad l\in[1,NL-1] \tag{4.8}$$

$$\frac{NL+1}{2}-\frac{\mu_{s,t}}{\sigma_t^d}\ge\sum_{l=1}^{NL}b_{s,t,l}\ge\frac{NL-1}{2}-\frac{\mu_{s,t}}{\sigma_t^d} \tag{4.9}$$

Expressions (4.8) and (4.9) characterize a novel variant of the formulation of EENS considering the probability distributions of forecast errors of wind and load as proposed in this dissertation. Constraint (4.8) makes use of the fact that if one interval causes load shedding, then any interval on its right must also cause load shedding. In other words, we only need to find the interval, in which $x_{s,t}=0$ lies. As stated before, the probability distribution of $x_{s,t}$ differs from that of e_t^d by shifting to the left or right depending on $\mu_{s,t}$. Constraint (4.9) takes advantage of this fact to find the location of $x_{s,t}=0$.

Of course, one can divide the distribution of $x_{s,t}$ into smaller intervals, such as σ_t^d/N by simply substituting σ_t^d/N for σ_t^d in (4.6), (4.7) and (4.9). With small intervals, the result will be more accurate, but require more computational resources. Finally, the summation of $EENS_{s,t}$ weighted by probabilities of corresponding scenarios is the total EENS of the system during period t.

$$\begin{aligned} EENS_t &= \sum_{s=0}^{NW} EENS_{s,t} p_{s,t} \\ &= \sum_{s=0}^{NW} \left\{ \sum_{l=1}^{NL} \left[\left(\frac{NL+1}{2} - l \right) \sigma_t^d - \mu_{s,t} \right] a_{s,t,l} b_{s,t,l} \right\} p_{s,t} \\ &= \sum_{s=0}^{NW} \left\{ \sum_{l=1}^{NL} \left[\left(\frac{NL+1}{2} - l \right) \sigma_t^d - \sum_{i \in A_{s,t}} R_{it} - \sum_{j \in U_{s,t}} P_{jt} \right] a_{s,t,l} b_{s,t,l} \right\} p_{s,t} \end{aligned} \tag{4.10}$$

It should be noted that the proposed formulation of EENS is independent of the specific probability distribution of net demand forecast error. For different distributions of net demand forecast errors, we just need to adjust the probability of each interval, which is $a_{s,t,l}$, and they can be calculated in advance. To this point, the proposed formulation can be applied to any form of probability distribution of net demand forecast error as long as it is continuous.

So far, EENS are formulated as the summation of products of two binary variables and a continuous variable, which can be linearized just as in Bouffard and Galiana (2004). By linearization, the more efficient mixed integer linear programming (MILP) solver,like CPLEX can be used.

4.3 Proposed SCUC Formulation

UC provides the best combination of generators to turn on and optimally schedules these generators to balance the demand over a specific study period. When security is considered in UC, this process becomes much more complex due to not only the

coupling of energy and spinning reserve output of generators but also the issue of quantifying spinning reserves. Generally, the more spinning reserve, the more reliable the system will operate. Still, a trade-off needs to be made between the additional operating cost and reliability.

4.3.1 Objective Function

The objective function of conventional UC considers only operating and start-up cost of generators over all periods of the scheduling horizon. In the proposed formulation, the spinning reserve requirements are determined by simultaneously optimizing the operating cost, start-up cost, reserve cost and expected cost of load shedding (ECLS). The ECLS is expressed as the value of lost load (VOLL) (Kariuki and Allan, 1996) multiplied by the approximation of EENS as developed in Section 4.2. This approach has the advantage of being self-contained in the sense that it does not need another EENS target or spinning reserve constraint because the spinning reserve provision is based on an internal cost/benefit analysis. In order to keep the MILP form, piece-wise linear approximation of the cost curves of generators is used. The objective function of SCUC is stated as

$$\begin{aligned} \min_{P_{it},u_{it},R_{it}} \quad & \sum_{t=1}^{NT}\{\sum_{i=1}^{NG}[C_i\left(P_{it},u_{it}\right)+S_i\left(u_{it},u_{i,t-1}\right)+q_{it}R_{it}] \\ & +VOLL_t\cdot\sum_{s=0}^{NW}EENS_{s,t}p_{s,t}\} \end{aligned} \tag{4.11}$$

4.3.2 Constraints

The objective function must be minimized subject to a number of constraints.

1. Power balance

$$\sum_{i=1}^{NG}P_{it}=D_t \qquad \forall t \tag{4.12}$$

2. Output limits of generators

$$P_i^{\min} u_{it} \leq P_{it} \leq P_i^{\max} u_{it} \qquad \forall i, \forall t \tag{4.13}$$

$$P_{it} + R_{it} \leq P_i^{\max} \qquad \forall i, \forall t \tag{4.14}$$

3. Spinning reserve limits of generators

$$0 \leq R_{it} \leq u_{it} R_i^{\max} \qquad \forall i, \forall t \tag{4.15}$$

4. Ramp limits of generators

$$P_{it} - P_{i,t-1} \leq RU_i u_{i,t-1} + R_i^{start}(u_{it} - u_{i,t-1}) \qquad \forall i, \forall t \tag{4.16}$$

$$P_{it} - P_{i,t-1} \geq -RD_i u_{it} - R_i^{shut}(u_{i,t-1} - u_{it}) \qquad \forall i, \forall t \tag{4.17}$$

$$R_i^{start} = \max RU_i, P_i^{min} \qquad \forall i \tag{4.18}$$

$$R_i^{shut} = \max RD_i, P_i^{min} \qquad \forall i \tag{4.19}$$

It should be noted that the trajectories of generators' start-up and shut-down process are neglected in the proposed model. Constraint (4.16) ensures that the increment in the output power ($\triangle P_{it} = P_{it} - P_{i,t-1}$) cannot be greater than the ramp limits of the generator, or if it is starting-up to its minimum stable generation. The ramp-down constraint (4.17) is formulated in an equivalent way.

5. Minimum up time

$$u_{it} = 1 \quad \forall t \in \left[1, t_i^{\text{up}} - t_i^{\text{H}}\right], \, t_i^{\text{up}} > t_i^{\text{H}} > 0 \tag{4.20}$$

$$\begin{cases} u_{it} - u_{i,t-1} \leq u_{i,t+1} \\ u_{it} - u_{i,t-1} \leq u_{i,t+2} \\ \vdots \qquad\qquad\qquad\qquad\qquad\qquad \forall t \in [1, NT-1] \\ u_{it} - u_{i,t-1} \leq u_{i,\min\left\{t+t_i^{\text{up}}-1, NT\right\}} \end{cases} \tag{4.21}$$

6. Minimum down time

$$u_{it} = 1 \quad \forall t \in \left[1, t_i^{\text{down}} + t_i^{\text{H}}\right], -t_i^{\text{down}} < t_i^{\text{H}} < 0 \tag{4.22}$$

$$\begin{cases} u_{i,t-1} - u_{it} \leq 1 - u_{i,t+1} \\ u_{i,t-1} - u_{it} \leq 1 - u_{i,t+2} \\ \vdots \qquad\qquad\qquad\qquad\qquad\qquad \forall t \in [1, NT-1] \\ u_{i,t-1} - u_{i,t} \leq 1 - u_{i,\min\left\{t+t_i^{\text{down}}-1, NT\right\}} \end{cases} \tag{4.23}$$

7. Transmission flow limits in the base scenario

$$\sum_{i=1}^{NG} GSF_{ki} P_{it} - \sum_{j=1}^{ND} GSF_{kj} D_{jt} \leq F_k^{max} \qquad \forall k, \forall t \tag{4.24}$$

4.4 Case Study

In this section, the proposed method for quantifying spinning reserve is demonstrated on a modified IEEE Reliability Test System (Grigg et al., 1999). In this system, there are 26 thermal generators and the hydro units have been removed. The ramp rates, failure rates and quadratic cost coefficients are taken from Wang and Shahidehpour (1993). For simplicity, the unit quadratic cost curves in Wang and Shahidehpour (1993) are converted into piece-wise linear cost curves. In addition, we assume that all units offer reserve at rates q_i equal to 10% of their highest incremental cost of producing energy as in Bouffard and Galiana (2004). The load from Wang and Shahidehpour (1993) is modified by adding another 250 MW for

each period to balance the wind power. The load forecast error is assumed to be Gaussian distribution with zero mean and a standard deviation 3% of the forecast load (Bouffard and Galiana, 2008). VOLL is set to be 4,000 $/MWh (Ortega-Vazquez and Kirschen, 2009).

In order to show the effect of wind power penetration on the system reliability, we add 6 wind farms at bus 1, bus 2, bus 7, bus 16, bus 17 and bus 22, respectively. Each wind farm has 70 wind generators with capacity 1.5 MW (GE, 2008). So, the total wind power capacity is 630 MW, 20.0% of the total conventional generation capacity. The correlation coefficients of two forecast errors of wind power in the same wind farm are set to be 0.3 and that of wind turbines between wind farms at bus 16 and bus 17 are set to be 0.2 (Söder., 1993; Doherty and O'Malley, 2005). In addition, the wind speed forecasting error is set to be a Gaussian distribution with zero mean. The standard deviations fall within the range of 5%˜20% in the examples. The forecast net demand, that is, the system forecast load minus the expected output of wind generators, is shown in Table 4.1.

Table 4.1: Forecast net demand

Hour	Load (MW)	Hour	Load (MW)	Hour	Load (MW)
1	1495.2	9	2369.8	17	2460.3
2	1557.8	10	2480.3	18	2474.7
3	1532.7	11	2561.4	19	2461.0
4	1546.1	12	2419.8	20	2591.1
5	1620.6	13	2435.0	21	2624.7
6	1737.1	14	2371.3	22	2546.4
7	1872.2	15	2508.0	23	2309.4
8	2246.3	16	2662.7	24	1924.5

The DC power flow is used to simulate the transmission flow limits in the base scenario. For simplicity, the system is divided into 2 areas, connected by 4 transmission lines from bus 11 to bus 14; bus 12 to bus 23; bus 13 to bus 23 and bus 15 to bus 24, respectively. It is assumed that no congestion occurs inside these two areas, and hence we only consider the transfer limits between areas.

The model is coded in a MATLAB environment and solved using a MILP solver CPLEX 12.2. With a pre-specified duality gap of 0.5%, the running time is about 180 seconds on a 2.66 GHz Windows-based PC with 4 G bytes of RAM.

4.4.1 Comparison of Traditional and Proposed Methods

Firstly, we solve the traditional UC maintaining the quantity of spinning reserve as the capacity of the largest generator in the system, which is 400 MW. Using this result, we calculate the EENS. Then, we solve the UC problem again by the proposed SCUC. The comparison of spinning reserve and EENS between traditional and the proposed methods is shown in Fig. 4.2. The comparison of the resulting generator schedules is shown in Fig. 4.3.

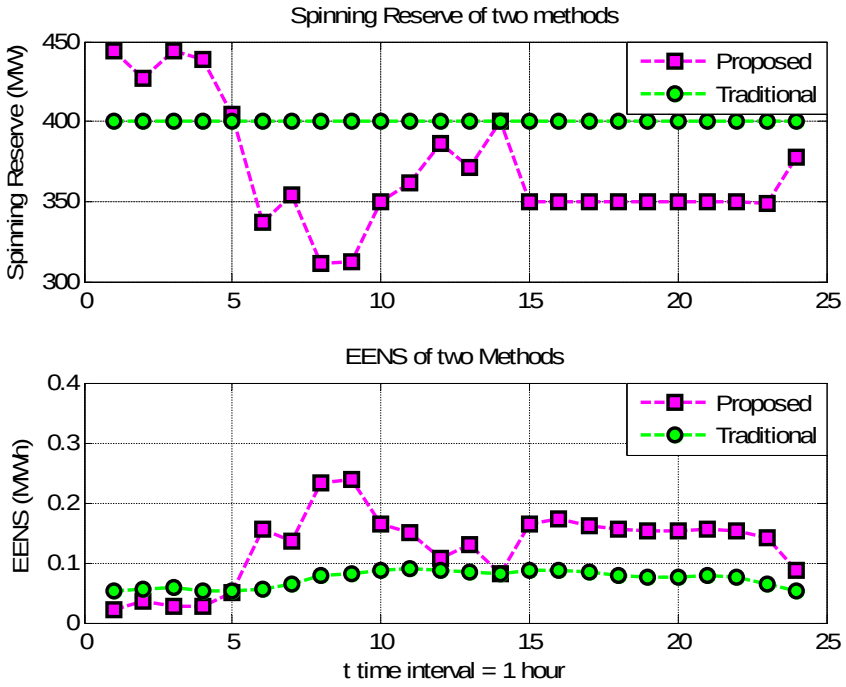

Figure 4.2: Comparison of spinning reserve and EENS between proposed and traditional methods: traditional method is conservative

From Fig. 4.2, we see that the scheduling result of traditional UC, which maintains 400 MW spinning reserve, is generally more reliable than that of the proposed

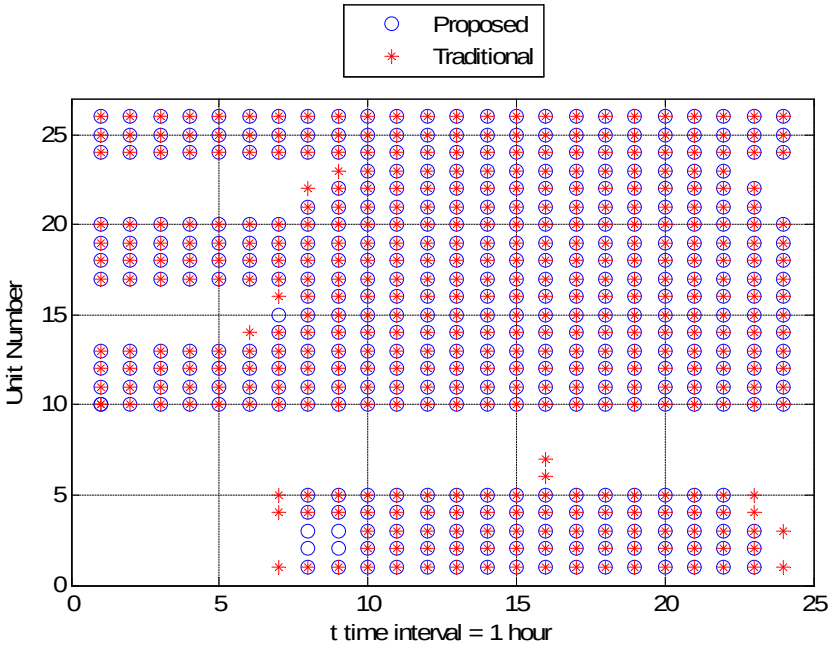

Figure 4.3: Comparison of generator schedules between proposed and traditional methods: less units are committed by proposed method

SCUC. Consequently, the total cost of traditional UC is slightly higher than that of the proposed SCUC as shown in Table 4.2. Specifically, the expected cost of load shedding by the proposed SCUC is increased, while the operating costs including energy cost, start-up cost and spinning reserve cost are reduced by a total off 1.12%. The overall cost of the proposed SCUC is reduced by 0.38% compared to that of the traditional UC. In other words, better operating efficiency can be reached by reducing the reliability level of the traditional UC. More simply, the spinning reserve requirement of 400 MW is very conservative.

Another point that should be noted is the trade-off between providing additional spinning reserve and load shedding as shown in Fig. 4.2. When the system load level is low, the EENS level is low. The reason is that the cost of providing extra spinning reserve is low due to the light load during these periods (Hour 1 to Hour 5), so additional spinning reserve is more economic than load shedding. On the contrary,

when the system load level is high (Hour 15 to 24), more expensive units have been committed, and as a result, the cost of providing extra spinning reserve is high. Therefore, the EENS during these periods is much higher than that during low load levels. During the period of load increase (Hour 6 to Hour 10), the cost of spinning reserve is the highest because extra generators need to be committed and the start-up cost of these generators results in a large increase in the cost of additional spinning reserve. Hence, the EENS during these periods is the highest (Fig. 4.2).

In addition, we can see that fewer units are committed by the proposed method than the traditional method as shown in Fig. 4.3. This again verifies the traditional UC with a spinning reserve minimum is conservative.

Table 4.2: Comparison of costs between traditional and proposed methods

Model	Total Cost ($)	Operating Cost ($)	ECLS ($)
Traditional UC	725054.76 (100%)	717982.43 (100%)	7072.33
Proposed UC	722295.33 (99.62%)	709905.32 (98.88%)	12390.01

4.4.2 Relationship Between VOLL and Spinning Reserve

The quantities of spinning reserve and EENS under different VOLL values are shown in Fig. 4.4. As the VOLL value increases from 2000 $/MWh to 8000 $/MWh (Ortega-Vazquez and Kirschen, 2009), both the resultant quantity of spinning reserve and EENS value vary significantly. This is because the increase of VOLL value changes the equilibrium point between energy cost, reserve cost and expected cost of load shedding. As the VOLL value increases, additional spinning reserve becomes more economic than load shedding. Consequently, the quantity of spinning reserve increases, while the value of EENS decreases.

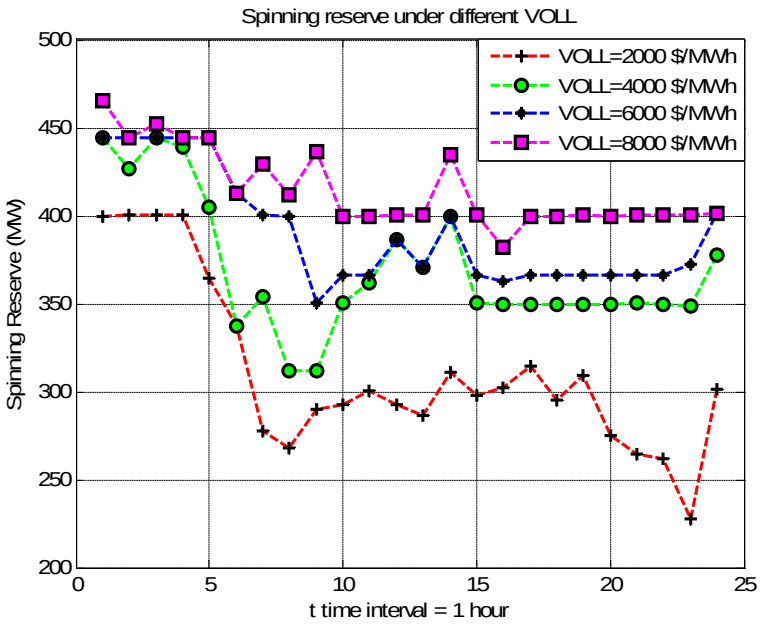

(a) Spinning reserve increases with higher VOLL value

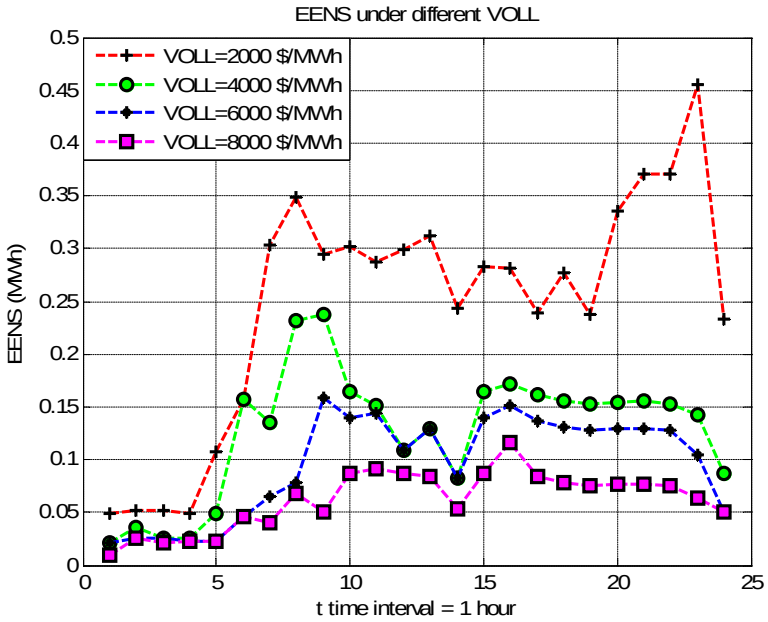

(b) EENS decreases with higher VOLL value

Figure 4.4: Spinning reserve and EENS under different VOLL values

4.4.3 Relationship Between Load Forecast Error and Spinning Reserve

The optimal spinning reserve and corresponding EENS under different load forecast errors are shown in Fig. 4.5. As the standard deviation of load forecast error rises from 2.5% to 4% (Bouffard and Galiana, 2008), both the resultant quantity of spinning reserve and the value of EENS increase. Similar to the discussion above, the increase of load forecast error changes the equilibrium point. As the load forecast error increases, the energy cost, reserve cost and expected cost of load shedding share the extra cost caused by increasing load uncertainty. The total cost of the system under different load forecast errors is shown in Table 4.3.

Table 4.3: Total cost of system under different load forecast errors

σ_t^l (%)	2.5	3.0	3.5	4.0
Total Cost ($)	721039.56 (99.30%)	722295.33 (99.48%)	723818.36 (99.68%)	726097.22 (100%)

4.4.4 Relationship Between ORR and Spinning Reserve

The optimal spinning reserve and corresponding EENS value under different ORR of generators are shown in Fig. 4.6. As the ORR of the 350 MW generator increases (Grigg et al., 1999), both the resultant quantity of spinning reserve and the value of EENS increase. Similar to the analysis above, the energy cost, reserve cost and expected cost of load shedding share the extra cost caused by increasing generation uncertainty. In particular, this result verifies that the reliability of generators plays an important role in the proposed SCUC. The total cost of system under different ORR values is shown in Table 4.4.

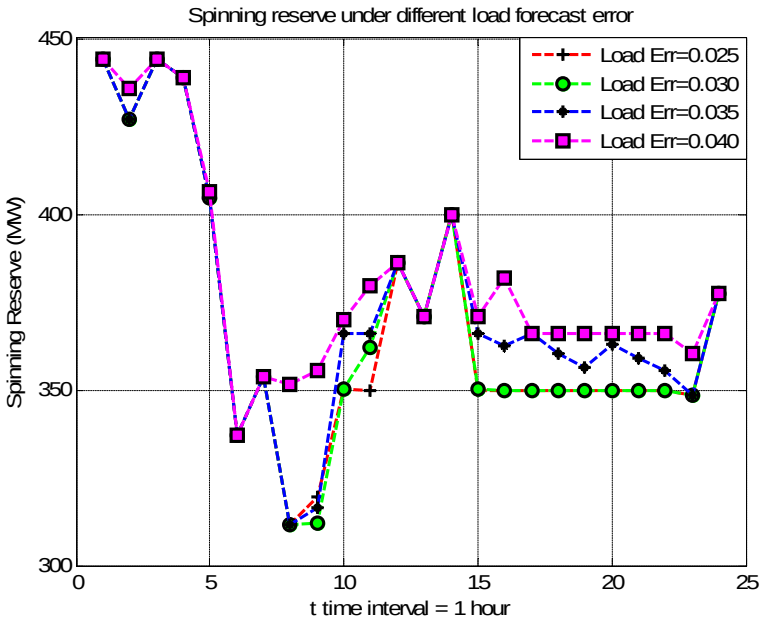

(a) Spinning reserve increases with higher load forecast error

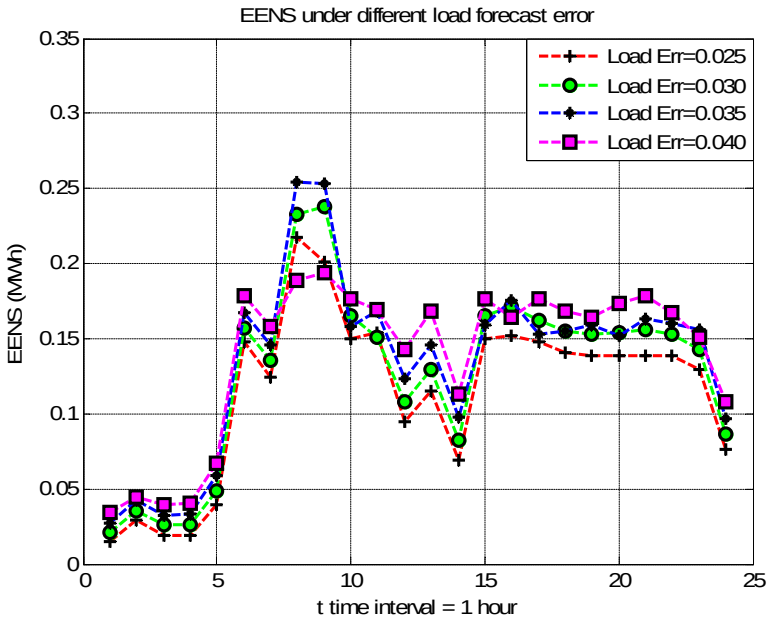

(b) EENS increases with higher load forecast error

Figure 4.5: Spinning reserve and EENS under different load forecast errors

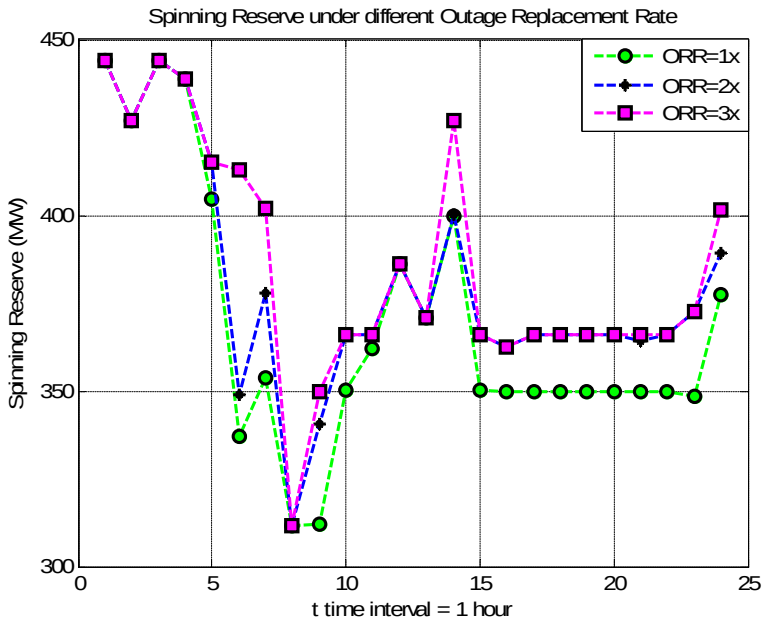

(a) Spinning reserve increases with higher ORR

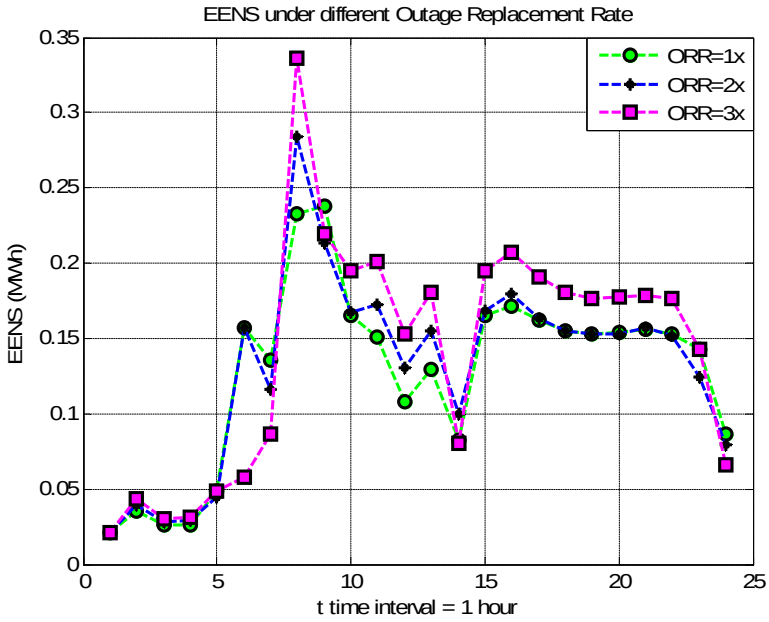

(b) EENS increases with higher ORR

Figure 4.6: Spinning reserve and EENS under different ORR

Table 4.4: Total cost of system under different ORR

Scaling factor of ORR	1	2	3
Total Cost ($)	722295.33 (99.44%)	724463.56 (99.73%)	726356.93 (100%)

4.4.5 Relationship Between Wind Speed Forecast Error and Spinning Reserve

The optimal spinning reserve and corresponding EENS value under different wind speed forecast errors are shown in Fig. 4.7. The optimal spinning reserve increases as the standard deviation of wind speed forecast error increases (Ahlstrom et al., 2005). Similar to the analysis of load forecast error, the energy cost, reserve cost and expected cost of load shedding share the extra cost of increasing wind speed uncertainty. The total cost of system under different wind speed forecast errors is shown in Table 4.5.

Table 4.5: Total cost of system under different wind speed forecast errors

Scaling factor of $\sigma^{w}_{i,r,t}$	0.5	1.0	2.0
Total Cost ($)	721675.14 (99.64%)	722295.33 (99.73%)	724252.17 (100%)

4.4.6 Impact of Transfer Limits on Spinning Reserve

Initially, the transfer limits of the four transmission lines are all 500 MW and the maximum power flow is only 247.47 MW (Grigg et al., 1999). In order to show the effect of transfer limits on spinning reserve, we reduce the limits to 220 MW and 200 MW, respectively. The optimal spinning reserve under different transfer limits is shown in Fig. 4.8.

The impact of transmission limits is variable. It may lead to increased spinning reserve as during Hour 1 to 5 and Hour 14. This arises due to scheduling changes

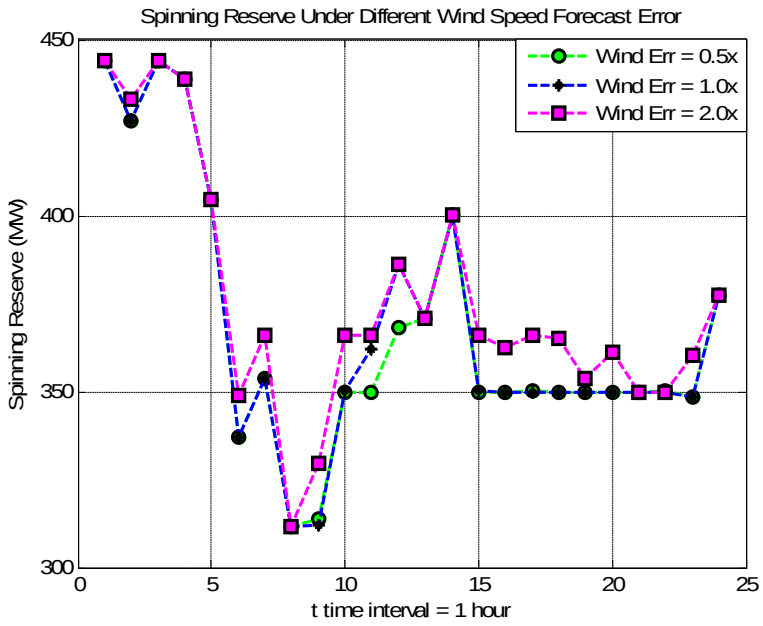

(a) Spinning reserve increases with higher wind speed forecast error

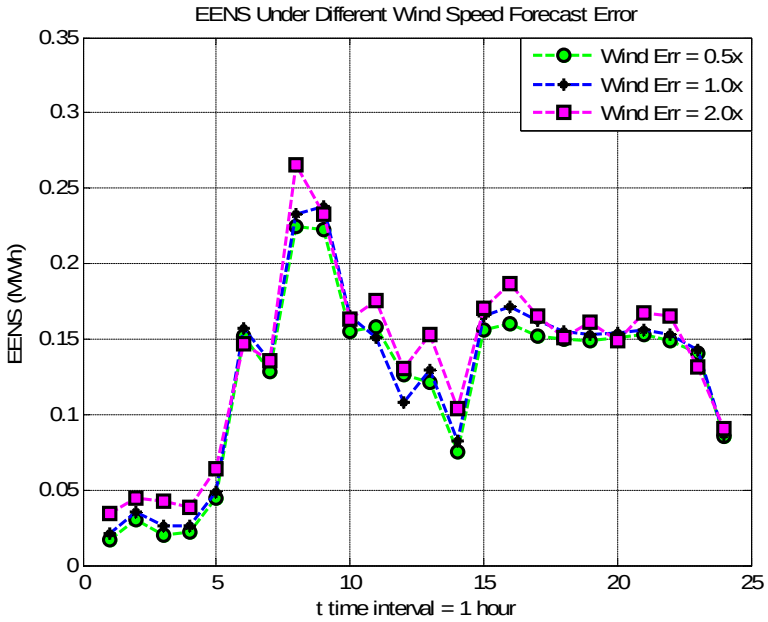

(b) EENS increases with higher wind speed forecast error

Figure 4.7: Spinning reserve and EENS under different wind speed forecast errors

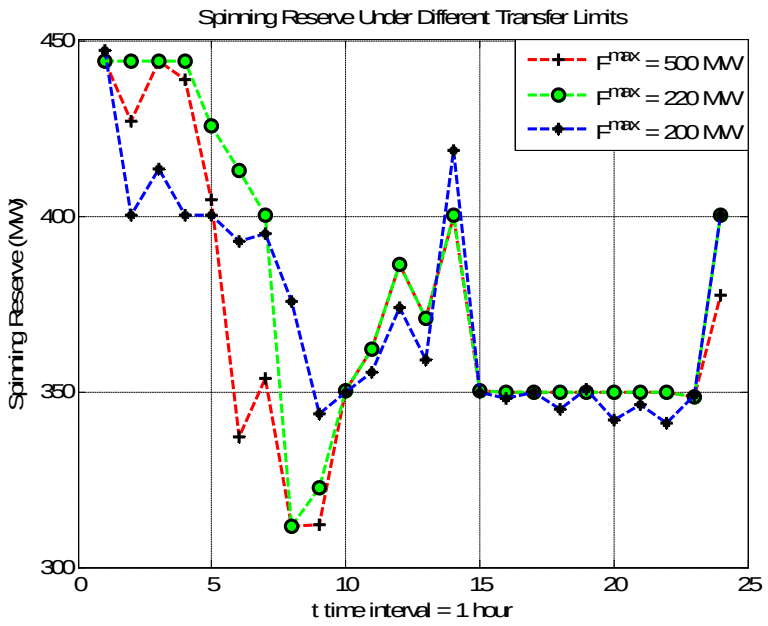

Figure 4.8: Spining reserve under different transfer limits

of the individual units. Specifically, the reductions in outputs of some units result in more spinning reserve available, while the increases in outputs of others have no effect on their spinning reserve. Thus, more spinning reserve is available. Still, further reduction of transfer limits may eventually reduce the optimal spinning reserve. When unit commitment changes, generally the spinning reserve increases, as in Hour 6 to 9. The reason is that more units are started during that period due to the transfer limits. It should be pointed out that the total operating cost always increases as the transfer limits are reduced regardless of the available reserve.

4.5 Conclusion

In this chapter, a new SCUC model, which integrates the stochastic wind forecast results into the day-ahead UC and extracts its value to system operation, is proposed. The approach determines the optimal amount of spinning reserve that minimizes the total cost of operating the system, i.e., balancing energy cost, start-up cost, reserve

cost and expected cost of load shedding. This new formulation of EENS considers the probability distribution of forecast errors of wind and load, as well as ORR of the various generators. Generally, the proposed method has two advantages: first, the method is capable of aggregating the probability distribution of wind and load forecast into UC; and second, the approach determines the optimal amount of spinning reserve in terms of the optimal trade-off between economic efficiency and reliability of system. The results of the case studies show the effect of uncertainties, such as ORR, load forecast error and wind forecast error, on the trade-off between economic efficiency and reliability of system.

Chapter 5

Day-ahead Unit Commitment Considering Demand Response

The main contribution of this chapter is to propose a full demand response model in which Demand Response Provider (DRP) could bid in the energy market as price responsive shiftable demand. Meanwhile, the same DRP could also bid in the spinning reserve market. It should be noted that the principle of demand providing spinning reserve is different from that of generators. A generator has to reduce the output in order to keep spinning reserve, whereas a consumer has to be scheduled in order to provide spinning reserve. In other words, a consumer has the potential to provide spinning reserve as long as it is scheduled in the energy market. For this reason, the proposed full demand response model could exploit more flexibility from demand than the previous mentioned models. The proposed full demand response model is incorporated in the co-optimized day-ahead energy and spinning reserve market in which the expected net cost under any credible system state, i.e. expected total cost of operation minus total benefit of demand, is minimized. The market clearing problem is formulated as a two-stage stochastic security constrained unit commitment (SCUC) problem and solved by mixed integer linear programming. The most economy solution

with a probabilistic spinning reserve scheme is obtained by balancing the energy plus spinning reserve cost and cost of expected energy not served (EENS).

The rest of this chapter is organized as follows. In Section 5.1, the model of full demand response is described. Then, the co-optimized day-ahead energy and spinning reserve market dispatch problem is formulated in Section 5.2. After that, results of case studies are presented in Section 5.3. Finally, the conclusions are given in Section 5.4.

The main content in this chapter can also be found in Liu and Tomsovic (2013a).

5.1 Model of Full Demand Response

Participating in the day-ahead market gives the consumers the opportunity to reduce their electricity charges by adjusting their activities once the market has cleared. However, not all consumers have the ability or motivation to adjust their demand as a function of prices. For this reason, demand can be divided into price taking and price responsive demands. This section will propose a full demand response model for the price responsive demands. The proposed model is actually a compound bidding mechanism, including price responsive shiftable demand bidding in energy market and spinning reserve bidding in the reserve market. The two bids are coupled since the amount of spinning reserve that a demand can provide depends on the accepted energy bids in the energy market.

Price responsive shiftable demand bids have been proposed in Su and Kirschen (2009). DRPs on behalf of consumers who have the means to reschedule their consumption can submit bids that are sensitive to electricity prices in the energy market. Hence, DRPs can shift the demand from periods of high electricity price to periods in which market price is comparatively low and maximize benefit over the complete scheduling horizon in day-ahead market.

A typical price responsive shiftable demand bid is shown in Fig. 6.2. In this bid, the following characteristics can be included:

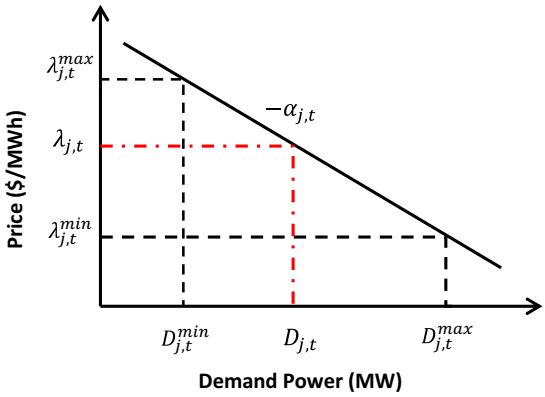

Figure 5.1: A typical price responsive shiftable demand bid

- minimum energy consumption at any period D_{jt}^{min};
- maximum energy consumption at any period D_{jt}^{max};
- total energy consumption over the scheduling horizon;
- demand pickup/drop rate;
- minimum up/down time limits.

It is clear from the negative slop bidding curve of Fig. 6.2 that DRPs would only accept that amount of demand for which the bidding price λ_{jt} is less than or equal to the market price (i.e. LMP). The benefit functions of a DRP can be determined by integral of the bidding curve from 0 to D_{jt}

$$B_{jt}(D_{jt}) = \left(\lambda_{jt}^{max} + \alpha_{jt} D_{jt}^{min}\right) D_{jt} - 0.5\alpha_{jt} \left(D_{jt}\right)^2 \tag{5.1}$$

The quadratic benefit function of a DRP can be approximated by piecewise linear functions like generation units (Wang et al., 2003). The detailed mathematical model is shown in 5.2.2

The spinning reserve bids are coupled with the price responsive shiftable demand bids since it is constrained by the accepted energy bids. DRPs on behalf of consumers

who have the means to reduce their scheduled consumption in the energy market when a contingency happens can submit bids in the spinning reserve market. It should be noted that the price responsive shiftable demand bids make use of the flexibility of demand in the day-ahead scheduling before the realization of system contingencies, while the spinning reserve bids utilize the flexibility of rescheduling the previous scheduled demand when system is in contingency. In fact, the price responsive shiftable demand bids are DRPs' adaption to price in the first stage, while the spinning reserve bids are DRPs' adaption to contingencies in the second stage. They are physically different.

The spinning reserve bids that DRPs can submit are quite flexible. In particular, the following characteristic can be included:

- conventional price-volume bid at a specific period;
- maximum spinning reserve at any period;
- maximum daily curtailment;
- demand pickup/drop rate.

Similar to generation units, the cost of providing spinning reserve by DRPs includes two parts: capacity cost and deployment cost. The deployment cost can be obtained from the benefit function as in subsection 5.2.4. In addition, the demand recovery effect after deploying spinning reserve is considered in the model.

5.2 Formulation of SCUC with Full Demand Response

This section describes a market clearing process that accept complex bids from both generation and demand sides. The market operator collects all offers and bids and then performs a multi-period optimization to determine the optimal production and

consumption schedules as well as the required amount of spinning reserve from both sides. The optimization problem is formulated as a two-stage stochastic mixed-integer linear programming model. The first stage involves the network-constrained unit commitment with probabilistic spinning reserve requirements in the base case without contingency and the second stage involves the recourse in scenarios where contingencies are realized. The formulation of the problem includes the objective function, the first stage and second stage constraints and the linking constraints, which bind the market decisions to the actual operation of the power system Morales et al. (2009).

5.2.1 Objective Function

The objective function minimizes the expected net cost (i.e. combined energy cost, spinning reserve cost, the expected cost of deploying spinning reserve in all scenarios weighted by probabilities of corresponding scenarios minus the total benefit

of demand). The expected net cost (ENC) is shown in (5.2).

$$
\begin{aligned}
Min_{p_{Git},u_{Git},p_{Djt},u_{Djt},R_{it},R_{jt},r_{Git},r_{Dit},L^{\omega}_{jt}} \quad & \sum_{t=1}^{NT}\sum_{i=1}^{NG}\sum_{m=1}^{Noit}[\lambda_{Git}(m)p_{Git}(m)+A_i u_{Git}] \\
& -\sum_{t=1}^{NT}\sum_{j=1}^{ND}\sum_{m=1}^{Nojt}[\lambda_{Djt}(m)p_{Djt}(m)+B_j u_{Djt}] \\
& +\sum_{t=1}^{NT}\sum_{i=1}^{NG} S_{it}\left(u_{Git},u_{Gi,t-1}\right) \\
& +\sum_{t=1}^{NT}\sum_{i=1}^{NG}\left(C^{U}_{it}R^{U}_{it}+C^{D}_{it}R^{D}_{it}\right) \\
& +\sum_{t=1}^{NT}\sum_{j=1}^{ND}\left(C^{U}_{jt}R^{U}_{jt}+C^{D}_{jt}R^{D}_{jt}\right) \\
& +\sum_{\omega=1}^{NW}\pi_{\omega}\left\{\sum_{t=1}^{NT}\sum_{i=1}^{NG}\sum_{m=1}^{Noit}\lambda_{Git}(m)r_{Git}(m)\right. \\
& \qquad +\sum_{t=1}^{NT}\sum_{j=1}^{ND}\sum_{m=1}^{Nojt}\lambda_{Djt}(m)r_{Djt}(m) \\
& \qquad \left.+\sum_{t=1}^{NT}\sum_{j=1}^{ND}VOLL_{jt}L^{\omega}_{jt}\right\} \qquad (5.2)
\end{aligned}
$$

The objective function includes eight terms [from line 1 to line 8 in (5.2)]:

1. the energy cost of generators;
2. the minus benefit of DRPs;
3. the start up cost of generators;
4. the cost of scheduling up- and down-spinning reserve from generators;
5. the cost of scheduling up-and down-spinning reserve from DRPs;
6. the cost associated to the actual deployment of up- and down-spinning reserve by generators;

7. the cost associated to the actual deployment of up- and down-spinning reserve by DRPs;

8. the cost of involuntary load shedding.

As stated in (5.2), all terms are in mixed-integer linear form except 3) the startup cost of generators. Nonetheless, it can be recast into mixed-integer linear form just as in Ortega-Vazquez (2006). The optimization variables include $p_{Git}(m)$, u_{Git}, $p_{Djt}(m)$, u_{Djt}, R^U_{it}, R^D_{it}, R^U_{jt}, R^D_{jt}, $r_{Git}(m)$, $r_{Dit}(m)$ and L^{ω}_{jt}.

5.2.2 First-Stage Constraints

Production Limits

$$P_{it} = \sum_{m=1}^{Noit} p_{Git}(m) + u_{Git} P_i^{min} \quad \forall i,\ \forall t \tag{5.3}$$

$$0 \leq p_{Git}(m) \leq p_{Git}^{max}(m) \quad \forall i,\ \forall t\, \forall m \tag{5.4}$$

Equation (5.3) and (5.4) approximate the energy cost function of generators by blocks Aminifar et al. (2009).

Demand Limits

$$D_{jt} = \sum_{m=1}^{Nojt} p_{Djt}(m) + u_{Djt} D_{jt}^{min} \quad \forall j,\ \forall t \tag{5.5}$$

$$0 \leq p_{Djt}(m) \leq p_{Djt}^{max}(m) \quad \forall i,\ \forall t\, \forall m \tag{5.6}$$

$$\sum_{t=1}^{NT} D_{jt} \triangle t \leq E_j \quad \forall j \tag{5.7}$$

$$0 \leq D_{jt} \leq \frac{E_j}{\triangle t} \quad \forall j,\ \forall t \tag{5.8}$$

Similar to production limits, equation (5.5) and (5.6) approximate the benefit function of DRPs by blocks. Equation (5.7) specifies the total energy consumption over the scheduling horizon and equation (5.8) specifies the maximum amount of energy that can be consumed in a single period.

Market Equilibrium

$$\sum_{i=1}^{NG} P_{it} = \sum_{j=1}^{ND} \left(D_{jt} + D_{jt}^{F}\right) \quad \forall t \tag{5.9}$$

Transmission Flow Limits

$$\sum_{i=1}^{NG} GSF_{ki} P_{it} - \sum_{j=1}^{ND} GSF_{kj} \left(D_{jt} + D_{jt}^{F}\right) \leq F_{k}^{max} \quad \forall k, \forall t \tag{5.10}$$

DC power flow is used to simulate the transmission constraints. Similarly, the opposite direction flow limit can be obtained.

Scheduled Reserve Determination Constraints

Generation-side:

$$0 \leq R_{it}^{U} \leq RU_i \tau \quad \forall i, \forall t \tag{5.11}$$

$$0 \leq R_{it}^{D} \leq RD_i \tau \quad \forall i, \forall t \tag{5.12}$$

$$R_{it}^{U} + P_{it} \leq P_{i}^{max} u_{Git} \quad \forall i, \forall t \tag{5.13}$$

$$R_{it}^{D} + P_{i}^{min} u_{Git} \leq P_{it} \quad \forall i, \forall t \tag{5.14}$$

Demand-side:

$$0 \leq R_{jt}^{U} \leq RD_j \tau \quad \forall j, \forall t \tag{5.15}$$

$$0 \leq R_{jt}^{D} \leq RU_j \tau \quad \forall j,\ \forall t \tag{5.16}$$

$$R_{jt}^{U} + D_{jt}^{min} u_{Djt} \leq D_{jt} \quad \forall j,\ \forall t \tag{5.17}$$

$$R_{jt}^{D} + D_{jt} \leq D_{jt}^{max} u_{Djt} \quad \forall j,\ \forall t \tag{5.18}$$

Ramping Rate Limits

Generation-side:

$$P_{it} - P_{i,t-1} \leq RU_i u_{Gi,t-1} + R_i^{\text{start}} \left(u_{Git} - u_{Gi,t-1}\right) \quad \forall i,\ \forall t \tag{5.19}$$

$$P_{it} - P_{i,t-1} \geq -RD_i u_{Git} - R_i^{\text{shut}} \left(u_{Gi,t-1} - u_{Git}\right) \quad \forall i,\ \forall t \tag{5.20}$$

$$R_i^{\text{start}} = max\left\{RU_i, P_i^{\min}\right\} \quad \forall i \tag{5.21}$$

$$R_i^{\text{shut}} = max\left\{RD_i, P_i^{\min}\right\} \quad \forall i \tag{5.22}$$

It should be noted that the trajectories of generators' startup and shut-down process are neglected in the proposed model. Constraint (5.19) ensures that the increment in the output power ($\triangle P_{i,t} = P_{i,t} - P_{i,t-1}$) cannot be greater than the ramp limits of the generator, or if it is startup to its minimum stable generation. The ramp-down constraint (5.20) is formulated in an equivalent way.

Demand-side:

$$D_{jt} - D_{j,t-1} \leq RU_j u_{Dj,t-1} + R_j^{\text{start}} \left(u_{Djt} - u_{Dj,t-1}\right) \quad \forall j,\ \forall t \tag{5.23}$$

$$D_{jt} - D_{j,t-1} \geq -RD_j u_{Djt} - R_j^{\text{shut}} \left(u_{Dj,t-1} - u_{Djt}\right) \quad \forall j,\ \forall t \tag{5.24}$$

$$R_j^{\text{start}} = \max\left\{RU_j, D_j^{\min}\right\} \quad \forall j \tag{5.25}$$

$$R_j^{\text{shut}} = \max\left\{RD_j, D_j^{\min}\right\} \quad \forall j \tag{5.26}$$

The minimum up/down time constraints are imposed through binary variables u_{Git} and u_{Djt} (Carrión and Arroyo, 2006). For the sake of conciseness, the mathematical formulations of them are omitted.

5.2.3 Second Stage Constraints (Depending on Scenario ω)

Power Balance

$$\sum_{i=1}^{NG} P_{it\omega} = \sum_{j=1}^{ND} \left(D_{jt\omega} + D_{jt}^{F} - L_{jt\omega}\right) \quad \forall t, \forall \omega \tag{5.27}$$

Transmission Flow Limits

$$\begin{aligned} \textstyle\sum_{i=1}^{NG} GSF_{ki} P_{it\omega} - \sum_{j=1}^{ND} GSF_{kj} \left(D_{jt\omega} + D_{jt}^{F} - L_{jt\omega}\right) \\ \leq F_{k}^{max} \qquad \forall k, \forall t, \forall \omega \end{aligned} \tag{5.28}$$

Involuntary Load Shedding Limits

$$0 \leq L_{jt\omega} \leq L_{jt}^{max} \quad \forall j, \forall t\,, \forall \omega \tag{5.29}$$

Demand Recovery Limit

$$\sum_{t=1}^{NT} D_{jt\omega} \geq \gamma\% \sum_{t=1}^{NT} D_{jt} \quad \forall j, \forall \omega \tag{5.30}$$

Equation (5.30) specifies the recovery limit of demand j. The recovery rate γ is a characteristic of individual demand, determined by the properties of activity facilitated by through the use of electricity.

5.2.4 Constraints Linking First and Second Stage Variables

Generator Power Output

$$P_{it\omega} = P_{it}\xi_{it\omega} + r_{it\omega}^{U} - r_{it\omega}^{D} \quad \forall i, \forall t\,, \forall \omega \tag{5.31}$$

In order to consider the reliability of generators, $\xi_{it\omega}$ is a binary variable where 1 represents the healthy state of a generator and 0 otherwise.

Demand Consumption

$$D_{jt\omega} = D_{jt} + r^{D}_{jt\omega} - r^{U}_{jt\omega} \quad \forall j, \forall t, \forall \omega \tag{5.32}$$

Deployed Spinning Reserve Constraints

Generation-side:

$$r^{U}_{it\omega} \leq R^{U}_{it}(1 - H_{t\omega})\xi_{it\omega} \quad \forall i, \forall t, \forall \omega \tag{5.33}$$

$$r^{D}_{it\omega} \leq R^{D}_{it}(1 - H_{t\omega})\xi_{it\omega} \quad \forall i, \forall t, \forall \omega \tag{5.34}$$

Health indicator $H_{t\omega}$ is a binary variable where 1 represents no contingency happens in and before period t and 0 otherwise. By introducing $H_{t\omega}$, the spinning reserve can only be deployed after a contingency happens.

Demand-side:

$$r^{U}_{jt\omega} \leq R^{U}_{jt}(1 - H_{t\omega}) \quad \forall j, \forall t, \forall \omega \tag{5.35}$$

$$r^{D}_{jt\omega} \leq R^{D}_{jt}(1 - H_{t\omega}) \quad \forall j, \forall t, \forall \omega \tag{5.36}$$

Decomposition of Deployed Spinning Reserve into Blocks

Generation-side:

$$r^{U}_{it\omega} - r^{D}_{it\omega} = \sum_{m=1}^{Noit} r_{Git\omega}(m) \quad \forall i, \forall t, \forall \omega \tag{5.37}$$

$$r_{Git\omega}(m) \leq p^{max}_{Git}(m) - p_{Git}(m) \quad \forall m, \forall i, \forall t, \forall \omega \tag{5.38}$$

$$-p_{Git}(m) \leq r_{Git\omega}(m) \quad \forall m, \forall i, \forall t, \forall \omega \tag{5.39}$$

Demand-side:

$$r^{U}_{jt\omega} - r^{D}_{jt\omega} = \sum_{m=1}^{Nojt} r_{Djt\omega}(m) \quad \forall j, \forall t, \forall \omega \tag{5.40}$$

$$r_{Djt\omega}(m) \leq p_{Djt}(m) \quad \forall m, \forall j, \forall t, \forall \omega \tag{5.41}$$

$$p_{Djt}(m) - p^{max}_{Djt}(m) \leq r_{Djt\omega}(m) \quad \forall m, \forall j, \forall t, \forall \omega \tag{5.42}$$

Equation (5.37) decompose the deployed spinning reserve into blocks. Equation (5.38) and (5.39) enforce that the blocks of spinning reserve are added (or subjected in case of down-spinning reserve) to blocks of energy (Morales et al., 2009). Thus, the cost of deployment of spinning reserve is as expressed in the objective function (5.2). Similarly, the deployed spinning reserve from demand-side can be decomposed into blocks.

In the proposed two-stage model, decisions made in the first stage include commitment status of units, scheduled power output and consumption and up/down spinning reserve from both generation and demand sides. Decisions made in the second stage include deployment of spinning reserve from both sides and involuntary load shedding. It should be noted the decisions on commitment status of units is only made in the first stage and doesn't change in any scenario. The deployment of spinning reserve and involuntary load shedding are determined in each scenario in order to survive the contingency.

5.3 Case study

5.3.1 Test System Data

In this section, the proposed full demand response model is demonstrated on a modified IEEE Reliability Test System (Grigg et al., 1999). In this system, there

are 26 thermal generators and the hydro units have been removed. The ramp rates, failure rates and quadratic cost coefficients are taken from Wang and Shahidehpour (1993). For simplicity, the unit quadratic cost curves in Wang and Shahidehpour (1993) are converted into piece-wise linear cost curves. In addition, we assume that all units offer capacity cost of up and down spinning reserve at the rates of 10% of their highest incremental cost of producing energy Bouffard and Galiana (2004). The deployment cost of spinning reserve from units is calculated according there actual cost of energy.

The analysis is conducted for a 24-h scheduling horizon and the forecast demand is shown as in Table 5.1 (Wang and Shahidehpour, 1993). The demand forecast error is neglected. Each demand contains two parts: fixed part and responsive part. The proposed full demand response model is for the responsive part delegated to a DRP at each bus. The price elasticity of DRPs' offer price is set as 0.1\$/MW^{2}h (Singh et al., 2011). The maximum and minimum energy consumption of all DRPs is set as 200 MW and 0MW, respectively. The maximum energy bidding price of DRPs is set as 45 \$/MWh. Based on these parameters, DRPs' benefit functions are calculated, and then linearized into 3 pieces. DRPs offer capacity cost of spinning reserve at the rate of 20% of benefit of energy. The deployment cost of spinning reserve from DRPs is calculated according there actual energy cost. VOLL is set to be 4,000 \$/MWh (Parvania and Fotuhi-Firuzabad, 2010).

A two-state Markov model is used to simulate the uncertainties of units (Billinton and Allan, 1996). A set of scenarios is constructed based on "$n-1$" contingency rules. Only single order contingency events are taken into account since multiple order contingency events have relatively small probabilities while consuming far more computational resources. So, we have 26 fault scenarios. The transmission constraints are included in both the first and second stages by using DC power flow.

Three cases are considered in the simulation. In case 1, no demand response is considered. In case 2, 10% of the demand is considered as responsive demand, which can bid in both energy and spinning reserve market. In case 3, 20% of the demand

is considered as responsive demand. The recovery rate of each load after deployed as spinning reserve is set as 0.7. The model is coded in a MATLAB environment and solved using a MILP solver CPLEX 12.2. With a pre-specified duality gap of 0.1%, the running time of each case is about 8 minutes on a 2.66 GHz Windows-based PC with 4 G bytes of RAM.

Table 5.1: Forecast demand

Hour	Load (MW)	Hour	Load (MW)	Hour	Load (MW)
1	1700	9	2540	17	2550
2	1730	10	2600	18	2530
3	1690	11	2670	19	2500
4	1700	12	2590	20	2550
5	1750	13	2590	21	2600
6	1850	14	2550	22	2480
7	2000	15	2620	23	2200
8	2430	16	2650	24	1840

5.3.2 Comparison of Unit Commitment Results

The results of unit commitment with different percentages of demand response are presented in Fig. 5.2. As can be seen, when there is no demand response, units 1-5, 14-16 and 21-23 need to be committed during the peak load hours and decommitted during the valley load hours. When there is 10% demand response, this difference between peak load and valley load is mitigated by shifting load from peak hours to valley hours. Consequently, more units can be committed through the whole dispatching horizon. In this case, unit 1-5 and unit 14-16 are committed for all 24 hours and unit 23 is keeping off all the time. This effect is more obvious when the demand response in increased to 20%. In this case, the unit commitment status is the same for all 24 hours. In this way, the times of starting up and shutting down of units are greatly decreased.

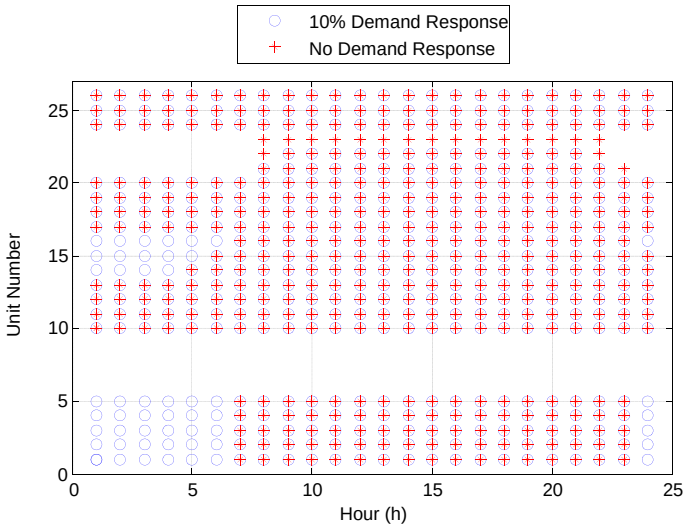

(a) Unit status of case 1 and 2

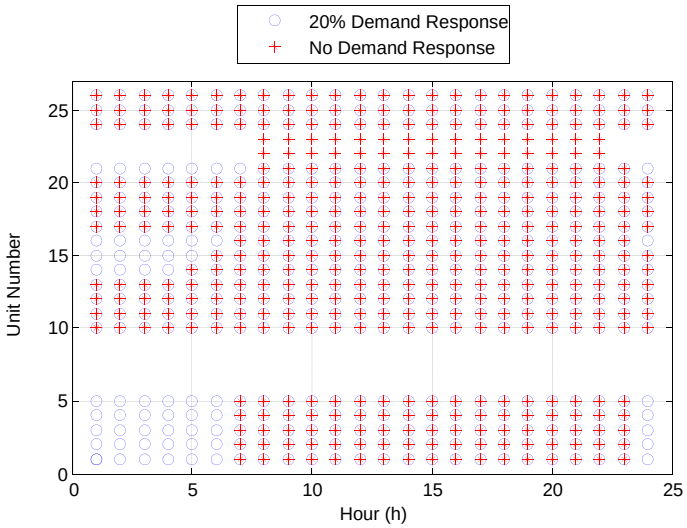

(b) Unit status of case 1 and 3

Figure 5.2: Comparison of unit status with different percentages of demand response: more demand response; more uniform unit commitment results

5.3.3 Comparison of Total Demand

The total demand profiles with different percentages of demand response are shown in Fig. 5.3. As can be seen, demands are shifted from the peak hours (Hour 8-22) to valley hours (Hour 23-7). As demand response is increased to 20 %, the demand profile is almost flat. This is as expected.

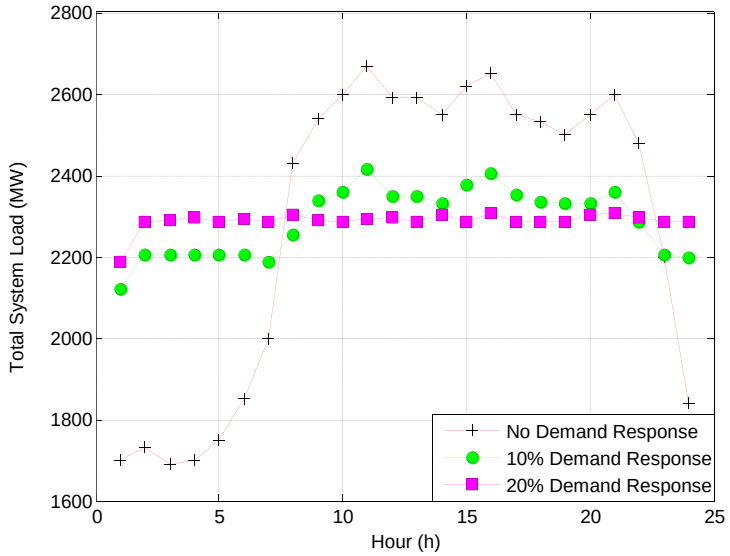

Figure 5.3: Demand profiles under three cases: more demand response; flatter demand profile

5.3.4 Comparison of Spinning Reserve and EENS

The spinning reserve and EENS profiles with different percentages of demand response are shown in Fig. 5.4. It can be seen that both the spinning reserve and EENS profiles are fluctuating in case 1 without demand response. This is due to the starting up and shutting down of units when demand is changing. As demand response is introduced, these profiles become flat as a result of more consistent unit commitment results. It should also be noted that the EENS values with demand response are a little higher than the ones without demand response. The reason is that fewer units are committed

since demand could provide spinning reserve instead of generators as well as demand profile becomes flat. In addition, the cost of spinning reserve from DRPs is much expensive than that from generators. This results in less spinning reserve and higher EENS.

5.3.5 Comparison of Spinning Reserve Provided by Generation and Demand

The comparison of spinning reserve provided by generators and demand when there are 10% demand response is presented in Fig. 5.5. As can be seen that DRPs provide spinning reserve in both peak and valley load hours. There are two reasons for demand providing more spinning reserve during valley hours than that during peak hours. Firstly, there is more demand response during valley load hours since responsive demand is shifted from peak hours to valley hours. Secondly, unit 21 and 22 are committed at hour 8 and 9 separately, as a result, additional inexpensive spinning reserve are available from these two generators.

It should be noted that not all the responsive demand is scheduled as spinning reserve at the same time (Fig. 5.3). It may be more economical to cut more load or scheduling spinning reserve from generators instead of scheduling more spinning reserve from DRPs.

5.3.6 Comparison of Total Cost

The total operating costs of system with different percentages of demand response are presented in Fig. 5.6. As can be seen, the total cost decreases as the percentage of demand response increases, i.e. the flexibility of demand increases. However, it should be noted that the slope of reduction is not consistent. In fact, the slop of reduction decreases as the percentage of demand response increase. Particularly, when the demand response increases from 15% to 20%, the total cost reduction is very small.

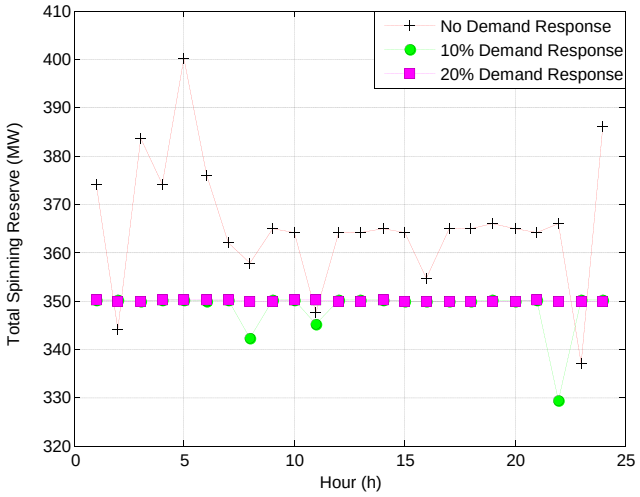

(a) Spinning reserve under three cases

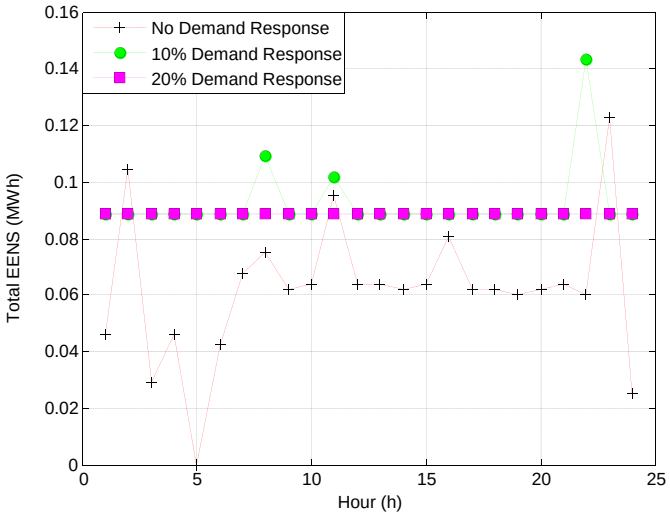

(b) EENS under three cases

Figure 5.4: Spinning reserve and EENS under different percentage of demand response: more demand response; more uniform spinning reserve and EENS

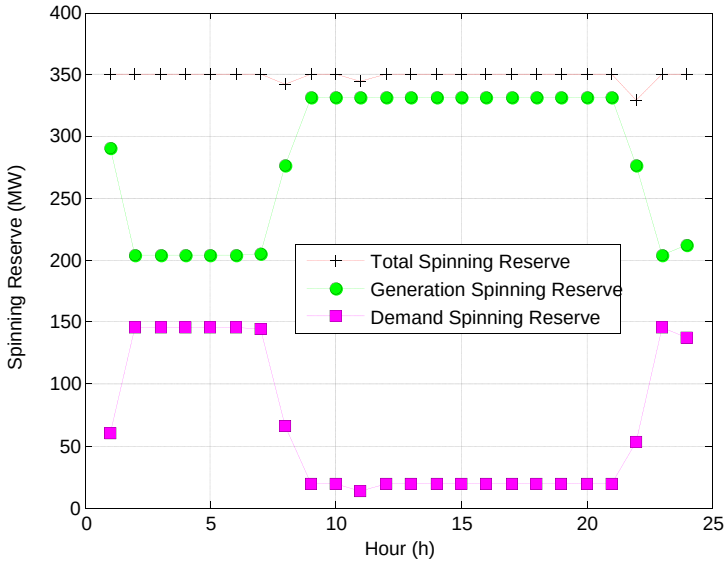

Figure 5.5: Comparison of spinning reserve from generators and demand

This is because the load profile is already flat and spinning reserve from demand is sufficient. Additional flexibility from demand cannot make changes greatly.

5.3.7 Comparison of LMP

The LMP of system with different percentages of demand response are presented in Fig. 5.7. As can be seen, the LMP of system without demand response is unstable and fluctuating with the load profile. There is a great price difference between the peak hour (9-22) and valley hours (23-7). When 10% of demand response is introduced, this price difference is reduced and the high price hours are also reduced. With 20% of demand response, the LMP of system is almost a constant value.

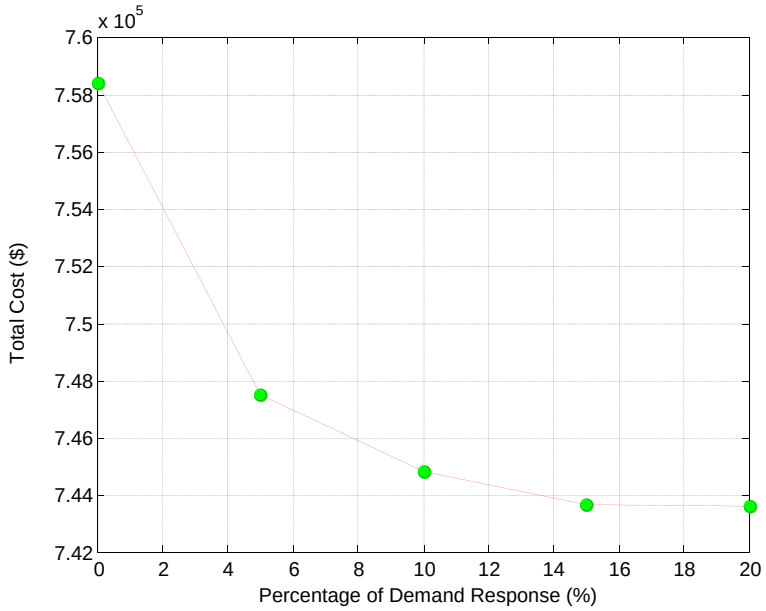

Figure 5.6: Total cost under different percentages of demand response: more demand response; lower cost but with diminishing effect

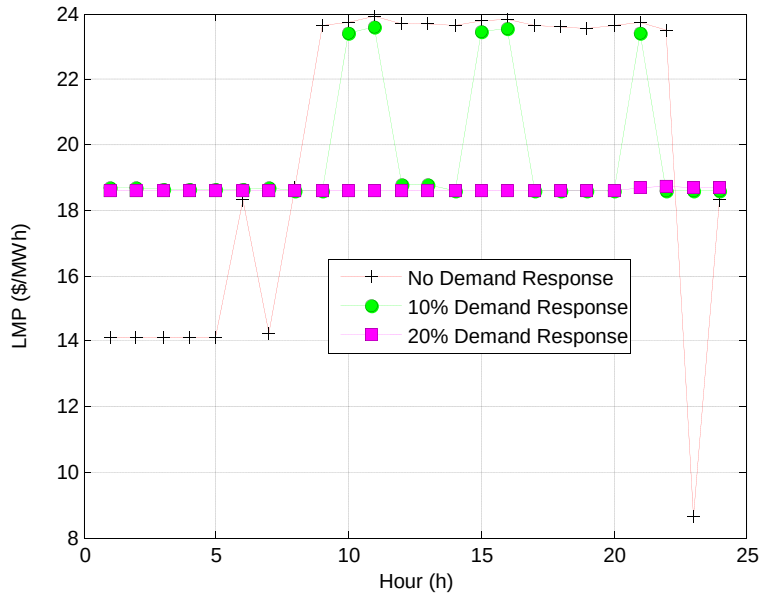

Figure 5.7: LMP under different percentages of demand response: more demand response; flatter LMP

5.3.8 Comparing Results of Shiftable Demand and Proposed Full Demand Response

In order to show the advantages of proposed full demand response model over the price responsive shiftable demand model, the dispatching results of SCUC with proposed model is compared with that of SCUC with shiftable demand model in this subsection.

Comparing Unit Commitment Results

The results of unit commitment with 10% full demand response and 10% shiftable demand are compared in Fig. 5.8a. As can be seen, the full demand response model, with fewer units committed since DRPs can also provide spinning reserve in the proposed full demand response model, leads to lower committed capacity from generators. Specifically, DRPs provide comparable amount of spinning reserve with the proposed full demand response model during hours 1-8 and 22-24 as shown in Fig. 5.5. With these additional reserve, unit 21 doesn't need to be committed during hour 1-7 and 23-24 as well as unit 22 during hour 7-8 and 22-24. In contrast, these units have to be committed to provide spinning reserve with the shiftable demand model. The same effect can be seen when the full demand response and shiftable demand are increased to 20% as in Fig. 5.8b. With 20% of shiftable demand, unit 22 is committed during hours 2-22 and decommitted during other hours. Compared to the proposed full demand response model, unit 22 does not need to be committed and the unit commitment status is the same for all 24 hours. In this way, the frequency of starting up and shutting down of the units is decreased.

Comparing Total Demand

The total demand profiles with different percentages of full demand response and shiftable demand are compared in Fig. 5.9. As can be seen, with 10% full demand response model, the total demand during peak hours (Hour 9-21) is higher than that with 10% of shiftable load, i.e. the one with shiftable can shift more load from peak

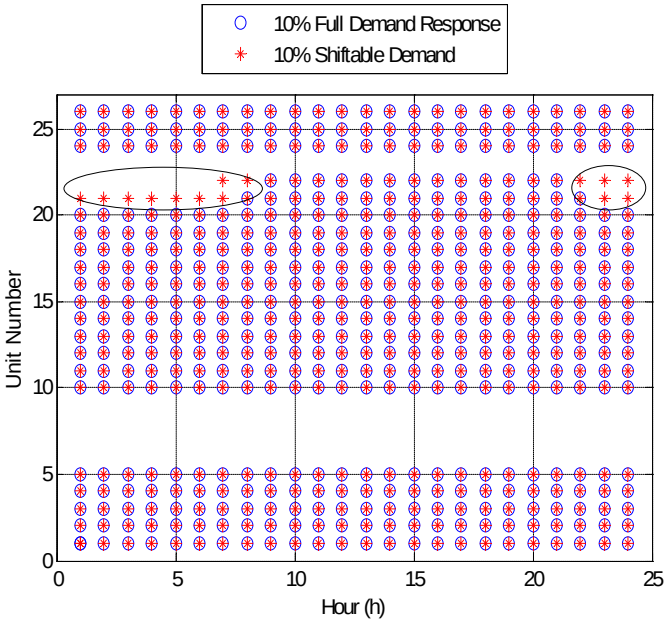

(a) 10% full demand response vs. 10% shiftable demand

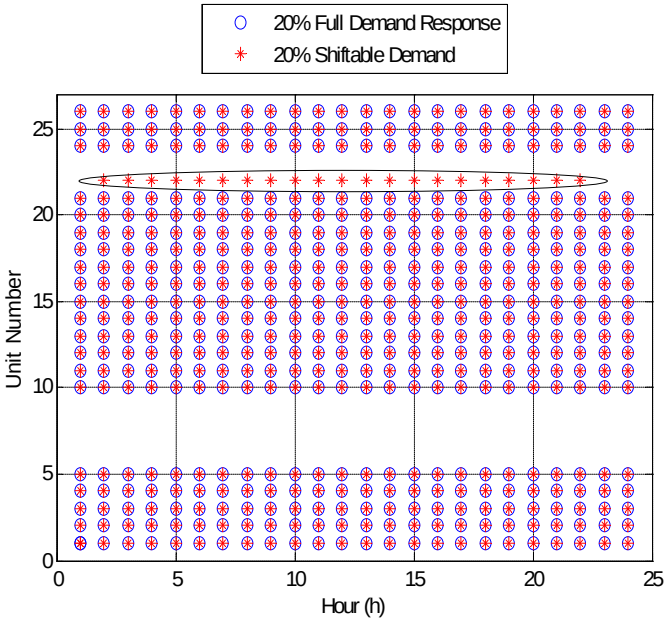

(b) 20% full demand response vs. 20% shiftable demand

Figure 5.8: Comparison of unit status between full demand response and shiftable demand: with full demand response, less units are committed

hours to valley hours. This is due to the reason that it is more economic keeping some responsive load and providing spinning reserve during peak hours compared to shifting them to valley hours and starting up additional units during the valley hours. When the responsive demand penetration increases to 20%, the demand profile with shiftable demand is higher than that with full demand response during hour 3-22. This is due to unit 22 is shut down at hour 23 and 24 as shown in Fig. 5.8b, hence demand reduced during hours 23and 24 is shifted to other hours.

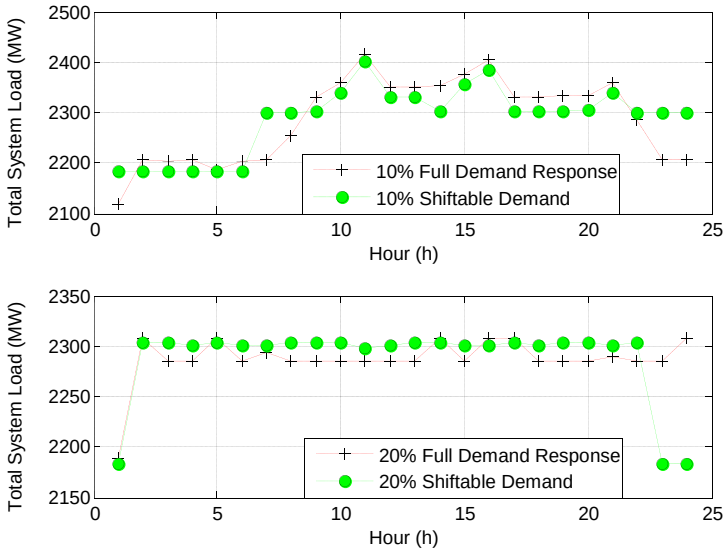

Figure 5.9: Comparison of total demand: full demand response vs. shiftable demand

Comparing Spinning Reserve and EENS

The spinning reserve and EENS profiles with 10% full demand response and 10% shiftable demand are shown in Fig. 5.10a. As can be seen, with full demand response model, the spinning reserve level is lower than that with shiftable demand at hours 7-9,14, 17-20 and 22-24. Consequently, the EENS with full demand response is higher than that with shiftable demand. Although demand can provide spinning reserve with the full demand response model, the spinning reserve that generators can provide is reduced under the same unit commitment since less demand is shifted as shown in Fig.

5.9. In addition, the spinning reserve from DRPs is more expensive than that from generators. This explains why the spinning reserve level with full demand response is slightly lower than with shiftable demand during hours 9, 14 and 17-20. During hours 7-8 and 22-24, additional units are committed with shiftable demand as shown is Fig. 5.8a. This results in the spinning reserve level with full demand response is further lower than with shiftable demand in these hours. The same effect can be seen in Fig. 5.10b during hours 2-22, when the full demand response and shiftable demand are increased to 20%.

Table 5.2: Classified costs with different models of demand response

Percentage of Demand Response (%)	10		20	
Demand Response Model	Shiftable	Full	Shiftable	Full
Energy Cost ($)	718,649.03	707,448.80	718,450.08	702,622.56
Reserve Scheduling Cost of Generators ($)	17,511.56	14,391.42	17,758.99	13,362.94
Reserve Scheduling Cost of DRPs ($)	0	13,154.07	0	17,087.28
Reserve Deployment Cost of Generators ($)	854.56	797.85	859.70	782.85
Reserve Deployment Cost of DRPs ($)	0	172.53	0	237.24
Involuntary Load Shedding Cost ($)	8,271.40	8,870.22	7,809.82	8,518.18

Classified and Total Costs

The classified costs with different models of demand response are presented in Table 5.2. It can be seen that the energy cost and reserve scheduling cost of generators are significantly decreased when the proposed full demand response model is introduced. Specifically, the energy cost (including start-up cost) is reduced by 1.56% and 2.11% when the percentage of demand response is 10% and 20% respectively. This is because the proposed full demand response model leads to less committed capacity and less

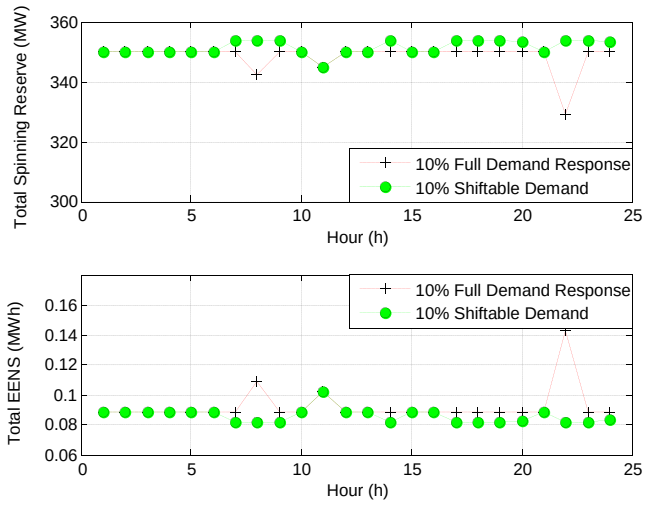

(a) 10% full demand response vs. 10% shiftable demand

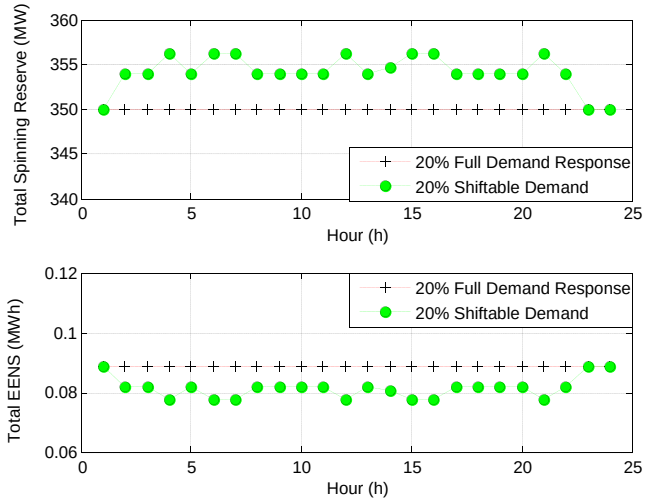

(b) 20% full demand response vs. 20% shiftable demand

Figure 5.10: Comparison of spinning reserve and EENS between full demand response and shiftable demand: with full demand response, more uniform spinning reserve and EENS

starting up and shutting down of the units. This ensures that more units are operating continuously and efficiently. With the proposed model, DRPs can provide spinning reserve instead of generators. Consequently, the reserve scheduling and deployment cost of DRPs cannot be neglected. It should be noted that the involuntary load shedding cost with proposed model can be higher than that with shiftable demand. This is because fewer units are committed since DRPs can also provide spinning reserve. In addition, the cost of spinning reserve from DRPs is more expensive than that from generators. This results in less spinning reserve and higher involuntary load shedding cost. Nevertheless, compared with the very high VOLL, the increase in the cost of spinning reserve has a very small effect on the amount of involuntary load shedding.

Table 5.3: Comparison of total costs: full demand response vs. shiftable demand

Percentage of Responsive Demand	Shiftable Demand	Full Demand Response
10%	$ 745,286.56 (100%)	$ 744,835.23 (99.96%)
20%	$ 744,878.61 (100%)	$ 743,611.20 (99.83%)

The total operating costs of the system with different percentages of full demand response and shiftable demand are compared in Table 5.3. The total cost with 10% full demand response model is slightly reduced by 0.06% relative to that with 10% shiftable demand. With 20% full demand response, the total cost can be slightly reduced by 0.17%.

With 20% full demand response, the total cost reduction rates under different capacity cost of spinning reserve from DRPs are shown in Fig. 5.11. As can be seen, when DRPs offer capacity cost of spinning reserve at the rate of 20% of the highest marginal benefit of energy, the total cost can be slightly reduced by 0.17%. However, when DRPs offer capacity cost of spinning reserve at the rate of 10% of the highest marginal benefit of energy, the total cost can be reduced by 1.77%, which is

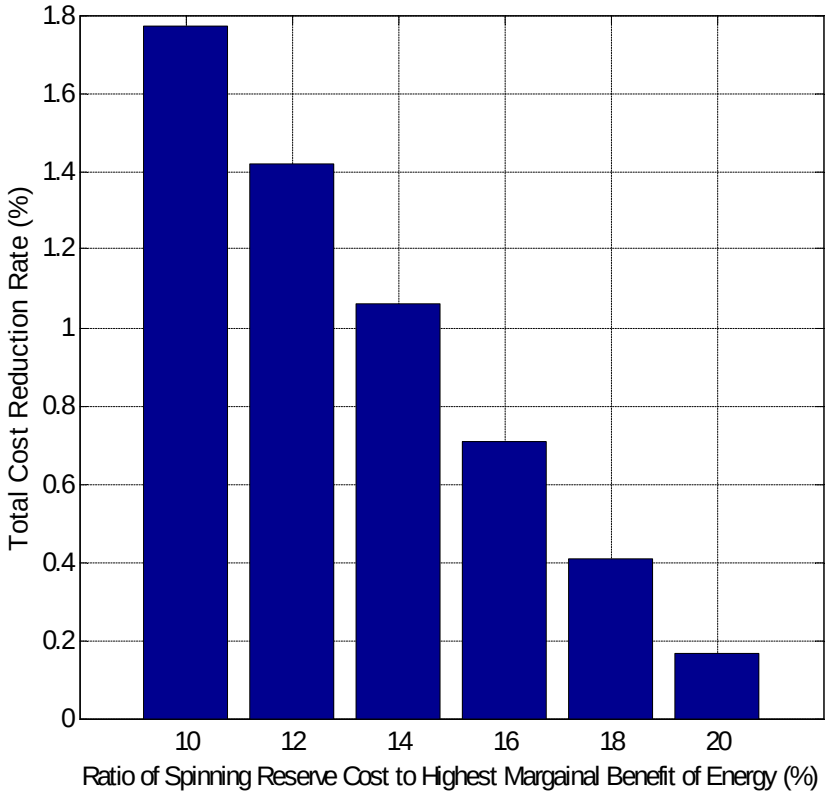

Figure 5.11: Total cost reduction rates with different capacity cost of spinning reserve from DRPs: cheaper reserve from DRPs, higher cost reduction rate

significant. In this case, the average capacity cost of spinning reserve from DRPs is reduced to 4.17 $/MW/h, which is still much higher than that from generators (2.12 $/MW/h).

5.4 Conclusion

In this chapter, a new full demand response model which allows one demand to bid in both energy market and spinning reserve market is proposed. A co-optimized day-ahead energy and spinning reserve market is proposed to maximize the expected social welfare, i.e. minimize the expected net cost under any credible system state and solved by mixed integer linear programming. Numerical simulation results on the

IEEE Reliability Test System show that the proposed model of full demand response could reduce the system operating cost, reduce on/off commitment of generators, shave the peak load and reduce the fluctuations of system reliability and energy price. Particularly, simulation results have shown that the proposed full demand response model outperform conventional demand shifting bids in operating efficiency. In other words, the second stage flexibility of demand in the proposed model leads to higher operating efficiency.

Chapter 6

Robust Unit Commitment Considering Uncertain Demand Response

The main contribution of this Chapter is to propose a new robust UC model to correct the inconsistency that occurs when the effect of uncertain demand elasticity on social welfare is calculated. In the proposed model, the objective is to minimize the generalized social cost, which consists of generation cost, and opportunity cost of reduced demand or alternative cost of electricity consumption. In this model, a low elasticity of demand results in increased generalized social costs and more generation capacity is needed, i.e., the worst case is the scenario with the lowest price elasticity of demand, which is in consistent with practical system operation. A robust unit commitment model is developed to take into account the uncertain price elasticity of demand. Numerical simulations show that the proposed model can reduce both the average electricity price and the volatility of prices.

The rest of this Chapter is organized as follows. In Section 6.1, the proposed unit commitment model to minimize generalized social cost is formulated. The robust unit commitment model considering uncertainty demand elasticity is developed in Section

6.2. Results of numerical simulations are presented in Section 6.3. Conclusions are given in Section 6.4.

The following symbols used in this Chapter indicate demand reduction, not demand consumption as in the nomenclature at the beginning of the dissertation. Thus, they are redefined below. Others will be defined as required in the text.

u_{jt} 1 if demand j is scheduled to be reduced during period t and 0 otherwise.

$d_{jt}(m)$ Demand reduction from the m-th block of demand j's reduction curve during period t (MW). Limited to $d_{jt}^{max}(m)$.

D_{jt} Demand reduction for demand j during period t (MW).

λ_{jt} Corresponding price when demand j during period t is reduced by D_{jt} ($/MWh).

$\tilde{\alpha}_{jt}$ A random variable of the slop of price elastic demand reduction curve of demand j during period t ($/$MW^2h$).

$mc_{jt}(m)$ Marginal opportunity or alternative cost of the m-th block of demand j's reduction curve during period t ($/MWh).

B_j Opportunity or alternative cost demand j when it is reduced by D_j^{min} ($/h).

D_{jt}^{max} Maximum reduction of demand j during period t (MW).

D_{jt}^{min} Minimum reduction of demand j during period t (MW).

D_{jt}^{ref} Reference responsive demand of demand j during period t without reduction (MW).

λ_{jt}^{max} Corresponding price when demand j during period t is reduced by D_{jt}^{max} ($/MWh).

λ_{jt}^{min} Corresponding price when demand j during period t is reduced by D_{jt}^{min} (\$/MWh).

λ_{jt}^{ref} Reference price when demand j during period t is not reduced (\$/MWh).

α_{jt} The slope of price elastic demand reduction curve of demand j during period t ($\$/MW^2h$).

e_{jt}^{m} The m-th elbow point of the piece-wise linear price elastic demand reduction curve of demand j during period t (MW).

$\triangle\alpha_{jt}$ Deviation from the nominal slop of price elastic demand reduction curve of demand j during period t ($\$/MW^2h$).

The main content in this chapter can also be found in Liu and Tomsovic (2013b).

6.1 Proposed UC Model Aimed to Minimize Generalized Social Cost

In this section, we first compare the proposed UC for minimizing generalized social cost with a traditional UC for maximizing social welfare. The mathematical formulation of proposed UC is presented. Consumers have the opportunity to reduce their electricity charges by adjusting their activities according to the market clearing results. However, some consumers will not have the ability or sufficient incentive to adjust their demand as a function of price. For this reason, demand is divided into fixed and price elastic demands.

A typical market equilibrium is shown in Fig. 6.1a. The maximum social welfare, which consists of consumers' surplus and suppliers' surplus, occurs at the intersection of the electricity supply and demand curves $\left(D_{jt}^{0}, \lambda_{jt}^{0}\right)$. At the same point, the generalized social cost, which consists of generation cost and opportunity cost of the reduced demand or the alternative cost of electricity consumption is minimized.

The generalized social cost can be seen as the complement of social welfare. When the social welfare is maximized, the generalized social cost is minimized and vice versa. With a deterministic supply and demand curves, a UC that minimizes generalized social cost is equivalent to a UC that maximizes social welfare.

When the demand curve is uncertain, as depicted in Fig. 6.1b, minimizing generalized social cost may no longer be equivalent to maximizing social welfare. The worst scenario in term of maximizing social welfare is when the demand curve is green with a flat slope, i.e., the price elasticity is highest, so that the social welfare is reduced by area A and the needed generation capacity is the minimum of all scenarios. In contrast, the worst scenario in term of minimizing generalized social cost is when the demand curve is grey with the greatest slope, i.e., the price elasticity is lowest, so that the generalized social cost is increased by area D and the needed generation capacity is the maximum of all scenarios. In fact, the worst scenario in term of maximizing social welfare is the best scenario in terms of minimizing generalized social cost, and vice versa.

The proposed UC model for minimizing generalized social cost is more appropriate than the traditional UC model for maximizing social welfare when the demand curve is uncertain. In real system operation, the worst scenario should be the estimated demand is much lower than the real-time demand because the price elasticity of demand is over-estimated and the real price elasticity of demand is much lower. As a result, the maximum generation capacity is needed and electricity price spikes appear. This is in contradiction with the traditional UC model for maximizing social welfare, whose worst scenario is the highest price elasticity and the needed generation capacity minimum of all scenarios. As to the proposed UC model for minimizing generalized social cost, the worst scenario is with the lowest price elasticity and the needed generation capacity maximum across all scenarios. This is consistent with practical system operation. Therefore, the proposed UC model is more appropriate than the traditional UC model when the demand curve is uncertain.

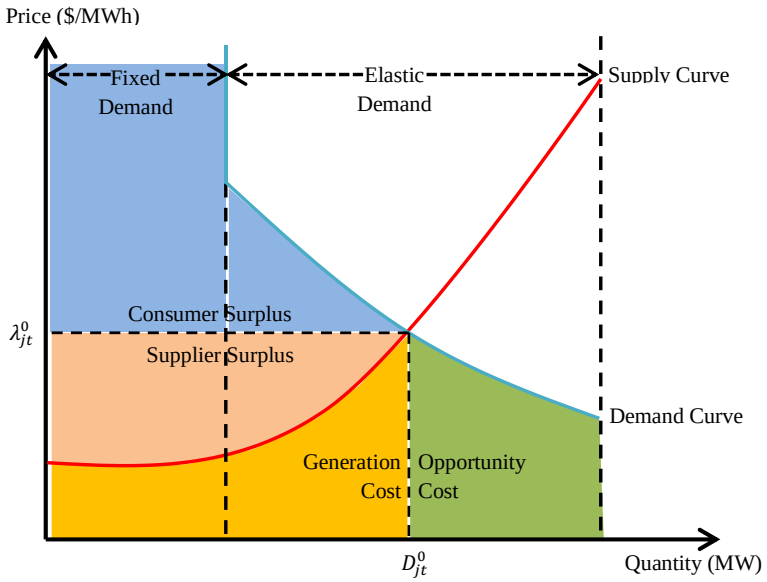

(a) Market equilibrium with deterministic demand curve: complementarity between social welfare and generalized social cost exists

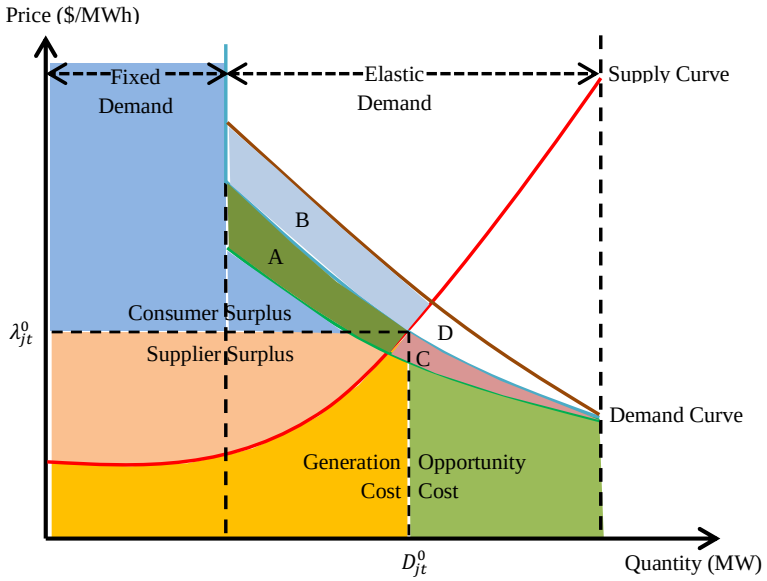

(b) Market equilibrium with uncertain demand curve: complementarity between social welfare and generalized social cost is lost

Figure 6.1: Market equilibrium with deterministic and uncertain demand curves

It should be noted that proposed UC model is not equivalent to the traditional UC model when, and only when, the demand curve is uncertain. With uncertainty, the demand curve encompasses area including A, B, C and D. Consequently, intersection of the electricity supply and demand curves changes from a single point into a curve. Under this situation, the complementarity between social welfare and generalized social cost no longer exists. In other words, maximizing social welfare is no longer equivalent to minimizing generalized social cost.

The proposed UC model to minimize the generalized social cost with deterministic demand curve (price elasticity) is as follows:

$$\begin{aligned} Min_{p_{it}(m),u_{it},d_{jt}(m),u_{jt},R_{it}} \quad & \sum_{t=1}^{NT}\sum_{i=1}^{NG}\sum_{m=1}^{NI}[\lambda_{it}(m)p_{it}(m)+A_i u_{it}] \\ & +\sum_{t=1}^{NT}\sum_{j=1}^{ND}\sum_{m=1}^{NJ}[mc_{jt}(m)d_{jt}(m)+B_j u_{jt}] \\ & +\sum_{t=1}^{NT}\sum_{i=1}^{NG}S_{it}\left(u_{it},u_{i,t-1}\right) \\ & +\sum_{t=1}^{NT}\sum_{i=1}^{NG}C_{it}R_{it} \end{aligned} \tag{6.1}$$

s.t.

$$P_{it}=\sum_{m=1}^{NI}p_{it}(m)+u_{it}P_i^{min} \quad \forall i,\ \forall t \tag{6.2}$$

$$0\le p_{it}(m)\le p_{it}^{max}(m) \quad \forall i,\ \forall t\ \forall m \tag{6.3}$$

$$D_{jt}=\sum_{m=1}^{NJ}d_{jt}(m)+u_{jt}D_{jt}^{min} \quad \forall j,\ \forall t \tag{6.4}$$

$$0\le d_{jt}(m)\le d_{jt}^{max}(m) \quad \forall j,\ \forall t,\ \forall m \tag{6.5}$$

$$\sum_{i=1}^{NG} P_{it} = \sum_{j=1}^{ND} \left(D_{jt}^{F} + D_{jt}^{ref} - D_{jt} \right) \quad \forall t \tag{6.6}$$

$$\sum_{i=1}^{NG} GSF_{ki} P_{it} - \sum_{j=1}^{ND} GSF_{kj} \left(D_{jt}^{F} + D_{jt}^{ref} - D_{jt} \right) \leq F_{k}^{max} \quad \forall k, \forall t \tag{6.7}$$

$$R_{it} + P_{it} \leq P_{i}^{max} u_{it} \quad \forall i, \forall t \tag{6.8}$$

$$P_{it} + R_{it} \leq TR \quad \forall i, \forall t \tag{6.9}$$

In the above formulation, the objection function (6.1) is the generalized social cost, including energy cost of generators (line 1), opportunity cost of reduced demand (line 2), startup cost of generators (line 3) and spinning reserve cost (line 4). All terms are in mixed-integer linear form except the startup cost of generators (line 3), which can be simply recast into mixed-integer linear form as in Ortega-Vazquez (2006). Constraints (6.2) and (6.3) approximate the energy cost of generators by blocks (Aminifar et al., 2009). Similarly, the opportunity cost of reduced demand is linearized and approximated by (6.4) and (6.5). The market equilibrium is enforced by (6.6). A DC power flow is used to represent the transmission constraints in (6.7). The coupling relationship between energy and spinning reserve is represented in constraint (6.8). The minimum amount of spinning reserve is ensured by (6.9) (Wood, 1982). Additionally, each unit or demand is subject to its own operating constraints, including minimum up and down time, initial condition, capacity limits and ramp limits. See Carrión and Arroyo (2006) for more details about the formulations of these constraints.

6.2 Robust UC with Uncertain Price Elasticity of Demand

In this section, we first introduce a price elastic demand reduction curve to represent the price elasticity. Then, the model of uncertain price elasticity is introduced. The robust UC with uncertain price elasticity of demand is formulated.

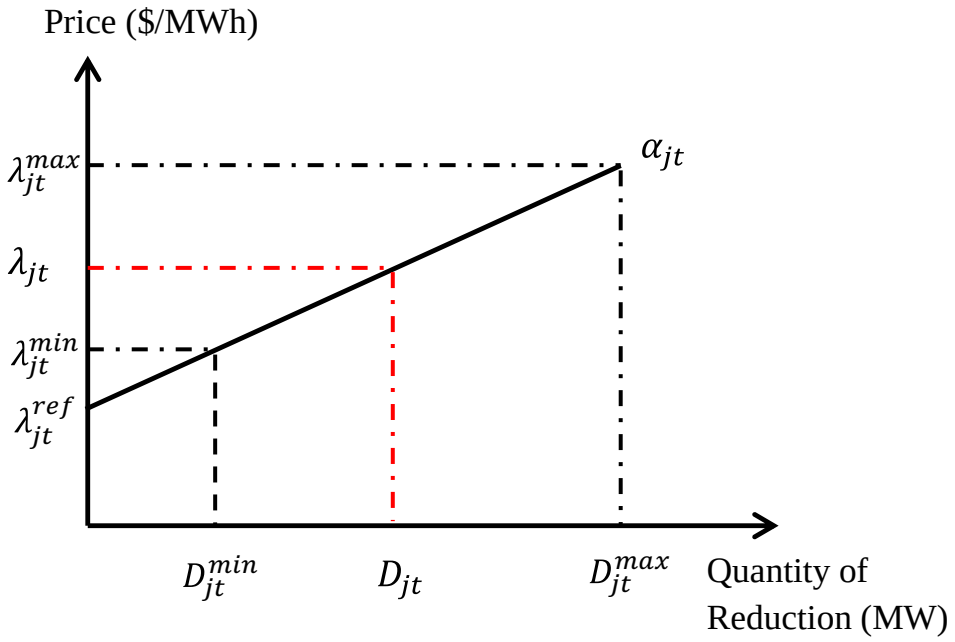

Figure 6.2: A typical price elastic demand reduction curve

A typical price elastic demand reduction curve is shown in Fig. 6.2. The demand reduction increases monotonically with electricity price increase. The slope of the curve α_{jt} represents the price elasticity of demand. The electricity price λ_{jt} of a consumer corresponding to reduction of demand by D_{jt} can be represented as

$$\lambda_{jt} = \lambda_{jt}^{ref} + \alpha_{jt} D_{jt} \tag{6.10}$$

The opportunity cost or alternative cost of reduced demand can be determined by the integral of the curve from 0 to D_{jt}.

$$OC_{jt}(D_{jt}) = \lambda_{jt}^{ref} D_{jt} + 0.5\alpha_{jt} (D_{jt})^2 \tag{6.11}$$

The quadratic cost function (6.11) can be approximated by piecewise linear functions similar to that for generation units (Ortega-Vazquez, 2006) as shown in Fig. 6.3. The marginal cost $mc_{jt}(m)$ can be represented as

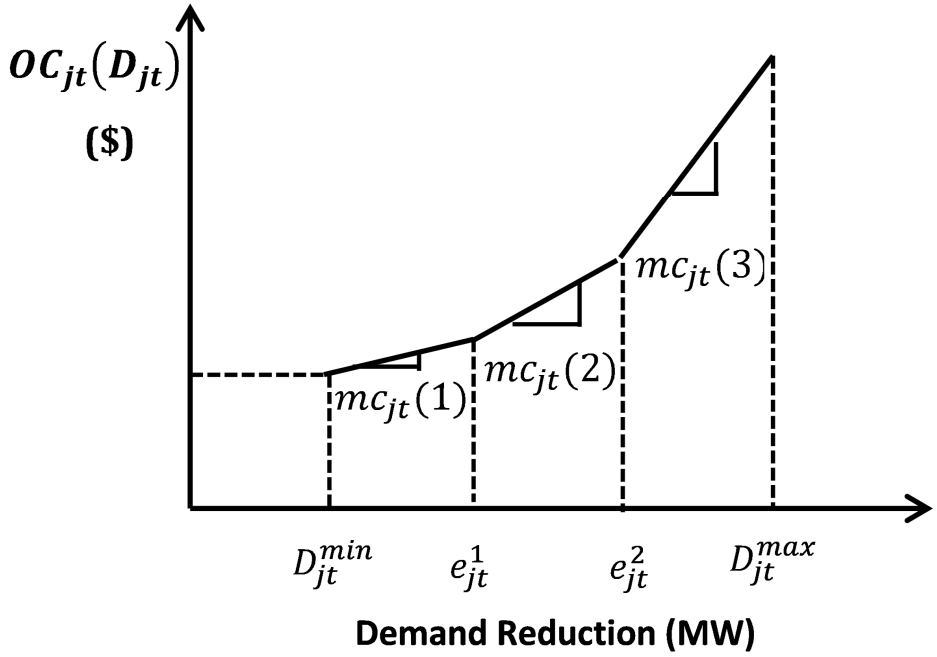

Figure 6.3: A typical piecewise linearization of quadratic cost function

$$\begin{cases} mc_{jt}(1) & = \lambda_{jt}^{ref} + 0.5\alpha_{jt}\left(D_{jt}^{min} + e_{jt}^{1}\right) \\ mc_{jt}(2) & = \lambda_{jt}^{ref} + 0.5\alpha_{jt}\left(e_{jt}^{2} + e_{jt}^{1}\right) \\ \vdots & \\ mc_{jt}(m) & = \lambda_{jt}^{ref} + 0.5\alpha_{jt}\left(e_{jt}^{m-1} + e_{jt}^{m}\right) \\ B_{jt} & = \lambda_{jt}^{ref} D_{jt}^{min} + 0.5\alpha_{jt}\left(D_{jt}^{min}\right)^{2} \end{cases} \tag{6.12}$$

In the proposed UC with deterministic price elasticity, we have deterministic estimates for the slope α_{jt} of the price elastic demand reduction curve. The parameter α_{jt} is very hard to quantify or estimate as mentioned before. Here, each α_{jt} is modeled as an independent, symmetric and bounded random variable (but with unknown distribution) $\tilde{\alpha}_{jt}$, that falls within $[\alpha_{jt} - \triangle\alpha_{jt},\ \alpha_{jt} + \triangle\alpha_{jt}]$, where $\triangle\alpha_{jt} \geq 0$.

To formulate a robust UC, we introduce an integer control parameter Γ_0, which takes values within the interval $[0,\ |J_0|]$, where $J_0 = \{(jt) \mid \triangle\alpha_{jt} > 0\}$. The parameter Γ_0 controls the level of robustness of the objective. We are interested in finding a solution that optimizes against all scenarios under which a number Γ_0 of price elasticities can vary in such a way as to maximally increase the objective function. If $\Gamma_0 = 0$, the uncertainty of price elasticity is completely ignored, while if $\Gamma_0 = |J_0|$, uncertainties in price elasticity are fully considered, leading to the most conservative solution (Baringo and Conejo, 2011; Bertsimas and Sim, 2003).

$$
\begin{aligned}
Min_{p_{it}(m),u_{it},d_{jt}(m),u_{jt},R_{it}} \quad & \sum_{t=1}^{NT}\sum_{i=1}^{NG}\sum_{m=1}^{NI}\left[\lambda_{it}(m)p_{it}(m)+A_i u_{it}\right] \\
& +\sum_{t=1}^{NT}\sum_{j=1}^{ND}\sum_{m=1}^{NJ}\left[mc_{jt}(m)d_{jt}(m)+B_j u_{jt}\right] \\
& +\sum_{t=1}^{NT}\sum_{i=1}^{NG}\left[S_{it}\left(u_{it},u_{i,t-1}\right)+C_{it}R_{it}\right] \\
& +Max_{\{S_0|S_0\subseteq J_0,|S_0|\leq\Gamma_0\}}\sum_{t=1}^{NT}\sum_{j=1}^{ND}\left\{\triangle\alpha_{jt}\left[u_{jt}\left(e_{jt}^{0}\right)^2/2\right.\right. \\
& \left.\left.+\sum_{m=1}^{NJ}d_{jt}(m)(e_{jt}^{m-1}+e_{jt}^{m})/2\right]\right\} \qquad (6.13)
\end{aligned}
$$

The proposed robust counterpart of equation (6.1) is (6.13), where $e_{jt}^{0}=D_{jt}^{min}$ and $e_{jt}^{NJ}=D_{jt}^{max}$. By the property of strong duality, the proposed robust UC with uncertain price elasticity of demand can be reformulated as:

$$
\begin{aligned}
Min_{p_{it}(m),u_{it},d_{jt}(m),u_{jt},R_{it},q_{jt},z_0} \quad & \sum_{t=1}^{NT}\sum_{i=1}^{NG}\sum_{m=1}^{NI}\left[\lambda_{it}(m)p_{it}(m)+A_i u_{it}\right] \\
& +\sum_{t=1}^{NT}\sum_{j=1}^{ND}\sum_{m=1}^{NJ}\left[mc_{jt}(m)d_{jt}(m)+B_j u_{jt}\right] \\
& +\sum_{t=1}^{NT}\sum_{i=1}^{NG}S_{it}\left(u_{it},u_{i,t-1}\right) \\
& +\sum_{t=1}^{NT}\sum_{i=1}^{NG}C_{it}R_{it} \\
& +\sum_{t=1}^{NT}\sum_{j=1}^{ND}q_{jt}+z_0\Gamma_0 \qquad (6.14)
\end{aligned}
$$

s.t.

(2) to (9)

$$z_0 + q_{jt} \geq \triangle \alpha_{jt} y_{jt} \qquad \forall jt \in J_0 \tag{6.15}$$

$$q_{jt} \geq 0 \qquad \forall jt \in J_0 \tag{6.16}$$

$$y_{jt} \geq 0 \qquad \forall jt \in J_0 \tag{6.17}$$

$$-y_{jt} \leq x_{jt} \leq y_{jt} \qquad \forall jt \in J_0 \tag{6.18}$$

$$x_{jt} = u_{jt} \left(e_{jt}^0\right)^2 /2 + \sum_{m=1}^{NJ} d_{jt}(m)(e_{jt}^{m-1} + e_{jt}^m)/2 \quad \forall jt \in J_0 \tag{6.19}$$

$$z_0 \geq 0 \tag{6.20}$$

The variables z_0 and q_{jt} are dual variables of the inner level maximum optimization problem in (6.13) , while x_{jt} and y_{jt} are auxiliary variables used to obtain equivalent linear expressions. A detailed description of how to obtain the robust problem from (6.13) is given in Bertsimas and Sim (2003). Again, each unit or demand is subject to its own operating constraints, including minimum up and down time, initial condition, capacity limits and ramp limits (Carrión and Arroyo, 2006).

6.3 Case Studies

The proposed full demand response model is demonstrated on a modified IEEE Reliability Test System (Grigg et al., 1999). In the modified system, there are 26 thermal generators and the hydro units have been removed. The ramp rates and quadratic cost coefficients are taken from Wang and Shahidehpour (1993). For simplicity, the unit quadratic cost curves in Wang and Shahidehpour (1993) are

converted into piece-wise linear cost curves. In addition, we assume that all units offer spinning reserve at the rate of 10% of their highest incremental cost for producing energy (Bouffard and Galiana, 2004).

The analysis is conducted for a 24-hour scheduling horizon and each time interval is set to be one hour. The forecast demand is as shown in Table 6.1. The UC with forecast demand is solved and the LMPs are calculated by minimizing the generation cost. These LMPs are set as the reference prices λ_{jt}^{ref} of the price elastic demand reduction curves as in Fig. 6.2. Then, each demand is divided into two parts: fixed and price elastic with a proportion of 80% and 20%, respectively. The price elasticity is set to 0.2\$/MW^{2}h (Singh et al., 2011). Based on these parameters, the price elastic demand reduction curves of the form in Fig. 6.2 are determined. The maximum and minimum reduced demand is set to be 200% and 50% of the price elastic portion, respectively. The opportunity cost or alternative cost of reduced demand is calculated and then linearized into piece-wise linear segments. Demand forecast error is neglected.

Table 6.1: Forecast demand

Hour	Load (MW)	Hour	Load (MW)	Hour	Load (MW)
1	1500	9	2340	17	2350
2	1530	10	2400	18	2330
3	1490	11	2470	19	2300
4	1500	12	2390	20	2350
5	1550	13	2390	21	2400
6	1650	14	2350	22	2280
7	1800	15	2420	23	2000
8	2230	16	2450	24	1640

All numerical simulations are coded in MATLAB and solved using the MILP solver CPLEX 12.2. With a pre-specified duality gap of 0.1%, the running time of each case is about 20 seconds on a 2.66 GHz Windows-based PC with 4 G bytes of RAM.

6.3.1 Effect of Robustness Level

In order to show the effect of Γ_0, we assume the slope of the demand reduction curves for all load falls within $[0.1, 0.3]$ \$/MW^{2}h (Singh et al., 2011). In addition, the robustness level is defined as $\Gamma_0/(NT \times NJ)$, where 0 means no robustness and 1 means fully robust. For different levels, the generalized social costs are calculated and shown as in Fig. 6.4.

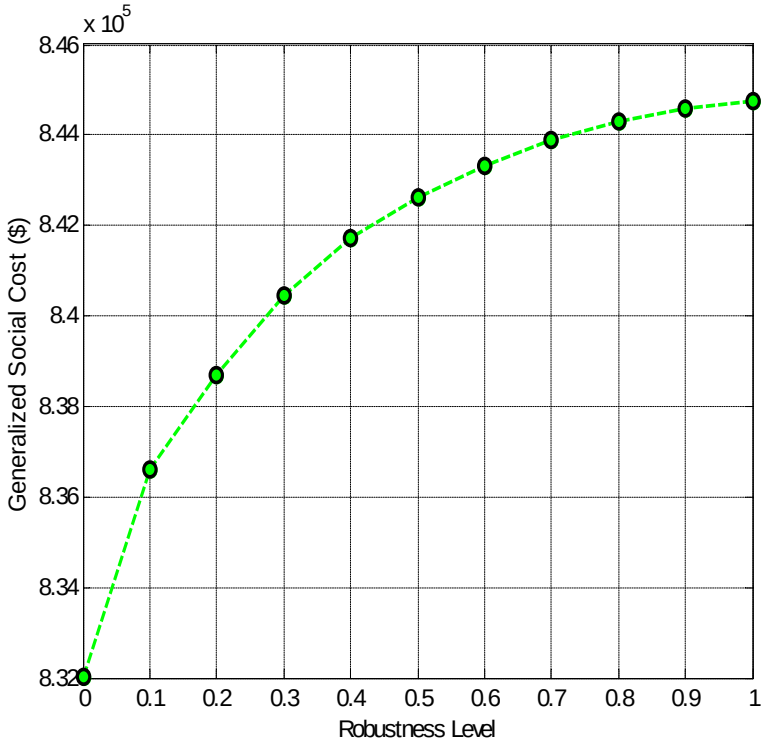

Figure 6.4: Effect of Robustness Level: more robust solution; higher cost

As can be seen in Fig. 6.4, the generalized social cost monotonically increases, but not linearly with the robustness level. We are trying to find an optimal solution that optimizes against all scenarios under which a number Γ_0 of price elasticities can vary in such a way as to maximally increase the objective function. Specifically, when the robust level is low, i.e., Γ_0 is small, the larger demands, which have major impact on the objective function, are considered. As a result, the generalized social cost and the solution robustness increase quickly. While if the robust level is high, i.e., Γ_0 is

big, the smaller demands, which have a minor impact on the objective function, are also taken into account. In this case, the generalized social cost and the robustness of solution increase more slowly. Thus, there is a diminishing return for considering greater uncertainty and we set the robustness level at 0.4 for the following studies.

6.3.2 Robustness against Uncertainty of Price Elasticity

The unit commitment results of proposed robust and deterministic methods are compared in Fig. 6.5. As can be seen, more units are committed at hours 7, 8 and 19-22 by the proposed robust method because the approach considers the worst-case scenario of demand price elasticities. In this worst-case scenario, the price elasticity of demand is over-estimated and the real price elasticity of DR is much lower as in Fig. 6.1b. As a result, the generation capacity is insufficient and electricity price spikes appear. By optimizing over this scenario, more units must be committed and additional generation capacity made available. Consequently, the electricity spikes are eliminated or reduced.

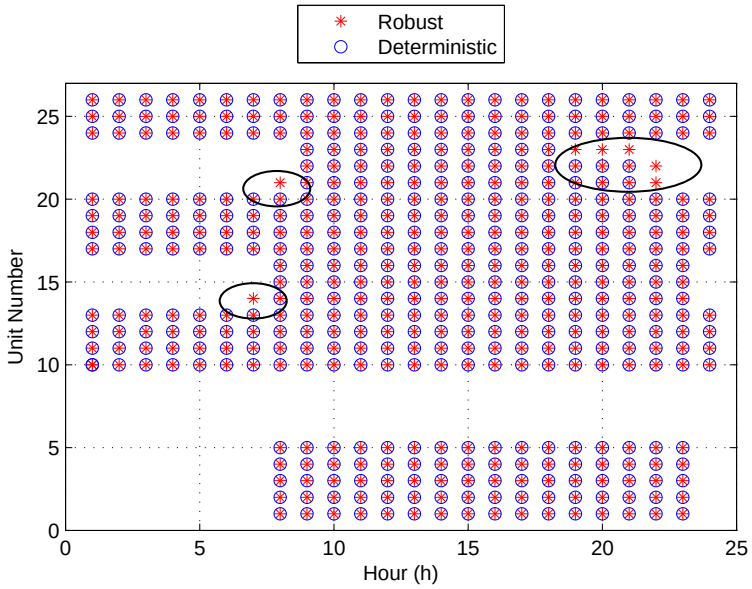

Figure 6.5: Comparison of unit status between proposed robust and deterministic methods

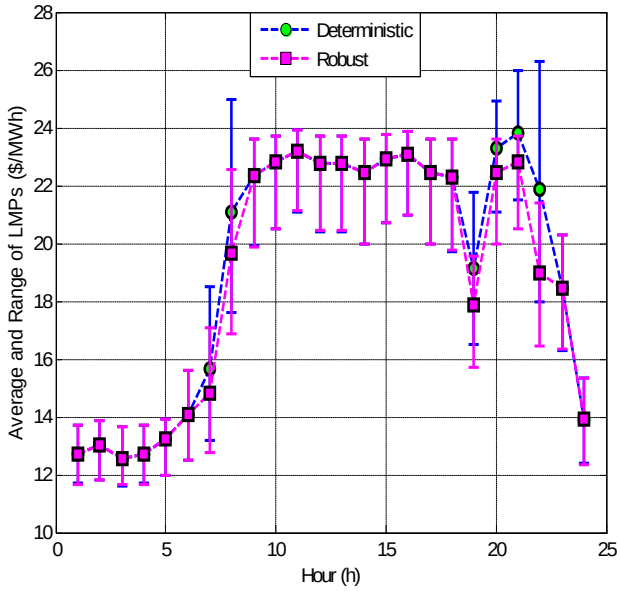

Figure 6.6: Comparison of average and range of LMPs between proposed robust and deterministic methods

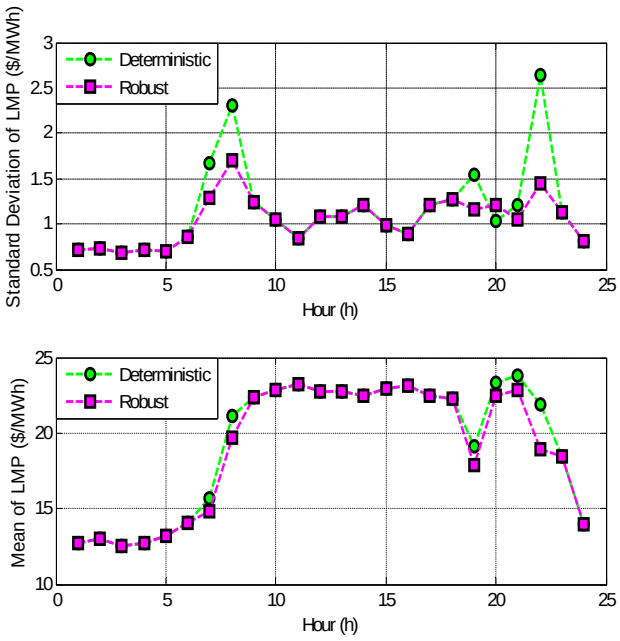

Figure 6.7: Comparison of mean and standard deviation of LMPs between proposed robust and deterministic methods

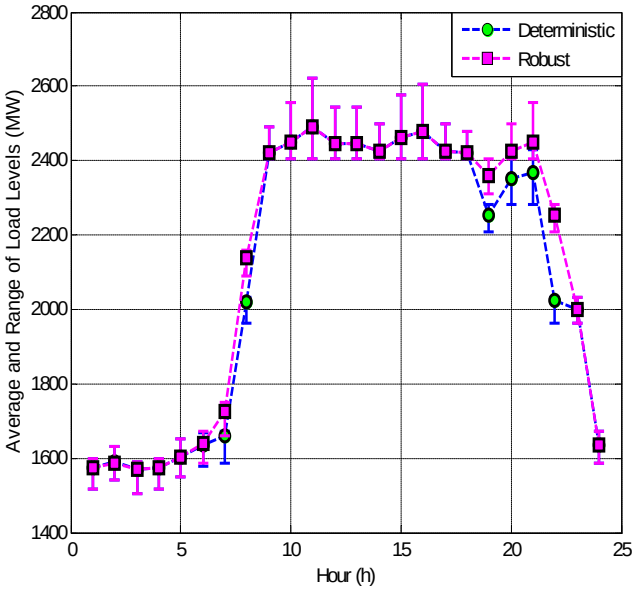

Figure 6.8: Comparison of mean and range of load levels between proposed robust and deterministic methods

A set of randomly sampled slopes of the demand reduction curves are generated based on a uniform distribution in the interval $[0.1, 0.3]$ \$/MW^{2}h. From the unit commitment results of these two methods, the LMPs are calculated for each sample slope and shown in Fig. 6.6. The vertical bars show the range of LMPs and the mark on each bar shows the average value. Compared to the deterministic UC, the proposed robust UC shows reduced variation.

Comparison of mean and standard deviation of LMPs between the proposed robust and deterministic methods is shown in Fig. 6.7. Generally, both the average and standard deviation of LMPs are reduced by the proposed method.

The load levels by these two methods for each scenario of demand elasticity are also calculated and shown in Fig. 6.8. As can be seen, both the peak and average load levels of the proposed robust method are higher than that of the deterministic method. This is because the average LMPs from the robust method are reduced as shown in Fig. 6.6. Moreover, less demand responds, so the load level is higher.

To summarize, the proposed robust method reduces both the mean and volatility of electricity prices. The price spikes are reduced or eliminated, while the average load levels are increased. It should be noted that these benefits are gained at the expense of increasing generalized social cost as shown in Fig. 6.4. Specifically, the total generation cost increases by 2.10% and the opportunity cost of the reduced demand decreases by 1.19%. In total, the generalized social cost increases by 1.16%. With reduced LMPs and increased unit load cost, the per unit sale profits of generators are reduced.

6.3.3 Robustness against Different Distributions of Price Elasticity

As mentioned before, the probability distribution for demand price elasticity is difficult to estimate. Thus, it is important for a UC solution to be robust against various distributions. Thus, a set of randomly sampled slopes for the demand reduction curves is generated that follows a normal distribution with mean 0.2 \$/MW^{2}h and standard deviation 0.2/2.88 \$/MW^{2}h (Singh et al., 2011). This results in 85% of samples falling between [0.1, 0.3] and negative samples are ignored (Bertsimas et al., 2013). Based on the unit commitment results of these two methods, the LMPs are calculated for each sample of price elasticities and shown in Fig. 6.9. The vertical bars show the ranges of LMPs and the mark on each bar shows the average value of LMPs. Compared to the deterministic UC, the proposed robust UC again significantly reduces volatility.

The mean and standard deviation of LMPs when the demand price elasticities are normally distributed are calculated and shown in Fig. 6.10. As can be seen, both the average and standard deviation of LMPs by the proposed robust method are reduced. The proposed UC method is robust against different probability distributions in elasticities.

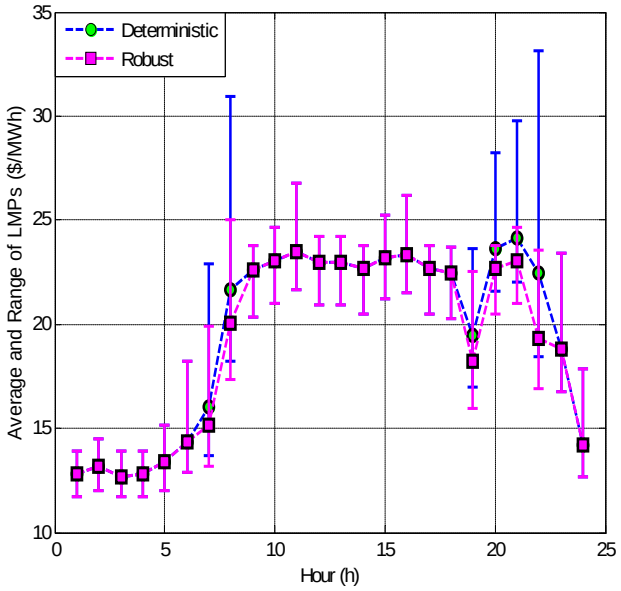

Figure 6.9: Comparison of average and range of LMPs with normally distributed price elasticities

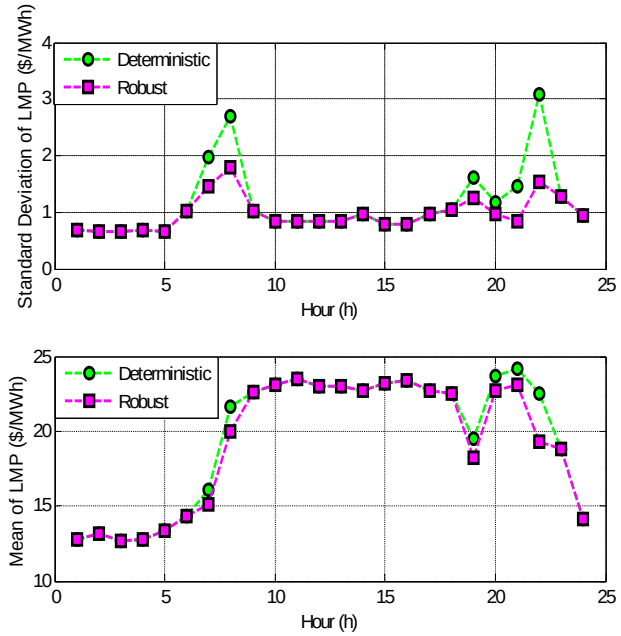

Figure 6.10: Comparison of mean and standard deviation of LMPs with normally distributed price elasticities

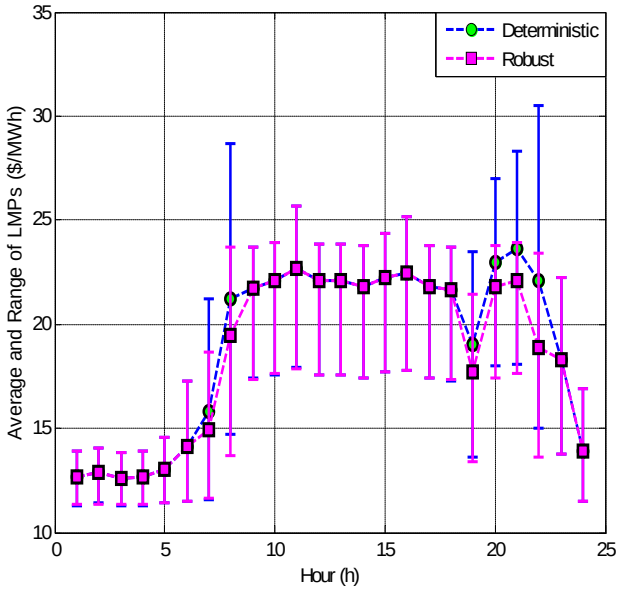

Figure 6.11: Comparison of average and range of LMPs for uniformly distributed price elasticities with high forecast error

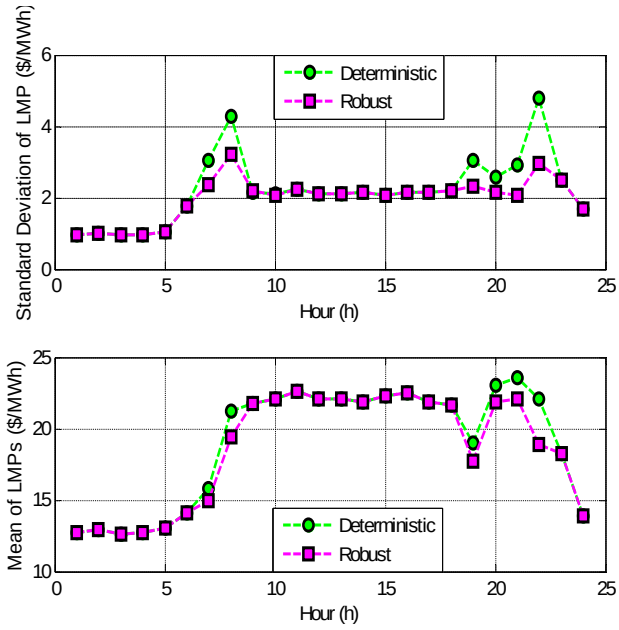

Figure 6.12: Comparison of mean and standard deviation of LMPs for uniformly distributed price elasticities with high forecast error

6.3.4 Robustness Against High Forecast Errors of Price Elasticity

In practice, the interval of demand price elasticity may also be difficult to accurately estimate. When the forecast errors of price elasticity are much higher than the estimation, i.e., the real interval of elasticity is much larger than the one used in the UC, it is important for the solution to remain robust. To evaluate this, the UC is solved for elasticity distributed uniformly in $[0.1, 0.3]$ \$/MW^{2}h and tested against the interval $[0.01, 0.39]$ \$/MW^{2}h (Singh et al., 2011). The LMPs are calculated for each sample and shown in Fig. 6.11. Compared to the deterministic UC, the proposed robust UC significantly reduces the price volatility even though the estimated interval is imprecise.

The mean and standard deviation of LMPs are calculated and shown in Fig. 6.12. As can be seen, both the average and standard deviation of LMPs are reduced compared to that of the deterministic method. Thus, the proposed UC method is robust against when the range of price elasticity is poorly understood.

6.4 Conclusions

In this chapter, a robust UC model to minimize the generalized social cost is proposed. Compared to the traditional UC to maximize the social welfare, the proposed UC model more effectively manages uncertainty in the demand response. The UC solution of the proposed model is robust against all possible modeled realizations of the uncertain demand response. Numerical simulation results on the IEEE Reliability Test System show that the solution can reduce both the average prices and price volatility to the deterministic UC. In particular, the robust UC significantly reduces or eliminates the occurrence of price spikes. In addition, the proposed UC method is robust against different probability distributions and high forecast errors in the demand elasticity.

Chapter 7

Conclusion and Future Work

7.1 Conclusion

In today's power system, operators are facing two critical changes. First, the large-scale integration of renewable energy sources, especially wind, is advancing rapidly in numerous countries. Second, demand response plays an increasing important role in the reliable and economic operation of power systems and the electricity markets. This work proposes solutions to effectively accommodate the uncertainties of wind and extract the flexibility of demand respond.

An hour-ahead economic dispatch model which considers uncertainty of wind power is proposed in Chapter 3. The uncertainty model of forecast wind power is established in section 3.1. The reliability index EDNS is formulated using this model. The uncertainty takes into account wind speed, load forecast and generator availability. A probabilistic model is proposed in the hour-ahead economic dispatch by using EDNS as a reliability constraint. Based on the monotonic relationship between EDNS and total spinning reserve, an iterative optimization scheme is used to find the solution through adjusting total spinning reserve to satisfy a predefined EDNS. The proposed probabilistic method can maintain a uniform system reliability level for all dispatch intervals.

The model proposed in Chapter 3 has two disadvantages. First, the assumption that total wind power forecast error follows Gaussian distribution is too restrictive. A method compatible for other distributions would be useful. Second, a predefined EDNS value needs to be specified for this model. To address these drawbacks, a more general model is developed in Chapter 4.

In Chapter 4, a new SCUC model, which integrates the stochastic wind forecast results into the day-ahead UC and analyze the sensitivity to parametric settings, is proposed. The approach determines the optimal amount of spinning reserve to minimize the total cost of operating the system, i.e., balancing energy cost, start-up cost, reserve cost and expected cost of load shedding. Generally, the proposed method has two advantages: first, the method is capable of aggregating various kinds of probability distributions of wind and load forecast errors into the UC; and second, the approach determines the optimal amount of spinning reserve in terms of the optimal trade-off between economic efficiency and system reliability. The results of the case studies show the effect of uncertainties, such as ORR, load forecast error and wind forecast error, on economic efficiency and system reliability.

In order to utilize the flexibility in demand, a full demand response model in which DRP could bid in the energy market and spinning reserve market is proposed in Chapter 5. The proposed model is incorporated into the co-optimized day-ahead energy and spinning reserve market. The market clearing problem is formulated as a two-stage stochastic SCUC and solved by MILP. The most economic solution with a probabilistic spinning reserve scheme is obtained by balancing the energy cost, spinning reserve cost and the cost of EENS. Numerical simulation results using the IEEE Reliability Test System show that the proposed model of full demand response can reduce the system operating cost, reduce cycling on/off of generators, shave peak load and reduce the fluctuations in system reliability and energy price. In particular, simulation results have shown that the proposed full demand response model outperforms conventional demand shifting bids in operating efficiency.

Response from demand side can be highly uncertain due to limited understanding of consumers' response to pricing signals.In this vein, a robust UC model to minimize the generalized social cost is proposed in Chapter 6. Compared to the traditional UC to maximize the social welfare, the proposed UC model more effectively manages uncertainty in the demand response. The UC solution of the proposed model is robust against all possible modeled realizations of the uncertain demand response. Numerical simulation results on the IEEE Reliability Test System show that the solution can reduce both the average prices and price volatility to the deterministic UC. In particular, the robust UC significantly reduces the occurrence of price spikes. In addition, the proposed UC method is robust against different probability distributions and large forecast errors in the demand elasticity.

7.2 Future Work

Based on the work to date, continuing research in various fields is needed for successful practical application of the presented methods.

- On day-ahead unit commitment

    1. The methods proposed in this thesis deal with the integration of wind power and demand response separately. It would be interesting to see how demand flexibility can contribute to allowing the maximum use of wind generation.
    2. The formulation of EENS in chapter 4 neglects transmission constraints. Including these constraints into the formulation of EENS without compromising the computational efficiency is challenging.

- On demand response

1. Demand can be classified into many types, all of which have different response characteristics. Constructing a DR model as a composite of these loads could improve scheduling.

Bibliography

(2008). *GE 1.5 MW SLE Wind Turbine Technical Specifications*. 57

Ahlstrom, L., Zavadil, R., and Grant, W. (2005). The future of wind forecasting and utility operations. *IEEE Power and Energy Magazine*, 3(6):57–64. 2, 65

Aminifar, F., Fotuhi-Firuzabad, M., and Shahidehpour, M. (2009). Unit commitment with probabilistic spinning reserve and interruptible load considerations. *IEEE Transaction on Power Systems*, 24(1):388–397. 75, 103

Anstine, L., Burke, R., Casey, J., Holgate, R., John, R., and Stewart, H. (1963). Application of probability methods to the determine of spinning reserve requirements for the pennsylvania-new jersey-maryland interconnection. *IEEE Transaction on Power Apparatus and Systems*, PAS-82(68):726–735. 17

Baboli, P., Moghaddam, M., and Eghbal, M. (2011). Present status and future trends in enabling demand response programs. In *Proceeding of IEEE Power and Energy General Meeting*, pages 1–6, San Diego, USA. IEEE PES. 6

Bai, J., Gooi, H., and Xia, L. (2008). Probabilistic reserve schedule with demand-side participation. *Electric Power Components and Systems*, 26(2):138–151. 25

Baldick, R. (1995). The generalized unit commitment problem. *IEEE Transaction on Power Systems*, 10(1):465–475. 21

Baringo, L. and Conejo, A. (2011). Offering strategy via robust optimization. *IEEE Transaction on Power Systems*, 26(3):1418–1425. 106

Bertsimas, D., Litvinov, E., Sun, X., Zhao, J., and Zheng, T. (2013). Adaptive robust optimization for the security constrained unit commitment problem. *IEEE Transaction on Power Systems*, 28(1):52–63. 23, 114

Bertsimas, D. and Sim, M. (2003). Robust discrete optimization and network flows. *Mathematical Programming Series B*, 93:49–71. 106, 108

Billinton, R. and Allan, R. (1996). *Reliability evaluation of power systems*. Plenum, New York, 2 edition. 20, 31, 81

Billinton, R. and Chowdhury, A. (1992). Incorporation of wind energy conversion systems in conventional generating capacity adequacy assessment. *IEE Proceedings of Generation, Transmission and Distribution*, 139(1):47–56. 28

Blatchfort, J. (2009). Participating intermittent resources program (prip) 101. Technical report, California Independent System Operator. 4

Bouffard, F. and Galiana, F. (2004). An electricity market with a probabilistic spinning reserve criterion. *IEEE Transaction on Power Systems*, 19(1):300–307. 17, 36, 53, 56, 81, 109, 138

Bouffard, F. and Galiana, F. (2008). Stochastic security for operations planning with significant wind power generation. *IEEE Transaction on Power Systems*, 23(2):306–316. 19, 23, 31, 57, 62

Carrión, M. and Arroyo, J. (2006). A computationally efficient mixed-integer linear formulation for the thermal unit commitment problem. *IEEE Transaction on Power Systems*, 21(3):1371–1378. 23, 78, 103, 108

Doherty, R. and O'Malley, M. (2005). A new approach to quantify reserve demand in systems with significant installed wind capacity. *IEEE Transaction on Power Systems*, 20(2):587–595. 19, 37, 42, 57

Dupačŏvá, J., Gröwe-Kuska, N., and Römisch, W. (2003). Scenario reduction in stochastic programming: An approach using probability metrics. *mathematical Programming*, 95(3):493–511. 23

Earle, R. (2000). Demand elasticity in the california power exchange day-ahead market. *The Electricity Journal*, 13(8):59–65. 8

Ericsen, P., Ackermann, T., Abildgarrd, H., Smith, P., Winter, W., and Rodríguez García, J. (2005). System operation with high wind penetration. *IEEE Power and Energy Magazine*, 3(5):65–74. 4

Fabbri, A., Roman, T., Abbad, J., and Quezada, V. (2005). Assessment of the cost associated with the wind generation prediction errors in a liberalized electricity market. *IEEE Transaction on Power Systems*, 20(3):1440–1446. 2, 29

FERC (2008). Wholesale competition in regions with organized electric markets, ferc order no. 719. Technical report, Federal Energy Regulatory Commission. 7

Gooi, H., Menders, D., Bell, K., and Kirschen, D. (1999). Optimal scheduling of spinning reserve. *IEEE Transaction on Power Systems*, 14(4):1485–1492. 17, 19

Grigg, C., Wong, P., Albrecht, P., Allan, R., Bhavaraju, M., Billinton, R., Chen, Q., Fong, C., Haddad, S., Kuruganty, S., Li, W., Mukerji, R., Patton, D., Rau, N., Reppen, D., Schneider, A., Shahidehpour, M., and Singh, C. (1999). The ieee reliability test system-1996. a report prepared by the reliability test system task force of the application of probability methods subcommittee. *IEEE Transaction on Power Systems*, 14(3):1010–1020. 36, 42, 56, 62, 65, 80, 108, 138

Han, X., Gooi, H., and Kirschen, D. (2001). Dynamic economic dispatch: Feasible and optimal solutions. *IEEE Transaction on Power Systems*, 16(1):22–28. 24

Karangelos, E. and Bouffard, F. (2012). Towards full integration of demandside resources in joint forward energy/reserve electricity markets. *IEEE Transaction on Power Systems*, 27(1):280–289. 25

Kariuki, K. and Allan, R. (1996). Evaluation of reliability worth and value of lost load. *IEE Proceedings of Generation, Transmission and Distribution*, 143(2):171–180. 54

Khodaei, A., Shahidehpour, M., and Bahramirad, S. (2011). Scuc with hourly demand response considering intertemporal load characteristics. *IEEE Transaction on Smart Grid*, 2(3):564–571. 25

Kirschen, D., Strbac, G., Cumperayot, P., and Menders, D. (2000). Factoring the elasticity of demand in electricity prices. *IEEE Transaction on Power Systems*, 15(2):612–617. 8

Kundur, P., Paserba, J., Ajjarapu, V., Andersson, G., Bose, A., C., C., N., H., Hill, D., Stankovic, A., Taylor, C., T., C., and V., V. (2004). Definition and classification of power system stability. *IEEE Transaction on Power Systems*, 19(2):1387–1401. 8

Lalor, G., Mullane, A., and O'Mally, M. (2005). Frequency control and wind turbine technologies. *IEEE Transaction on Power Systems*, 20(4):1905–1943. 4

Lindenberg, S. (2008). 20% wind energy by 2030: Increasing wind energy's contribution to us electricity supply. Technical report, U.S. Depart of Energy. 1

Liu, G. and Tomsovic, K. (2012a). Quantify spinning reserve for uniform system reliability considering wind power. In *Proceeding of the 12th International Conference on Probabilistic Methods Applied to Power*, pages 1–6, Istanbul, Turkey. IEEE PES. 27

Liu, G. and Tomsovic, K. (2012b). Quantifying spinning reserve in systems with significant wind power penetration. *IEEE Transaction on Power Systems*, 27(4):2385–2393. 48

Liu, G. and Tomsovic, K. (2013a). A full demand response model in co-optimized energy and reserve market. *Electric Power System Research, Revision under Review*. 70

Liu, G. and Tomsovic, K. (2013b). Robust unit commitment considering uncertain demand response. *IEEE Transaction on Power Systems, Under Review*. 99

Louton, C. and Hawkins, D. (2007). Renewable energy integration: Transmission and operating issues and recommendations for integrating renewable resources on

the california iso-controlled grid. Technical report, California Independent System Operator. 2, 3

Meibom, P., Barth, R., Hasche, B., Brand, H., Weber, C., and O'Malley, M. (2011). Stochastic optimization model to study the operational impacts of high wind penetrations in ireland. *IEEE Transaction on Power Systems*, 26(3):1367–1379. 20, 23

Morales, J., Conejo, A., and Pérez-Ruiz, J. (2009). Economic valuation of reserves in power systems with high penetration of wind power. *IEEE Transaction on Power Systems*, 24(2):900–910. 23, 73, 80

Muckstadt, J. and Koenig, S. (1977). An application of lagrangian relaxation to scheduling in power-generation systems. *Operations Research*, 25(3):387–403. 23

Ortega-Vazquez, M. (2006). *Optimizing the spinning reserve requirements*. PhD thesis, School of Electrical and Electronic Engineering, Manchester, U.K. 75, 103, 105

Ortega-Vazquez, M. and Kirschen, D. (2007). Optimizing the spinning reserve requirements using using a cost/benefit analysis. *IEEE Transaction on Power Systems*, 22(1):24–33. 18

Ortega-Vazquez, M. and Kirschen, D. (2009). Estimating the spinning reserve requirements in systems with significant wind power generation penetration. *IEEE Transaction on Power Systems*, 24(1):114–124. 20, 31, 57, 60

Papoulis, A. and Pillai, S. (2002). *Probability, Random Variables and Stochastic Processes*. McGraw-Hill, New York, 4 edition. 29

Parvania, M. and Fotuhi-Firuzabad, M. (2010). Demand response scheduling by stochastic scuc. *IEEE Transaction on Smart Grid*, 1(1):89–98. 25, 81

Rahimi, F. and Ipakchi, A. (2010). Demand response as a market resource under the smart grid paradigm. *IEEE Transaction on Smart Grid*, 1(1):82–88. 6, 10

Singh, K., Padhy, N., and Sharma, J. (2011). Influence of price responsive demand shifting bidding on congestion and lmp in pool-based day-ahead electricity markets. *IEEE Transaction on Power Systems*, 26(2):886–896. 25, 81, 109, 110, 114, 117

Singh, S. and Østergaard, J. (2010). Use of demand response in electricity markets: An overview and key issues. In *7th International Conference on the European Energy Market (EEM)*, pages 1–6, Madrid, Spain. IEEE PES. 7

Söder., L. (1993). Reserve margin planning for a wind-hydro-thermal power systems. *IEEE Transaction on Power Systems*, 8(2):564–571. 5, 9, 17, 29, 31, 36, 40, 57

Strbac, G. and Kirschen, D. (1999). Assessing the competitive of demand-side bidding. *IEEE Transaction on Power Systems*, 14(1):120–125. 8

Su, C. and Kirschen, D. (2009). Quantifying the effect of demand response on electricity markets. *IEEE Transaction on Power Systems*, 24(3):1199–1207. 70

Tan, Y. and Kirschen, D. (2006). Co-optimization of energy and reserve in electricity markets with demand-side participation in reserve services. In *Proceedings of Power Systems Conference and Exposition*, pages 1182–1198, Atlanta, USA. IEEE PES. 6

Thresher, R., Robinson, M., and Veers, P. (2007). To capture the wind. *IEEE Power and Energy Magazine*, 5(6):34–36. 4

Ummels, B., Gibescu, M., Pelgrum, E., Kling, W., and Brand, A. (2007). Impacts of wind power on thermal generation unit commitment and dispatch. *IEEE Transaction on Energy Conversion*, 22(1):44–51. 5, 9

Wang, C. and Shahidehpour, M. (1993). Effects of ramp-rate limits on unit commitment and economic dispatch. *IEEE Transaction on Power Systems*, 8(3):1341–1350. 56, 81, 108, 138

Wang, J., Redondo, N., and Galiana, F. (2003). Demand-side reserve offers in joint energy/reserve electricity markets. *IEEE Transaction on Power Systems*, 18(4):1300–1306. 7, 25, 71

Wang, L., Shahidehpour, M., and Li, Z. (2008). Security-constrained unit commitment with volatile wind power generation. *IEEE Transaction on Power Systems*, 43(6):1441–1448. 20, 23

Wang, M. and Gooi, H. (2011). Spinning reserve estimation in microgrids. *IEEE Transaction on Power Systems*, 26(3):1164–1174. 20

Wang, Q., Wang, J., and Guan, Y. (2013). Stochastic unit commitment with uncertain demand response. *IEEE Transaction on Power Systems*, 28(1):562–563. 26

Watson, S., Landberg, L., and Halliday, J. (1994). Application of wind speed forecasting to the integration of wind energy into a large scale power system. *Proceedings of IEE Generation, Transmission and Distribution*, 141(4):357–362. 2

Wight, D. (2006). Assessment of demand response and advanced metering: Staff report. Technical report, Federal Energy Regulatory Commission. 7

Wolfgang, O. and Doorman, G. (2011). Evaluating demand side measures in simulation models for the power market. *Electric Power System Research*, 81(3):790–797. 26

Wood, A. and Woolenberg, B. (1996). *Power Generation, Operation and Control*. Wiley, New York, 2 edition. 6, 14, 23

Wood, W. (1982). Spinning reserve constrained static and dynamic economic dispatch. *IEEE Transaction on Power Apparatus and Systems*, PAS-101(2):381–388. 6, 14, 103

Wu, H. and Gooi, H. (1999). optimal scheduling of spinning reserve with ramp constraints. In *Proceeding of IEEE Power and Energy Winter Meeting*, pages 785–790, New York, USA. IEEE PES. 18

Xia, L., Gooi, H., and Bai, J. (2005). A probabilistic reserve with zero-sum settlement scheme. *IEEE Transaction on Power Systems*, 20(2):993–1000. 35, 38

Zhao, C., Wang, J., Watson, J., and Guan, Y. (2013). Multi-stage robust unit commitment considering wind and demand response uncertainties. *IEEE Transaction on Power Systems*, 28(3):2708–2717. 26

Zhao, L. and Zeng, B. (2012). Robust unit commitment problem with demand response and wind energy. In *Proceeding of IEEE Power and Energy General Meeting*, pages 1–6, San Diego, USA. IEEE PES. 26

Appendices

A Proof of Monotonic Relationship Between $EDNS$ and Total Spinning Reserve

There are two steps to prove this monotonic relationship between $EDNS$ and SR. Firstly, when SR has a positive change $\Delta SR > 0$, it is needed to show that $\Delta SR - \sum_{m \in U_s} (\Delta P_{m,t} + \Delta R_{m,t}) \geq 0$. Then, $\Delta EDNS_{s,t} \leq 0$ for each scenario is shown. So, the their probabilistic weighted summation $\Delta EDNS \leq 0$. That proves the monotonic relationship between $EDNS$ and SR.

Let NB stands for the unbinding units satisfying $P_{m,t} + R_{m,t} < P_m^{max}$ and B stands for the binding units satisfying $P_{m,t} + R_{m,t} = P_m^{max}$. Since the cost of generating reserve is much less than the cost of generating energy, if $\exists\, R_{j,t} < R_j^{max}$ and $j \in NB$, when SR has a very small positive change $\Delta SR > 0$, then $\Delta P_j^t = 0$, $\Delta R_{j,t} \geq 0$ and $\Delta P_{i,t} = 0$, $\Delta R_{i,t} = 0$, $i \in B$.

Now if $R_{j,t} = R_j^{max}$, $\forall\, j \in NB$, the only way of increasing SR is to increase $R_{i,t}$ and decrease $P_{i,t}$, $i \in B$. That means the capacity binding units transfer the task of generating energy to other units in order to carry more spinning reserve. Particularly, we can prove $\Delta P_{i,t} \leq 0$ and $\Delta R_{i,t} \geq 0$, $\forall\, i \in B$ since the transition is from one optimum to another optimum.

For simplicity, assuming there is one unit k, such that $\Delta P_{k,t} > 0$ and $\Delta R_{k,t} < 0$, $k \in B$. When SR has a positive change $\Delta SR > 0$, there will be units $l \in L \subset B$ such that $\Delta P_{l,t} < 0$, $\Delta R_{l,t} > 0$ and $\Delta P_{l,t} + \Delta R_{l,t} = 0$ also, $\sum_{l \in L} \Delta R_{l,t} = \Delta SR - \Delta R_{k,t}$. We can divide this into two steps. Firstly, $\sum_{l \in L} \Delta P_{l,t} = -\Delta SR$, $\sum_{l \in L} \Delta R_{l,t} = \Delta SR$ and $P_{k,t}\, R_{k,t}$ stay the same. Secondly, the units in L transfer $\Delta P_{k,t}$ of load to unit k. The second step indicates the first order partial derivative of dual Lagrange function at $P_{k,t}$ is lower than that of unit l after first step, at $P_{l,t} + \Delta P_{l,t}$. So, it is much lower than that of unit l at $P_{l,t}$. In fact, we know that the first order partial derivative of dual Lagrange function at $P_{k,t}$ should be equal to that of unit l at $P_{l,t}$ since $P_{k,t}$ and $P_{l,t}$ are at a optimum before SR has a positive change. So, the assumption is not true, i.e. there is no unit such that $\Delta P_{k,t} > 0$ and $\Delta R_{k,t} < 0$, $k \in B$. Moreover,

the same result can be proved from the point of marginal reserve cost. In summary, $\Delta P_{i,t} \leq 0$ and $\Delta R_{i,t} \geq 0$, $\forall\, i \in B$.

Now, $\Delta P_{m,t} + \Delta R_{m,t} = 0$, $m \subset B$ and $\Delta P_{m,t} + \Delta R_{m,t} \geq 0$, $m \subset NB$. Then, we have $\Delta SR - \sum_{m \in U_s} (\Delta P_{m,t} + \Delta R_{m,t}) \geq 0$. Since

$$\begin{aligned} &\textstyle\sum_{m \subset U_s} (\Delta P_{m,t} + \Delta R_{m,t}) \\ &= \textstyle\sum_{m \subset U_s \cap NB} (\Delta P_{m,t} + \Delta R_{m,t}) \\ &\leq \textstyle\sum_{m \subset U_s \cap NB} \Delta R_{m,t} + \sum_{m \subset B} (-\Delta P_{m,t}) \\ &\leq \textstyle\sum_{m \subset U_s \cap NB} \Delta R_{m,t} + \sum_{m \subset B} (\Delta R_{m,t}) \\ &\leq \Delta SR \end{aligned} \tag{A.1}$$

The first step of the proof is done. Now, we move to the second step. The EDNS of scenario s during time interval t is

$$\begin{aligned} &E(e_t^d - \sum_{i \in A_s} R_{i,t} + \sum_{m \in U_s} P_{m,t} \mid e_t^d > \sum_{i \in A_s} R_{i,t} \\ &- \sum_{m \in U_s} P_{m,t}) \cdot P(e_t^d > \sum_{i \in A_s} R_{i,t} - \sum_{m \in U_s} P_{m,t}) \\ &= \int_0^\infty x \frac{\sigma_t^d}{\sqrt{2\pi}} e^{-\frac{\left[x + \left(SR - \sum_{m \in U_s} (P_{m,t} + R_{m,t})\right)\right]^2}{2\left(\sigma_t^d\right)^2}} dx \end{aligned} \tag{A.2}$$

Let $A = SR - \sum_{m \in U_s} (P_{m,t} + R_{m,t})$, which stands for the adequacy or deficiency of system after failure of generators $m \in U_s$ depending on the sign of A. When we increase SR by a small amount ΔSR, we have $\Delta A \geq 0$ and the new $EDNS_{s,t}^{\text{new}}$ is

$$
\begin{aligned}
EDNS_{s,t}^{\text{new}} &= \int_0^{\infty} x \frac{\sigma_t^d}{\sqrt{2\pi}} e^{-\frac{[x+(A+\Delta A)]^2}{2\left(\sigma_t^d\right)^2}} dx \\
&= \int_{\Delta A}^{\infty} (u - \Delta A) \frac{\sigma_t^d}{\sqrt{2\pi}} e^{-\frac{(u+A)^2}{2\left(\sigma_t^d\right)^2}} du \\
&= \int_{\Delta A}^{\infty} u \frac{\sigma_t^d}{\sqrt{2\pi}} e^{-\frac{(u+A)^2}{2\left(\sigma_t^d\right)^2}} du \\
&- \int_{\Delta A}^{\infty} \Delta A \frac{\sigma_t^d}{\sqrt{2\pi}} e^{-\frac{(u+A)^2}{2\left(\sigma_t^d\right)^2}} du \\
&= \int_0^{\infty} u \frac{\sigma_t^d}{\sqrt{2\pi}} e^{-\frac{(u+A)^2}{2\left(\sigma_t^d\right)^2}} du \\
&- \int_0^{\Delta A} u \frac{\sigma_t^d}{\sqrt{2\pi}} e^{-\frac{(u+A)^2}{2\left(\sigma_t^d\right)^2}} du \\
&- \int_{\Delta A}^{\infty} \Delta A \frac{\sigma_t^d}{\sqrt{2\pi}} e^{-\frac{(u+A)^2}{2\left(\sigma_t^d\right)^2}} du
\end{aligned}
\tag{A.3}
$$

The first term is the original $EDNS_{s,t}$. Since both the second and third term are non-positive, we can get $EDNS_{s,t}^{\text{new}} \leq EDNS_{s,t}$, i.e. $\Delta EDNS_{s,t} \leq 0$. Consequently, $\Delta EDNS_t = \sum_{s \in S} \Delta EDNS_{s,t} p_s \leq 0$. The second step of the proof is done.

B Mixed Integer linear programming models

B.1 Fuel Cost Function

The fuel cost characteristics of thermal generating units are non-convex and non-differentiable functions, but they are traditionally approximated by convex quadratic functions in unit commitment and economic dispatch programs. In the unit commitment formulation, the quadratic polynomial approximation of units' fuel cost functions can be further approximated by piecewise linear functions. These functions would be composed by elbow points, which are obtained by means of dividing the production range between the minimum output and the capacity of unit in a desired number of segments. Usually, the number of segments used is three in simulations. The incremental cost are such that the price at $P_i^{\min}$, e^1, e^1 and $P_i^{\max}$ are equal to those obtained with the polynomial function. A typical piecewise linearization of quadratic cost function is as shown in Figure B.1.

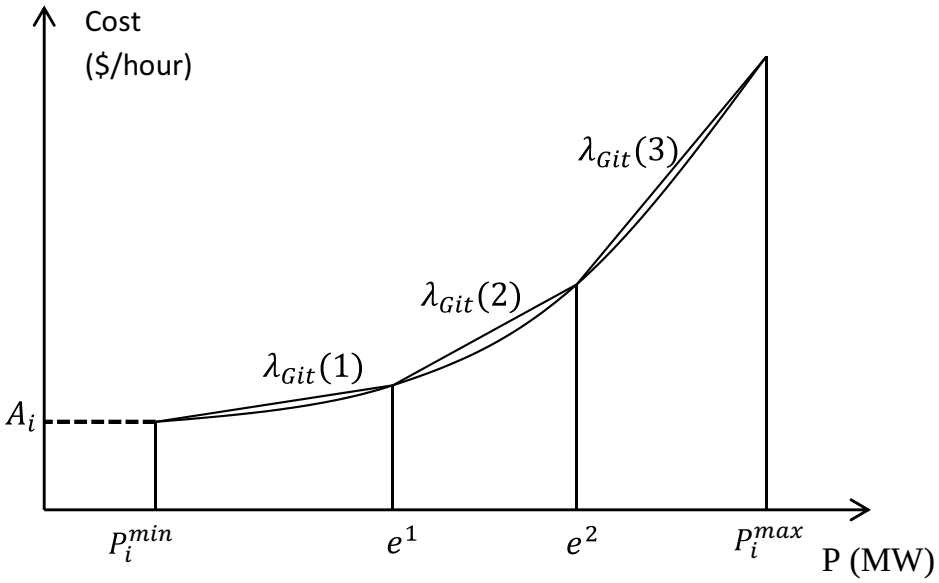

Figure B.1: Linearization of quadratic cost function

By replacing the quadratic cost function for the piecewise linear approximation, the analytical representation of cost function changes as follows:

$$C_i(P_{it}, u_{it}) = \sum_{m=1}^{3} \lambda_{Git}(m) p_{Git}(m) + A_i u_{Git} \tag{B.1}$$

$$P_{it} = \sum_{m=1}^{3} p_{Git}(m) + u_{Git} P_i^{min} \tag{B.2}$$

Due to the convexity of the approximated piecewise linear function, it is guaranteed that all units will be dispatched in such a way that the low incremental cost segment will be loaded first.

B.2 Generation limits

The generation limits are listed as follows:

$$0 \leq p_{Git}(1) \leq e^1 - P_i^{min} \tag{B.3}$$

$$0 \leq p_{Git}(2) \leq e^2 - e^1 \tag{B.4}$$

$$0 \leq p_{Git}(3) \leq P_i^{max} - e^2 \tag{B.5}$$

B.3 Start-up Cost

The start-up cost of unit i is K_i, SC_{it} is a binary variable satisfies:

$$\begin{cases} SC_{it} & \geq 0 \\ SC_{it} & \geq u_{Git} - u_{Gi,t-1} \end{cases} \tag{B.6}$$

So the start-up cost of unit i during period t ca be expressed as :

$$S_{it}(u_{Git,} u_{Gi,t-1}) = K_i SC_{it} \tag{B.7}$$

The minimum up and down time constraints of generators are formulated in mixed integer linear form.

B.4 Minimum Up- and Down-time

The minimum up-time constraints for unit i are given by:

$$u_{it} = 1 \quad \forall t \in \left[1, t_i^{\text{up}} - t_i^{\text{H}}\right],\ t_i^{\text{up}} > t_i^{\text{H}} > 0 \tag{B.8}$$

$$\begin{cases} u_{it} - u_{i,t-1} \leq u_{i,t+1} \\ u_{it} - u_{i,t-1} \leq u_{i,t+2} \\ \vdots \qquad\qquad\qquad\qquad \forall t \in [1, NT-1] \\ u_{it} - u_{i,t-1} \leq u_{i,\min\left\{t+t_i^{\text{up}}-1, NT\right\}} \end{cases} \tag{B.9}$$

Where t_i^{up} is the minimum number of periods that unit i has to be committed. t_i^{H} donates the number of periods that unit i was committed up to $t = 0$.

The minimum down time constraints for unit i are given by:

$$u_{it} = 1 \quad \forall t \in \left[1, t_i^{\text{down}} + t_i^{\text{H}}\right],\ -t_i^{\text{down}} < t_i^{\text{H}} < 0 \tag{B.10}$$

$$\begin{cases} u_{i,t-1} - u_{it} \leq 1 - u_{i,t+1} \\ u_{i,t-1} - u_{it} \leq 1 - u_{i,t+2} \\ \vdots \qquad\qquad\qquad\qquad \forall t \in [1, NT-1] \\ u_{i,t-1} - u_{i,t} \leq 1 - u_{i,\min\left\{t+t_i^{\text{down}}-1, NT\right\}} \end{cases} \tag{B.11}$$

Where t_i^{down} is the minimum number of periods that unit i has to be down. t_i^{H} donates the number of periods that unit i was decommitted up to $t = 0$.

C IEEE Reliability Test Systems

The IEEE Reliability Test System (Grigg et al., 1999) consists of 32 units, 24 buses, 17 loads and 38 transmission lines. The total generation capacity is 3405 MW. The quadratic approximation of the cost functions and ramp-up limits were taken from Wang and Shahidehpour (1993). For simplicity, the unit quadratic cost curves in Wang and Shahidehpour (1993) are converted into piece-wise linear cost curves. In addition, we assume that all units offer reserve at rates q_i equal to 10% of their highest incremental cost of producing energy as in Bouffard and Galiana (2004). Since hydro units' scheduling is much more complicated and constrained by precipitation, irrigation, fishery, even some political factors, the scheduling of hydro units is usually processed beforehand and separately in real practice. Therefore, the hydro units are neglected in the day-ahead unit commitment.

C.1 Unit Data

The type of generating units and their start-up cost are shown in Table C.1, in which CT stands for combustion turbine.

Table C.1: Unit type and start-up cost

Number of Units	Unit Type	Capacity (MW)	Start-up Cost ($)
5	Oil/Steam	12	68
4	Oil/CT	20	5
6	Hydro	50	0
4	Coal/Steam	76	655.6
3	Oil/Steam	100	566
4	Coal/Steam	155	1048.3
3	Oil/Steam	197	755
1	Oil/Steam	350	4468
2	Nuclear	400	10000

The mean time to failure (MTTF) and expected failure rate (λ) are shown in Table C.2.

Table C.2: Units' reliability data

Number of Units	Capacity (MW)	MTTF (Hour)	Expected Failure Rate λ (Hour^{-1})
5	12	2940	0.00034
4	20	450	0.00222
6	50	1980	0.00050
4	76	1960	0.00051
3	100	1200	0.00083
4	155	960	0.00104
3	197	950	0.00105
1	350	1150	0.00087
2	400	1100	0.00091

The minimum and maximum stable output of units and coefficients of the quadratic approximation of the cost function of each unit are shown in Table C.3.

The data for the piecewise approximation of the quadratic cost functions for the units except the hydro units is shown in Table C.4.

The generating units' minimum up- and down-times as well as history are shown in Table C.5

The generating units' maximum ramp-up and ramp-down rates are shown in Table C.6

C.2 Transmission System Data

The transmission network consists of 24 bus locations connected by 38 lines and transformers, as shown in Figure C.1.

The reactance and rating of transmission lines are shown in Table C.7. The locations of the generating units are shown in Table C.8. It can be seen that 10 of the 24 buses are generating stations.

Table C.3: Production limits and coefficients of quadratic cost function of units

Unit	$P_{\min}$(MW)	$P_{\max}$(MW)	a_i(\$/MW^{2}h)	b_i(\$/MWh)	c_i(\$/h)
1	2.4	12	0.02533	25.5472	24.3891
2	2.4	12	0.02649	25.6753	24.4110
3	2.4	12	0.02801	25.8027	24.6382
4	2.4	12	0.02842	25.9318	24.7605
5	2.4	12	0.02855	26.0611	24.8882
6	4	20	0.01199	37.5501	117.7551
7	4	20	0.01261	37.6637	118.1083
8	4	20	0.01359	37.7770	118.4576
9	4	20	0.01433	37.8896	118.8206
10	0	50	0	0.5	0
11	0	50	0	0.5	0
12	0	50	0	0.5	0
13	0	50	0	0.5	0
14	0	50	0	0.5	0
15	0	50	0	0.5	0
16	15.2	76	0.00876	13.3272	81.1364
17	15.2	76	0.00895	13.3858	81.2980
18	15.2	76	0.00910	13.3805	81.4641
19	15.2	76	0.00932	13.4073	81.6259
20	25	100	0.00623	18.0000	217.8952
21	25	100	0.00612	18.1000	218.3350
22	25	100	0.00598	18.2000	218.7552
23	54.24	155	0.00463	10.6940	142.7348
24	54.24	155	0.00473	10.7154	143.0288
25	54.24	155	0.00481	10.7376	143.3179
26	54.24	155	0.00487	10.7583	143.5972
27	68.95	197	0.00259	23.0000	259.1310
28	68.95	197	0.00260	23.1000	259.6490
29	68.95	197	0.00263	23.2000	260.1760
30	140	350	0.00153	10.8616	177.0575
31	100	400	0.00194	7.4921	310.0021
32	100	400	0.00195	7.5031	311.9120

C.3 Load Data

Bus load data at time of system peak (2850 MW) is shown in Table C.9. For times other than the system peak, the bus loads are assumed to have the same proportional

Table C.4: Piecewise linear approximation of quadratic cost functions

Unit	P_{min} (MW)	e^1 (MW)	e^2 (MW)	P_{max} (MW)	A_i ($/h)	$\lambda_{Git}(1)$ ($/MWh)	$\lambda_{Git}(2)$ ($/MWh)	$\lambda_{Git}(3)$ ($/MWh)
1	2.40	5.60	8.80	12	24.049	25.750	25.912	26.074
2	2.40	5.60	8.80	12	24.055	25.887	26.056	26.226
3	2.40	5.60	8.80	12	24.262	26.027	26.206	26.386
4	2.40	5.60	8.80	12	24.379	26.159	26.341	26.523
5	2.40	5.60	8.80	12	24.504	26.289	26.472	26.655
6	4.00	9.33	14.67	20	117.310	37.711	37.839	37.967
7	4.00	9.33	14.67	20	117.640	37.832	37.967	38.101
8	4.00	9.33	14.67	20	117.950	37.958	38.103	38.248
9	4.00	9.33	14.67	20	118.290	38.081	38.234	38.387
10	15.20	35.47	55.73	76	76.414	13.771	14.126	14.481
11	15.20	35.47	55.73	76	76.473	13.807	14.170	14.533
12	15.20	35.47	55.73	76	76.558	13.842	14.211	14.580
13	15.20	35.47	55.73	76	76.602	13.879	14.257	14.635
14	25.00	50.00	75.00	100	210.110	18.467	18.779	19.091
15	25.00	50.00	75.00	100	210.690	18.559	18.865	19.171
16	25.00	50.00	75.00	100	211.310	18.648	18.948	19.246
17	54.24	87.83	121.41	155	120.670	11.352	11.663	11.974
18	54.24	87.83	121.41	155	120.550	11.387	11.705	12.022
19	54.24	87.83	121.41	155	120.410	11.420	11.743	12.067
20	54.24	87.83	121.41	155	120.400	11.450	11.777	12.104
21	68.95	111.63	154.32	197	239.190	23.468	23.689	23.910
22	68.95	111.63	154.32	197	239.640	23.570	23.791	24.103
23	68.95	111.63	154.32	197	239.940	23.675	23.889	24.124
24	140.00	210.00	280.00	350	132.080	11.379	11.612	11.826
25	100.00	200.00	300.00	400	271.200	8.074	8.462	8.850
26	100.00	200.00	300.00	400	272.910	8.088	8.478	8.868

Table C.5: Units' minimum up/down-times and history

Number of Units	Capacity (MW)	Min up-time (Hour)	Min down-time (Hour)	Historyt_i^H (Hour)
5	12	1	1	-1
4	20	1	1	-1
6	50	1	1	-1
4	76	3	2	3
3	100	4	2	-3
4	155	5	3	5
3	197	5	4	-4
1	350	8	5	10
2	400	8	5	10

Table C.6: Units' ramp rates

Number of Units	Capacity (MW)	Max Ramp-up (MW/h)	Max Ramp-down (MW/h)
5	12	48.0	60.0
4	20	30.5	70.0
6	50	600	600
4	76	38.5	80.0
3	100	51.0	74.0
4	155	55.0	78.0
3	197	55.0	99.0
1	350	70.0	120
2	400	50.5	100

relation to system load as at the peak load conditions. The per unit bus loads are given in the last column of Table C.9.

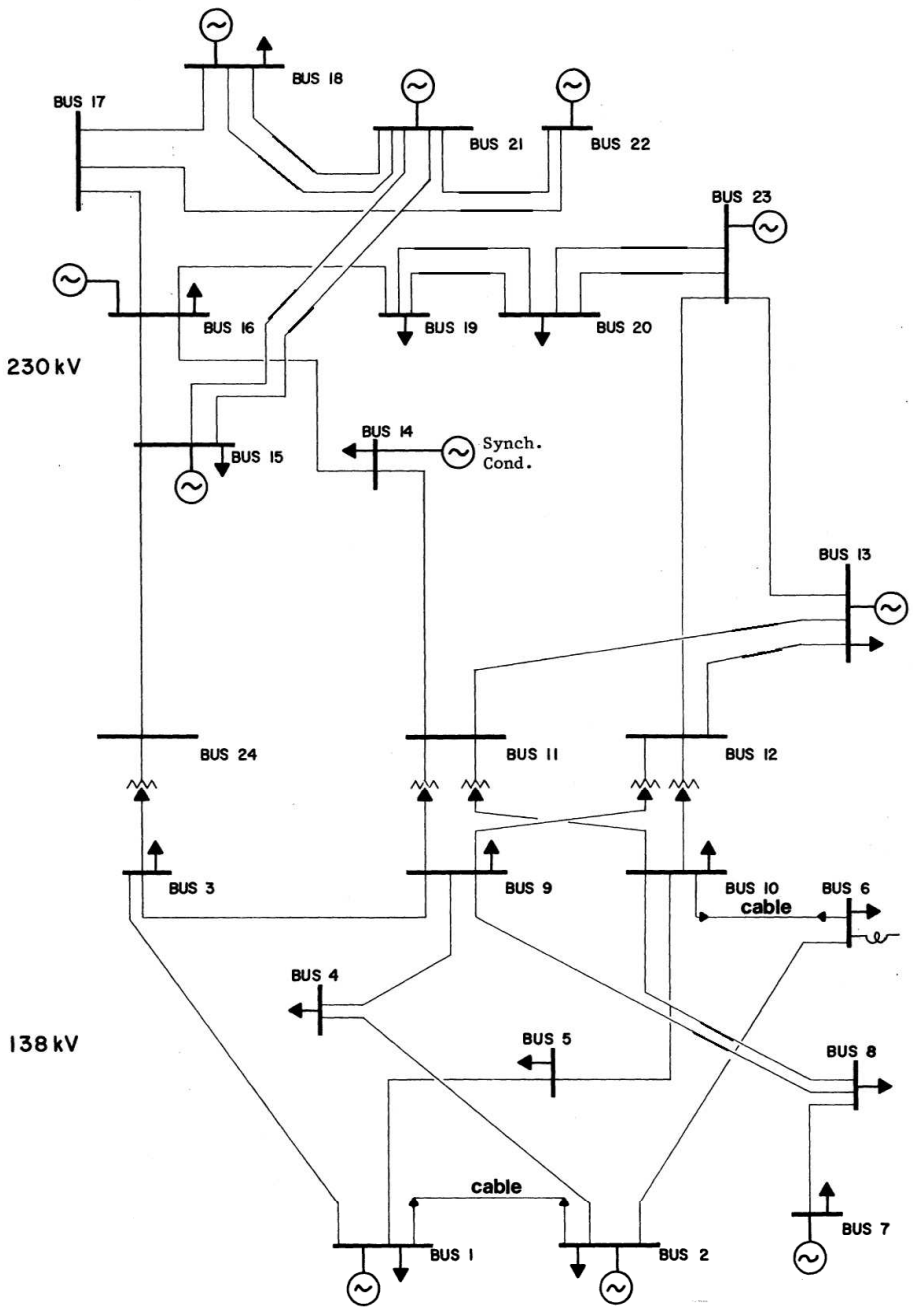

Figure C.1: IEEE Reliability Test System

Table C.7: Reactance and rating data of transmission lines

From Bus	To Bus	Reactance (P.U./100 MVA)	Rating (100 MVA)
1	2	0.0139	175
1	3	0.2112	175
1	5	0.0845	175
2	4	0.1267	175
2	6	0.1920	175
3	9	0.1190	175
3	24	0.0839	400
4	9	0.1037	175
5	10	0.0883	175
6	10	0.0605	175
7	8	0.0614	175
8	9	0.1651	175
8	10	0.1651	175
9	11	0.0839	400
9	12	0.0839	400
10	11	0.0839	400
10	12	0.0839	400
11	13	0.0476	500
11	14	0.0418	500
12	13	0.0476	500
12	23	0.0966	500
13	23	0.0865	500
14	16	0.0389	500
15	16	0.0173	500
15	21	0.0490	500
15	21	0.0490	500
15	24	0.0519	500
16	17	0.0259	500
16	19	0.0231	500
17	18	0.0144	500
17	22	0.1053	500
18	21	0.0259	500
18	21	0.0259	500
19	20	0.0396	500
19	20	0.0396	500
20	23	0.0216	500
20	23	0.0216	500
21	22	0.0678	500

Table C.8: Unit locations

Bus	Unit 1 (MW)	Unit 2 (MW)	Unit 3 (MW)	Unit 4 (MW)	Unit 5 (MW)	Unit 6 (MW)
1	20	20	76	76		
2	20	20	76	76		
7	100	100	100			
13	197	197	197			
15	12	12	12	12	12	155
16	155					
18	400					
21	400					
22	50	50	50	50	50	50
23	155	155	350			

Table C.9: Load Data

Bus	Load (MW)	Bus Load % of System Load
1	108	3.8
2	97	3.4
3	180	6.3
4	74	2.6
5	71	2.5
6	136	4.8
7	125	4.4
8	171	6.0
9	175	6.1
10	195	6.8
13	265	9.3
14	194	6.8
15	317	11.1
16	100	3.5
18	333	11.7
19	181	6.4
20	128	4.5
Total	2850	100

D Wind Data

D.1 Ten-minutes Wind Speed Forecast Results

This data is collected by Oregon State University for the United States Government, Department of Energy and Bonneville Power Administration. The data is in raw form collected directed from the data logger. The information of the data collection site is shown in Table D.1.

Table D.1: Data collection site information 1

Site Code	Site	Levels (ft)
101	Browning Depot, MT	80
102	Cape Blanco, OR	50
103	Goodnoe Hills, WA	50

The ten-minutes wind speed forecast results of these three sites on January, 29th, 2002 from 1300 hours to 1400 hours are shown in Table D.2.

D.2 Hourly Wind Speed Forecast Results

The information of the data collection site is shown in Table D.3.

The hourly wind speed forecast results of these six sites on January, 15th, 2006 are shown in Table D.4 to D.6.

Table D.2: Ten-minutes wind speed forecast results

Site Code	Time	Forecast Wind Speed (Mph)	Resultant Wind Speed (Mph)	Standard Deviation of Wind Speed (Mph)
101	1300	13.34	13.06	2.81
101	1310	14.08	13.79	3.00
101	1320	14.04	13.66	2.85
101	1330	13.41	13.08	2.56
101	1340	12.16	11.89	2.10
101	1350	11.86	11.58	2.40
101	1400	11.42	11.20	2.29
102	1300	8.34	7.50	2.31
102	1310	8.67	7.40	2.12
102	1320	11.35	9.56	1.45
102	1330	12.31	9.92	1.20
102	1340	12.44	10.06	1.26
102	1350	11.93	8.97	1.14
102	1400	11.64	8.92	1.31
103	1300	16.58	16.47	2.17
103	1310	16.42	16.32	1.99
103	1320	18.23	18.14	1.83
103	1330	17.16	17.05	2.04
103	1340	16.88	16.76	2.23
103	1350	16.96	16.87	1.95
103	1400	16.04	15.80	2.47

Table D.3: Data collection site information 2

Site Code	Location	Levels (ft)
CN	Chinook, OR	164
GU	Goodnoe Hills, WA	195
KZ	Kennewick, WA	86
SL	Sevenmile Hill, OR	50
VZ	Vansycle, OR	201
WO	Wasco, OR	100

Table D.4: Hourly wind speed forecast results at CN and GU

Hour	CN		GU	
	Forecast Wind Speed (Mph)	Standard Deviation of Wind Speed (Mph)	Forecast Wind Speed (Mph)	Standard Deviation of Wind Speed (Mph)
1	25.37	3.151	29.54	3.193
2	22.83	3.109	26.77	2.405
3	23.88	3.103	24.65	2.459
4	23.32	3.046	30.60	2.858
5	20.43	3.127	29.42	3.720
6	21.01	2.770	25.07	2.624
7	20.65	2.568	22.89	3.554
8	20.34	3.101	24.54	3.212
9	18.78	3.329	27.53	4.341
10	22.07	3.324	22.08	4.608
11	24.29	3.072	19.52	2.431
12	27.02	3.410	21.81	2.689
13	26.35	3.461	19.31	2.544
14	25.06	3.508	20.27	2.532
15	22.27	3.322	18.51	2.721
16	17.80	2.472	17.03	3.574
17	19.55	2.792	21.60	1.743
18	20.06	2.523	19.89	2.478
19	20.19	2.559	23.15	1.774
20	20.05	2.888	18.85	2.108
21	18.63	2.326	21.35	1.894
22	28.33	2.199	20.91	2.435
23	14.59	2.080	14.18	1.715
24	13.39	1.731	11.43	1.224

Table D.5: Hourly wind speed forecast results at KZ and SL

Hour	KZ		SL	
	Forecast Wind Speed (Mph)	Standard Deviation of Wind Speed (Mph)	Forecast Wind Speed (Mph)	Standard Deviation of Wind Speed (Mph)
1	30.14	2.131	19.71	2.859
2	27.09	2.809	19.14	2.506
3	27.51	2.336	16.21	3.231
4	25.56	2.213	15.04	1.759
5	28.31	1.652	1091	1.703
6	27.58	1.613	12.42	1.654
7	30.74	1.983	16.75	2.901
8	32.34	1.910	22.29	2.132
9	26.92	2.439	22.07	2.580
10	21.68	1.826	24.64	2.576
11	23.10	3.142	21.78	3.547
12	24.23	1.964	23.39	2.878
13	24.52	1.825	26.67	3.258
14	29.29	2.464	26.32	3.105
15	26.17	2.109	25.29	3.157
16	23.68	1.554	17.86	3.536
17	27.39	2.574	18.56	3.508
18	26.78	1.671	9.340	3.106
19	22.24	2.035	12.09	3.713
20	15.24	2.183	10.77	1.511
21	16.61	1.406	11.54	1.208
22	15.92	2.159	7.886	1.039
23	21.00	1.474	4.694	2.261
24	25.38	1.766	2.409	0.632

Table D.6: Hourly wind speed forecast results at VZ and WO

Hour	VZ		WO	
	Forecast Wind Speed (Mph)	Standard Deviation of Wind Speed (Mph)	Forecast Wind Speed (Mph)	Standard Deviation of Wind Speed (Mph)
1	34.65	2.439	12.23	2.503
2	34.80	2.068	10.07	1.602
3	33.36	2.502	14.83	2.510
4	31.53	1.808	14.37	2.046
5	31.30	2.099	13.96	2.144
6	32.93	1.869	11.91	2.065
7	33.49	1.772	16.92	2.908
8	31.38	1.704	18.05	3.163
9	30.20	2.097	12.38	3.357
10	27.92	2.007	10.81	1.797
11	26.74	1.980	12.04	1.917
12	26.40	2.872	11.86	2.902
13	23.90	1.902	11.06	2.773
14	24.71	1.650	12.23	3.399
15	23.80	1.565	10.33	3.737
16	22.45	1.311	13.50	2.859
17	23.21	1.908	13.91	3.464
18	30.25	1.413	11.60	5.719
19	29.59	1.136	6.942	1.504
20	28.26	1.708	6.366	1.740
21	27.90	1.432	6.455	0.593
22	24.03	2.644	6.636	0.770
23	21.74	1.147	9.960	2.087
24	21.50	0.940	9.730	1.411

Vita

Guodong Liu received his B.S. and M.S. degrees, both in electric power engineering, from Shandong University (China) in 2007 and Huazhong University of Science and Technology in 2009, respectively. He started his Ph.D. studies at The University of Tennessee, Knoxville, in August 2009. His current interests include power system operation and planning, power system reliability, and market simulation.